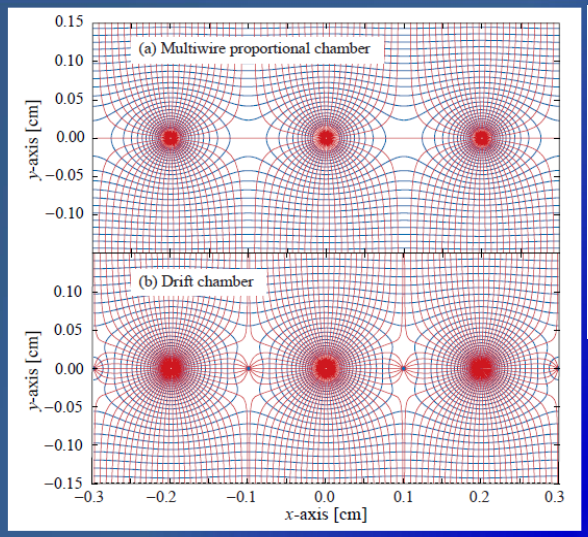

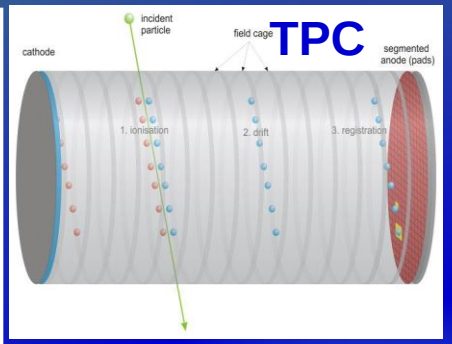

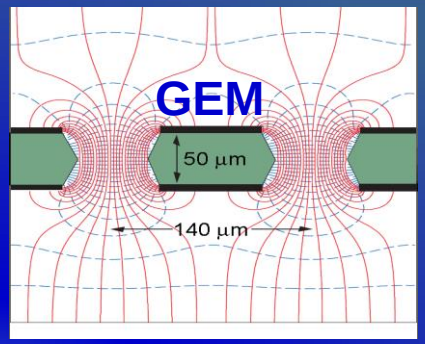

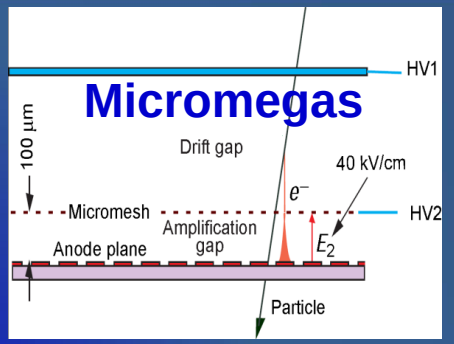

From (very) Basic Ideas to Rather Complex Gaseous Detector Systems

Maxim Titov, CEA Saclay, Irfu, France

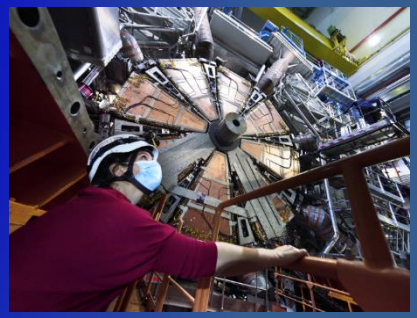

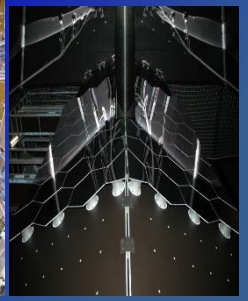

XI ICFA Instrumentation School, Tata Institute of Fundamental Research, Mumbai, India, Feb. 12-25, 2023

To make a collider experiment, one needs:

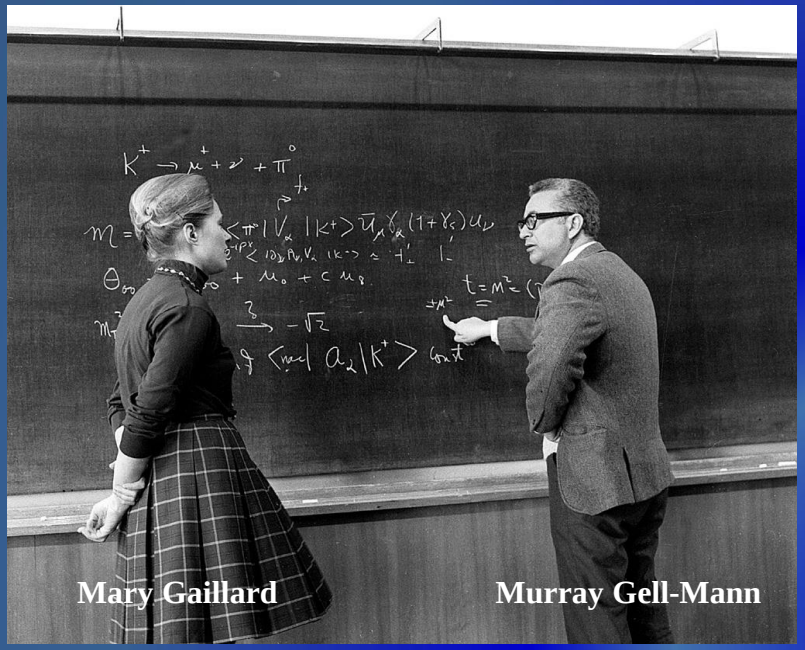

A theory:

and a cafeteria

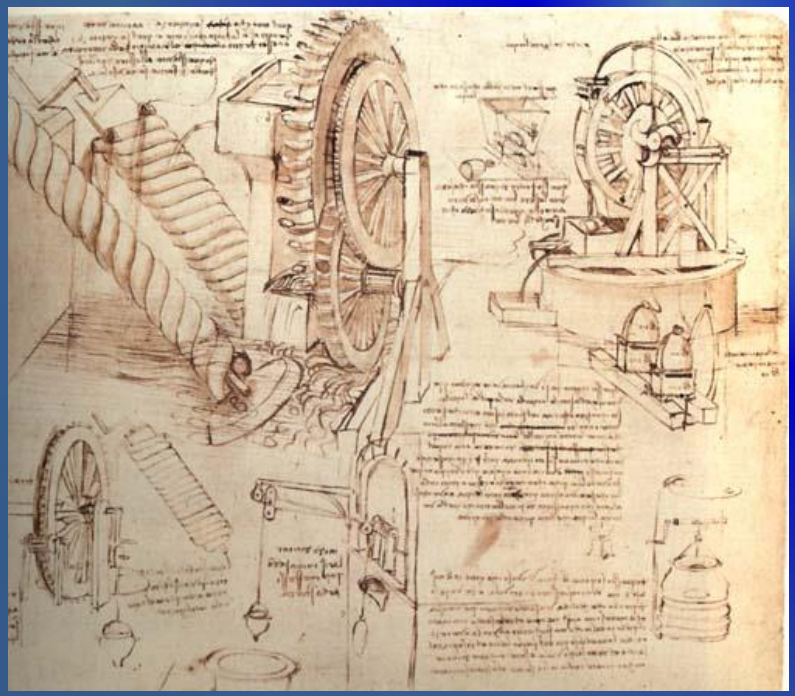

Clear and easy understandable drawings

and a tunnel for the accelerator and magnets and stuff

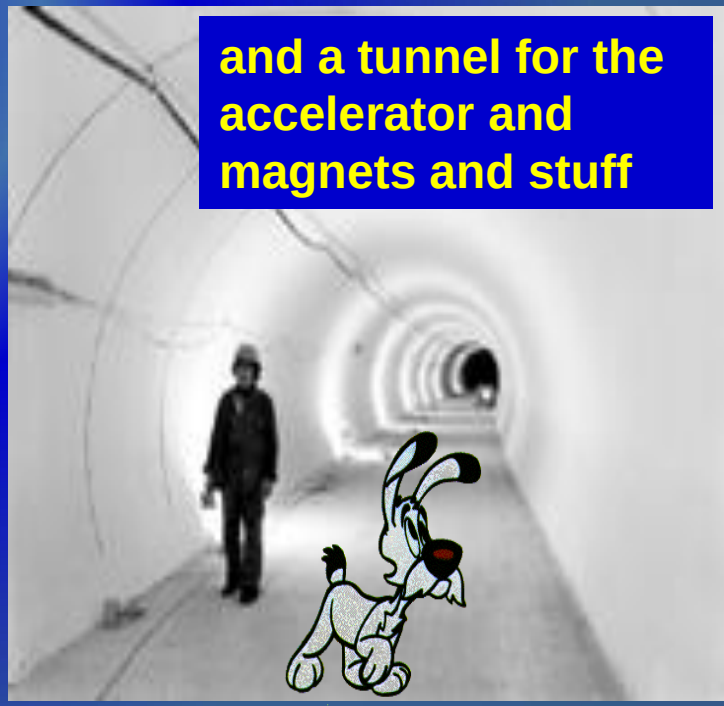

Easy access to the experiment

Physicists to operate detector/analyze data

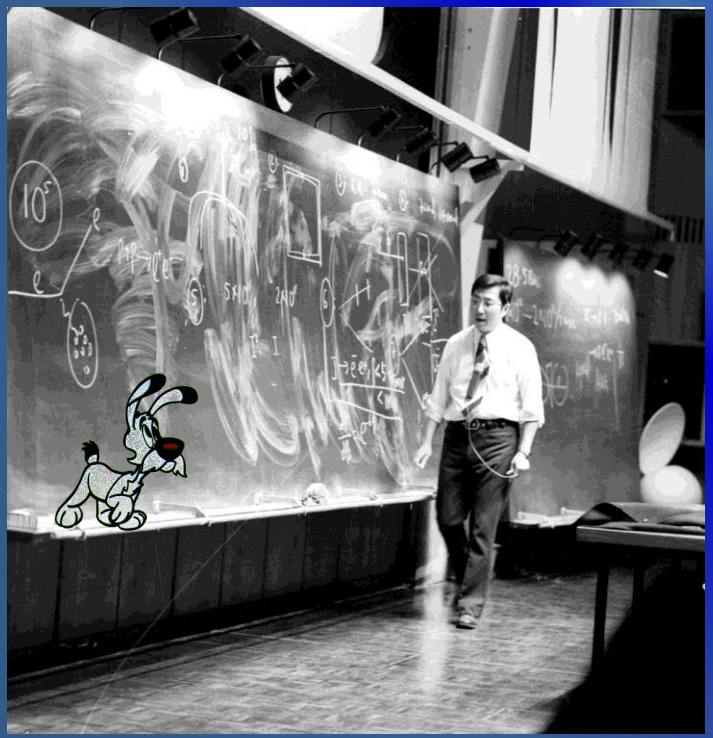

and a Nobel prize

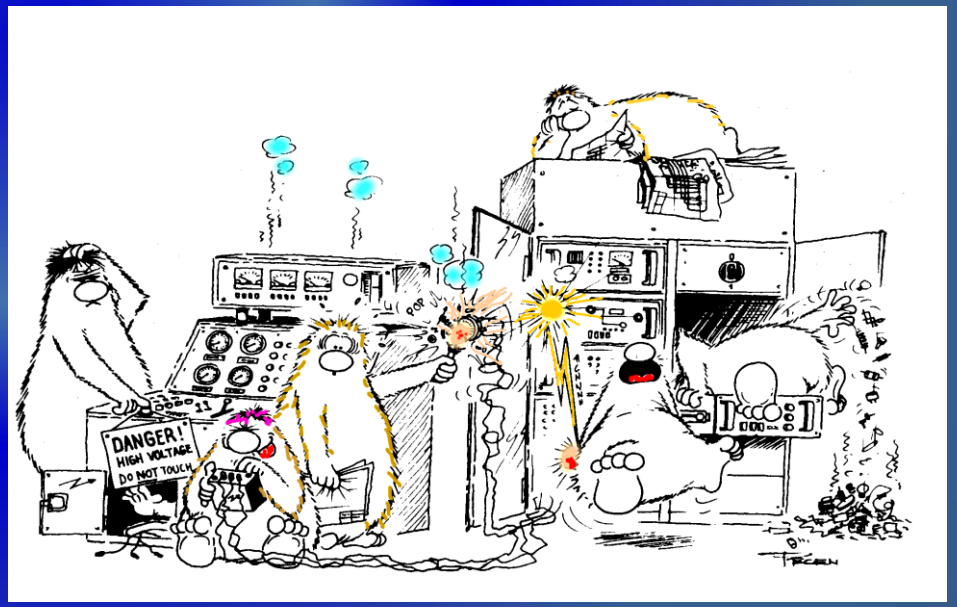

We will just concentrate on Particle Detectors – "Gaseous Detectors"

Gas-Based Detectors: A Brief History

Geiger Counter
H.GeigerW.Mueller 1928

PPC
Parallel Plate Counter

PC
Proportional Counter

Pestov
Counter
V.Pestov 1982

RPC
Resistive Plate Chambers
R.Santonico R.Cardarelli 1981

MWPC
Multiwire Proportional Chamber
G.Charpak et al 1968

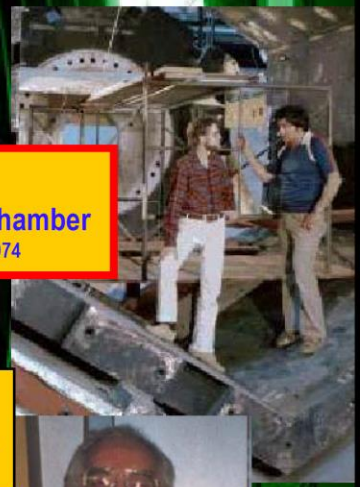

TPC
Time Projection Chamber
D.R.Nygren et al 1974

MSGC
Microstrip Gas Chambers
A.Oed 1988

GEM
Gas Electron Multiplier
F.Sauli 1997

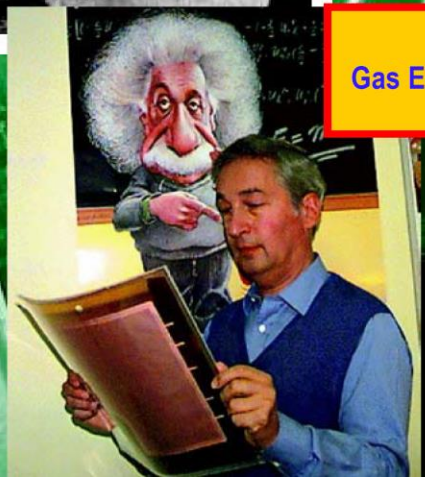

μM
Micromegas
I.Giomataris et al 1996

Family of Gaseous Detectors with a Glorious Tradition

1908: FIRST WIRE COUNTER USED BY RUTHERFORD IN THE STUDY OF NATURAL RADIOACTIVITY

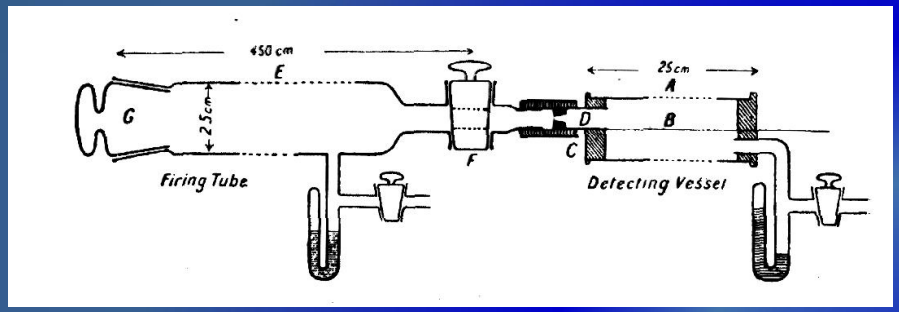

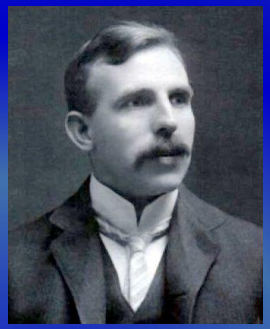

E. Rutherford and H. Geiger , Proc. Royal Soc. A81 (1908) 141

Nobel Prize in Chemistry in 1908

1968: MULTIWIRE PROPORTIONAL CHAMBER

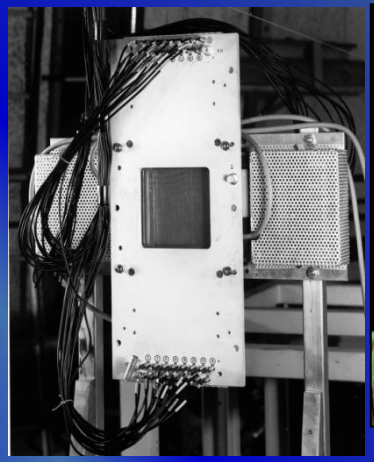

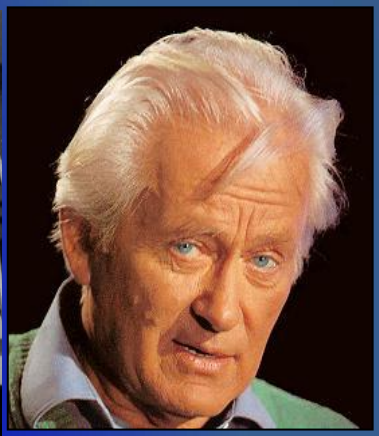

Nobel Prize in Physics 1992

1928: GEIGER COUNTER SINGLE ELECTRON SENSITIVITY

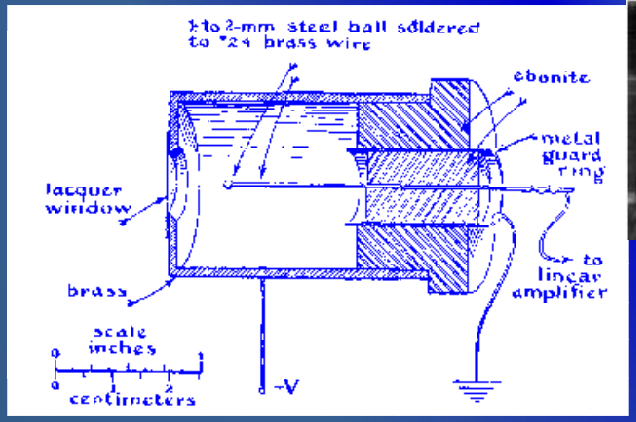

H. Geiger and W. Müller, Phys. Zeits. 29 (1928) 839

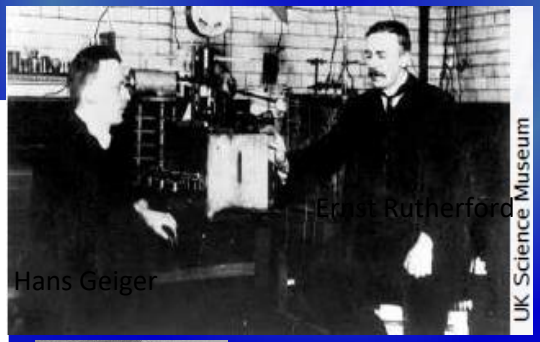

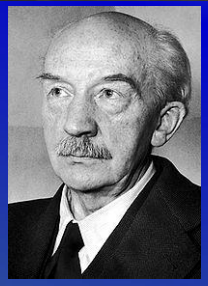

Walther Bothe Nobel Prize in Physics 1954 for the “coincidence method”

G. Charpak, Proc. Int. Symp. Nuclear Electronics (Versailles 10-13 Sept 1968)

1968: MWPC – Revolutionising the Way Particle Physics is Done

G. Charpak, F. Sauli and J.C. Santiard

Before MWPC: Detecting particles was a mainly a manual, tedious and labour intensive job – unsuited for rare particle decays

1968: George Charpak developed the MultiWire Proportional Chamber, (MWPC), which revolutionized particle detection & HEP,
and marked transition from Manual to Electronics era

1992:

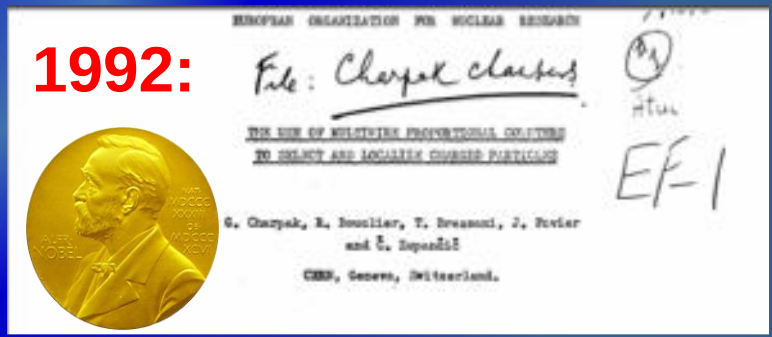
EUROPEAN ORGANIZATION FOR NUCLEAR RESEARCH
File: Charpak classes
THE USE OF MULTIWIRE PROPORTIONAL COUNTERS TO SELECT AND LOCALIZE CHARGED PARTICLES
G. Charpak, R. Bouclier, T. Bressani, J. Favier and C. Zupančič
CERN, Geneva, Switzerland.
EF-1

"Image" & "Logic (electronics)" tradition combined into the "Electronics Image" detectors during the 1970ies

Multi-Wire Proportional Chambers – Particle Physics Spin-Off

Biospace: Company Founded In 1989 by Georges Charpak

http://www.biospacelab.com:

Our digital autoradiography system leverages the gas detection technology invented by our founder Georges Charpak:

Nobel Prize in Physics in 1992.

~ 2000: LOW-DOSE 3D IMAGING

COMMERCIAL AUTORADIOGRAPHY SYSTEMS WITH GASEOUS DETECTORS

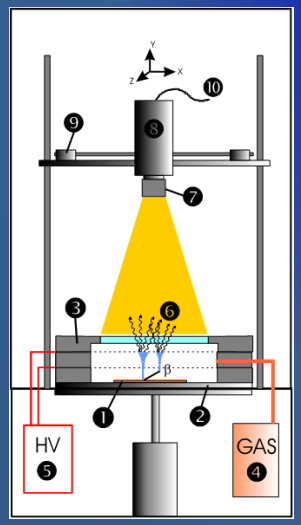

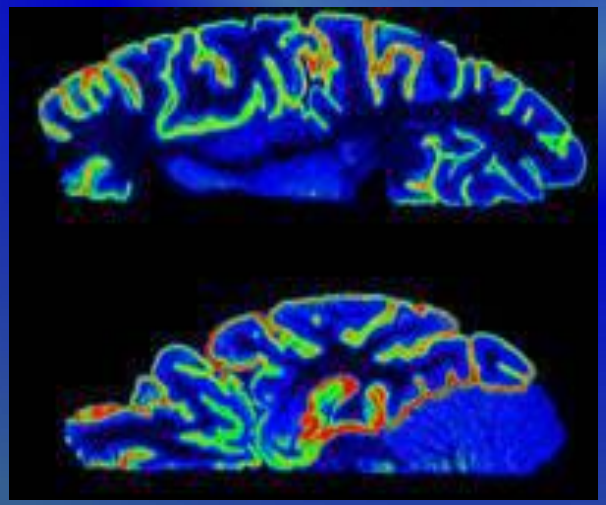

Georges Charpak with Friends

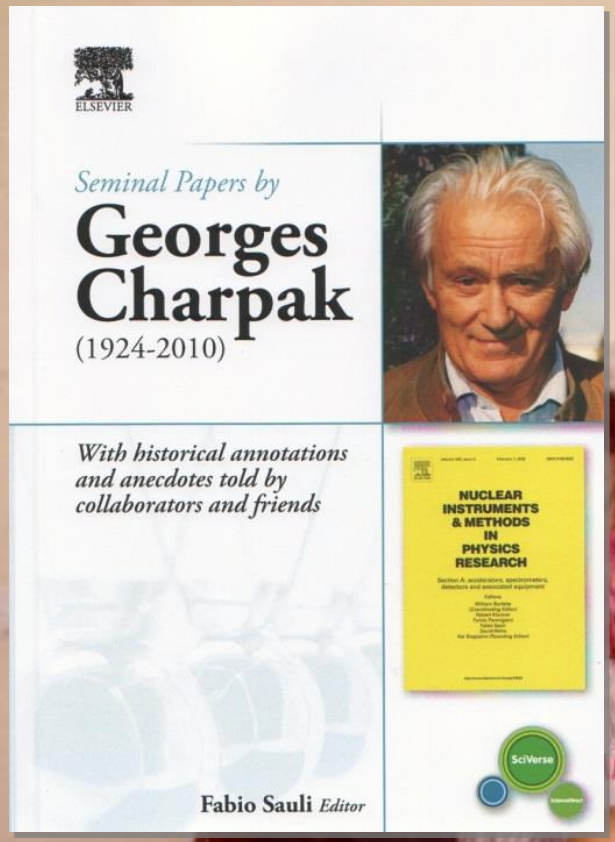

1983/1984: Discovery of W and Z Bosons at UA1/UA2

UA1 used the largest wire / drift chamber of its day (5.8 m long, 2.3 m in diameter)

It can now be seen in the CERN Microcosm Exhibition

Discovery of W and Z bosons
C. Rubbia & S. Van der Meer,

1984:

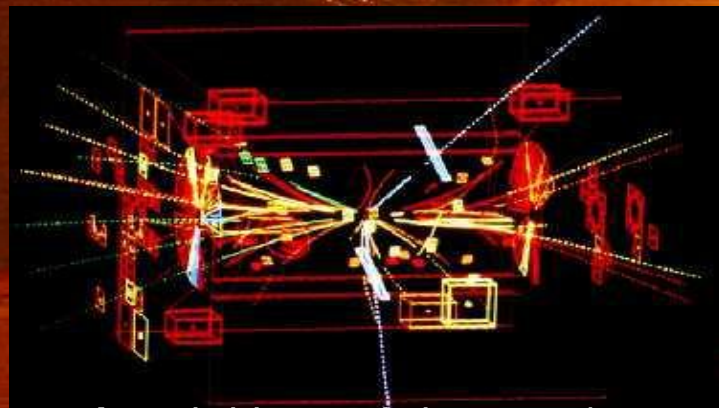

Z → *ee* (white tracks) at UA1/CERN

Time Projection Chamber (TPC) in Particle and Ion Physics

An ultimate drift chamber design is TPC concept - 3D precision tracking with low material budget & enables particle identification through differential energy loss dE/dx measurement or cluster counting dN_{cl}/dx techniques.

PEP4 (SLAC)

- ✓ **Invented by David Nygren (Berkeley) in 1974**
- ✓ **Proposed as a central tracking device for the PEP-4 detector @ SLAC 1976**
- ➢ **More (and even larger) were built, based on MPWC readout**
- ➢ **New generation of TPCs use MPGD-based readout: e.g. ALICE Upgrade, T2K, ILC, CepC**

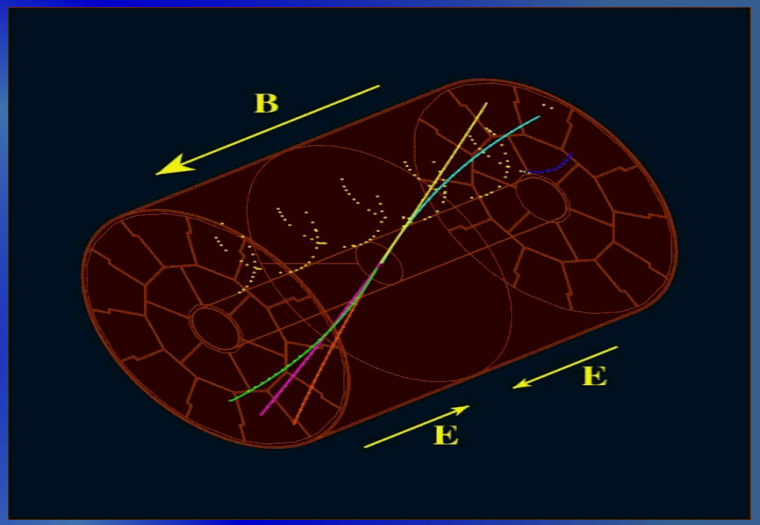

TOPAZ (KEK)

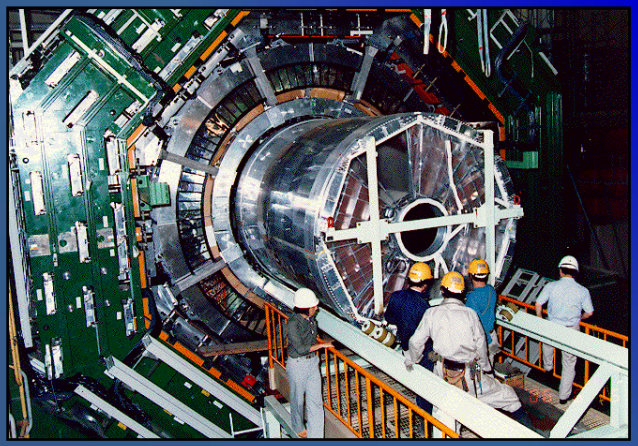

ALEPH (CERN)

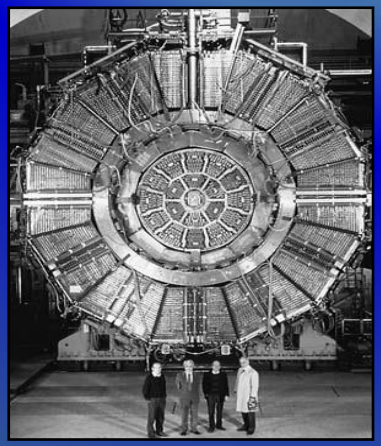

STAR (LBL)

DELPHI (CERN)

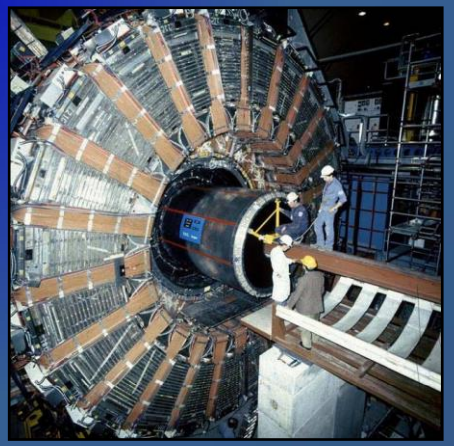

Modern Time Projection Chamber in ALICE Experiment @ LHC

Gaseous Detectors: From Wire/Drift Chamber → Time Projection Chamber (TPC) → Micro-Pattern Gas Detectors

Primary choice for large-area coverage with low material-budget (+ dE/dx measurement)

1990's: Industrial advances in photolithography has favoured the invention of novel micro-structured gas amplification devices (MSGC, GEM, Micromegas, …)

Rate Capability:
MWPC vs MSGC

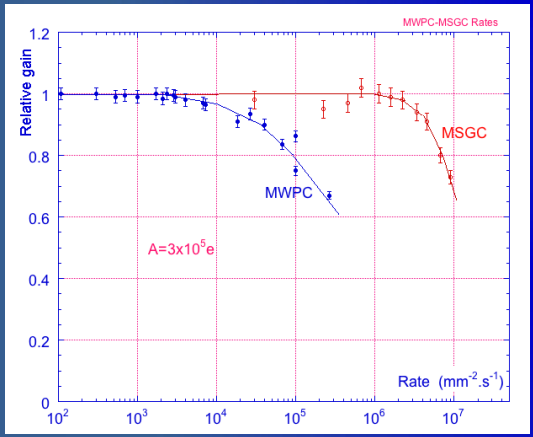

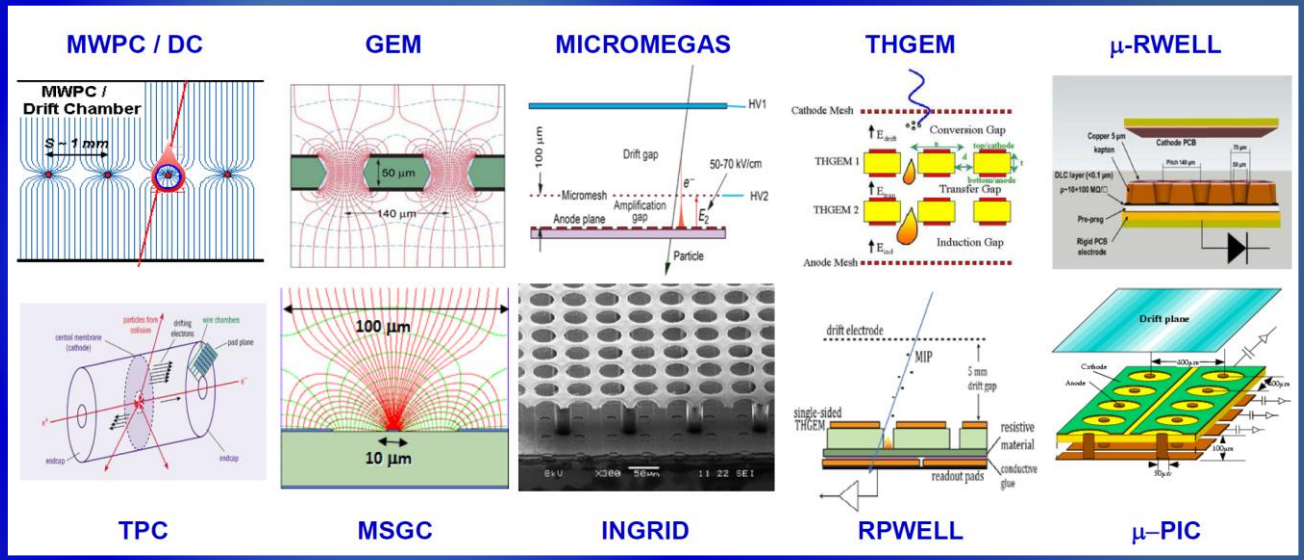

HL-LHC Upgrades: Tracking (ALICE TPC/MPGD); Muon Systems: RPC, CSC, MDT, TGC, GEM, Micromegas;

Future Hadron Colliders: FCC-hh Muon System (MPGD - OK, rates are comparable with HL-LHC)
Future Lepton Colliders: Tracking (FCC-ee / CepC - Drift Chambers; ILC / CePC - TPC with MPGD readout)
Calorimetry (ILC, CepC – RPC or MPGD), Muon Systems (OK)

Future Election-Ion Collider: Tracking (GEM, μWELL; TPC/MPGD), RICH (THGEM), TRD (GEM)

CERN-RD51 Collaboration & MPGD Technology Advances

RD51* CERN-based *"TECHNOLOGY - DRIVEN R&D COLLABORATION" *was established to advance MPGD concepts and associated electronics readout systems*

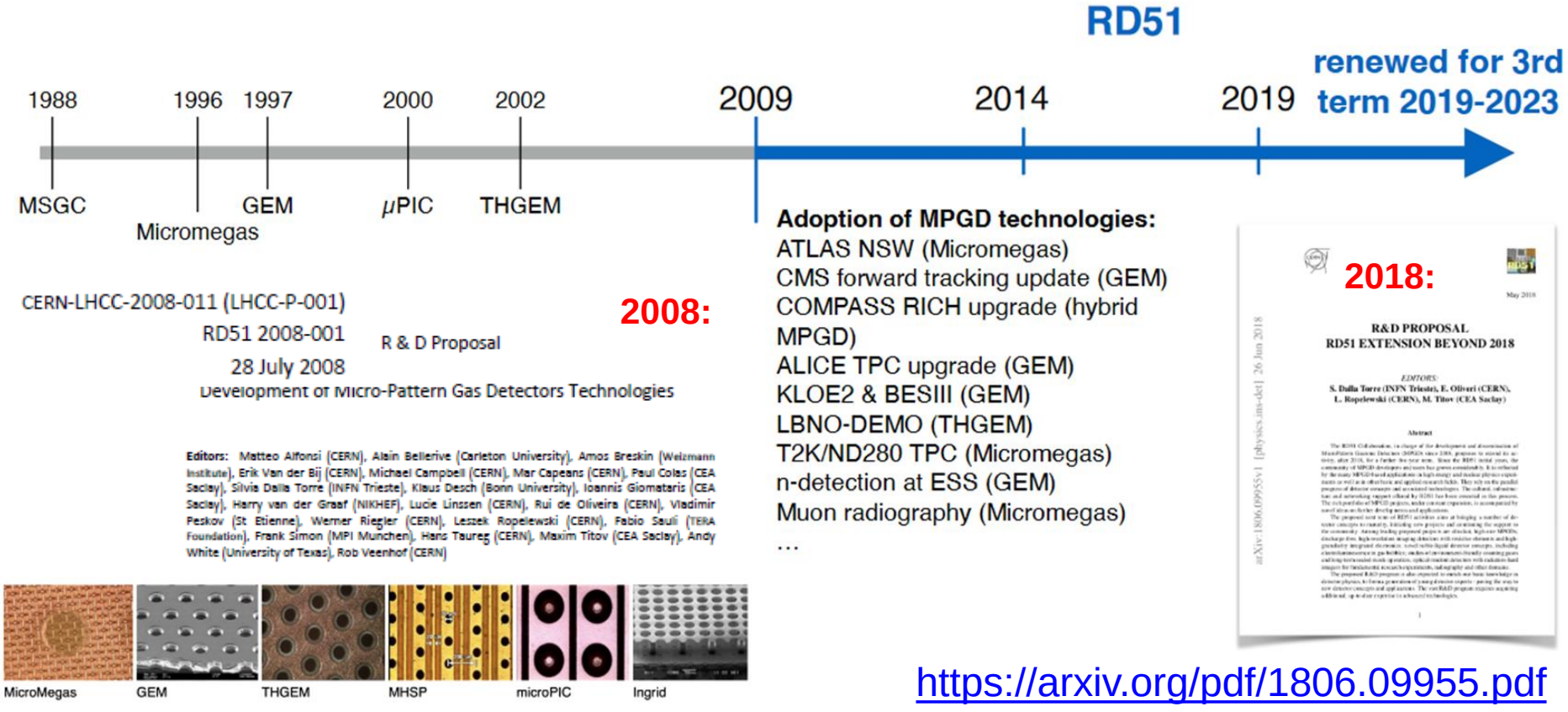

https://arxiv.org/pdf/1806.09955.pdf

- *Renewed by the CERN Research Board for the 3rd term 2019 – 2023*
- *Beyond 2023, RD51 will serve as a nuclei of the new DRD1 ("all gas detectors") collaboration, anchored at CERN, as part of the ECFA Detector R&D Roadmap implementation*

2014: RD51 Collaboration Meeting in Kolkata

International Workshop on Advanced Detectors IWAD 2014

& 14th RD51 Collaboration Meeting

October 27 - 31, 2014
Kolkata
India

Sponsor
Board of Research in Nuclear Science
Department of Atomic Energy

Advanced gaseous detectors play a major role in modern day particle physics experiments. As spinoff they also find wide range of applications in the areas of medical imaging, radiography among others. In this regard a two-day International Workshop on Advanced Detectors (IWAD) is being organized during 27-28 October 2014 at VECC-SINP campus, Kolkata, INDIA. The workshop would be followed by 14th RD51 collaboration meeting at the same venue.

Local Organizing Committee

Sudhee R. Banerjee	VECC
Subhasis Chattopadhyay (Chairman)	VECC
Sukalyan Chattopadhyay	SINP
Supriya Das	BI
Anand K. Dubey (Convener)	VECC
Nayana Majumdar	SINP
Supratik Mukhopadhyay (Co-Chairman)	SINP
Tapan K. Nayak	VECC
Lalit M. Pant	BARC
Satyajit Saha	SINP
Vikas Singhal	VECC

Areas to be covered in the workshop

27 – 28 October, 2014

- Micropattern Gas Detectors (MPGD)
- Resistive Plate Chambers (RPC)
- Applications of advanced detectors in High Energy Physics
- Medical and other applications of advanced detectors

International Advisory Committee

Amos Breskin	Weizmann Inst. Sc., Israel
Sunanda Banerjee	SINP, India
Giovanni Bencivenni	LNF-INFN, Italy
Rakesh K. Bhandari	IUAC, India
Sudeb Bhattacharya	SINP, India
Bikas K. Chakraborty	SINP, India
Paul Colas	CEA/IRFU Saclay, France
Vivek M. Datar	NPD, BARC, India
Klaus Desch	Bonn University, Germany
Ioannis Giomataris	CEA Saclay, France
Harry van der Graaf	NIKHEF, The Netherlands
Naba K. Mondal	TIFR, India
Sibaji Raha	Bose Institute, India
Leszek Ropelewski	CERN, Switzerland
Fabio Sauli	CERN, Switzerland
Christian J. Schmidt	GSI Darmstadt, Germany
Amar Sinha	BARC, India
Dinesh K. Srivastava	VECC, India
Hans Taureg	CERN, Switzerland
Maxim Titov	CEA Saclay, France
Silvia Dalla Torre	Trieste Univ. & INFN, Italy
Yogendra P. Viyogi	VECC, India
Andy White	Univ. of Texas, Arlington, USA

Contact

E-mail : rd51india@vecc.gov.in
Postal :
Anand Kumar Dubey, Convener
Variable Energy Cyclotron Center (VECC)
Department of Atomic Energy
1/AF, Bidhan Nagar, Kolkata – 700064, India
Phone : +91 33 2318 2416 / 2410
Fax : +91 33 2334 6871

Registration

No Registration Fee for RD51 Collaboration Members

	For others	
Indian Participants	Faculties : ₹ 2000/-	Students : ₹ 1000/-
Foreign Participants	Faculties : USD 60	Students : USD 30

For participation in IWAD please send one page abstract to
rd51india@vecc.gov.in
on or before
August 15, 2014.

http://indico.vecc.gov.in/indico/conferenceDisplay.py?confId=31

CERN Courier (5 pages) Volume, October 2015

CERN Courier October 2015
etector R&D

RD51 and the rise of micro-pattern gas detectors

Since its foundation, the RD51 collaboration has provided important stimulus for the development of MPGDs.

Improvements in detector technology often come from capitalizing on industrial progress. Over the past two decades, advances in photolithography, microelectronics and printed circuits have opened the way for the production of micro-structured gas-amplification devices. By 2008, interest in the development and use of the novel micro-pattern gaseous detector (MPGD) technologies led to the establishment at CERN of the RD51 collaboration. Q... ated for a five-year term, RD51 was later pr... years beyond 2013. While many of the MP... introduced before RD51 was founded (figu... niques becoming available or affordable, new... still being introduced, and existing ones are s...

In the late 1980s, the development of the m... ber (MSGC) created great interest because... capability, which was orders of magnitude ... chambers, and its position resolution of a few tens of micrometres at particle fluxes exceeding about 1 MHz/mm^2. Developed for projects at high-luminosity colliders, MSGCs promised to fill a gap between the high-performance but expensive solid-state detectors, and cheap but rate-limited traditional wire chambers. However, detailed studies of their long-term behaviour at high rates and in hadron beams revealed two possible weaknesses of the MSGC technology: the formation of deposits on the electrodes, affecting gain and performance ("ageing effects"), and spark-induced damage to electrodes in the presence of highly ionizing particles.

These initial ideas have since led to more robust MPGD structures, in general using modern photolithographic processes on thin insulating supports. In particular, ease of manufacturing, operational stability and superior performances for charged-particle tracking, muon detection and triggering have given rise to two main designs: the gas electron-multiplier (GEM) and the micro-mesh gaseous structure (Micromegas). By using a pitch size of a few hundred micrometres, both devices exhibit intrinsic high-rate capability (> 1 MHz/mm^2), excellent spatial and multi-track resolution (around 30 μm and 500 μm, respectively), and time resolution for single photoelectrons in the sub-nanosecond range.

Coupling the microelectronics industry and advanced PCB technology has been important for the development of gas detectors with increasingly smaller pitch size. An elegant example is the use of a CMOS pixel ASIC, assembled directly below the GEM or Micromegas amplification structure. Modern "wafer post-processing technology" allows for the integration of a Micromegas grid directly on top of a Medipix or Timepix chip, thus forming

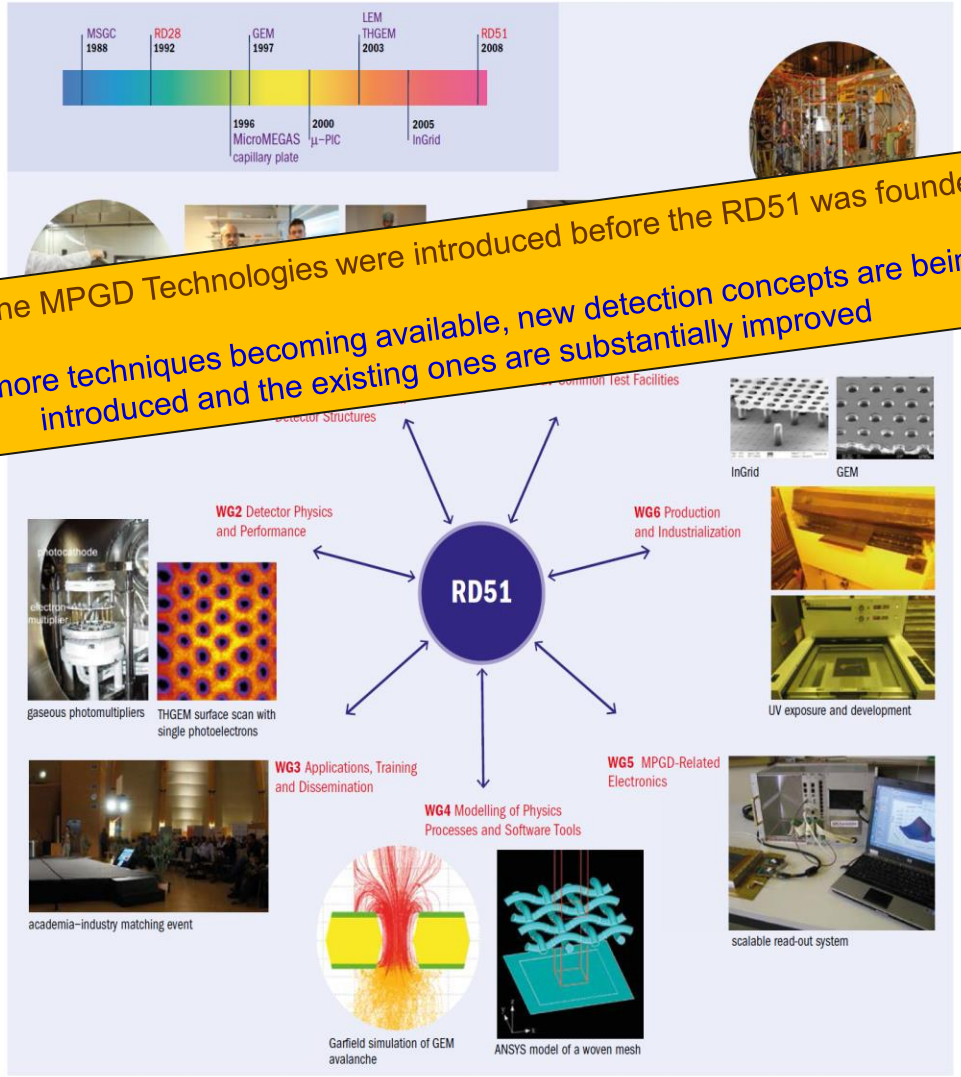

Fig. 1. The seven working groups of RD51, with illustrations of just a few examples of the different kinds of work involved. Top left: the 20-year pre-history of RD51. (Image credits: RD51 Collaboration.)

integrated read-out of a gaseous detector (InGrid). Using this approach, MPGD-based detectors can reach the level of integra-...actness and resolving power typical of solid-state pixel ...r applications requiring imaging detectors with large-...ge and moderate spatial resolution (e.g. ring-imaging ...RICH) counters), coarser macro-patterned structures ...resting economic solution with relatively low mass ...struction – thanks to the intrinsic robustness of the ...des. Such detectors are the thick GEM (THGEM), ...h multiplier (LEM), patterned resistive thick GEM (RETGEM) and the resistive-plate WELL (RPWELL).

RD51 and its working groups

The main objective of RD51 is to advance the technological development and application of MPGDs. While a number of activities have emerged related to the LHC upgrade, most importantly, RD51 serves as an access point to MPGD "know-how" for the worldwide community – a platform for sharing information, results and experience – and optimizes the cost of R&D through the sharing of resources and the creation of common projects and infrastructure. All partners are already pursuing either basic- or application-oriented R&D involving MPGD concepts. Figure 1 shows the organization of seven Working Groups (WG) that cover all of the relevant aspects of MPGD-related R&D.

WG1 Technological Aspects and Development of New Detector Structures. The objectives of WG1 are to improve the performance of existing detector structures, optimize fabrication methods, and develop new multiplier geometries and techniques. One of the most prominent activities is the development of large-area GEM, Micromegas and THGEM detectors. Only one decade ago, the largest MPGDs were around 40 × 40 cm^2, limited by existing tools and materials. A big step towards the industrial manufacturing of MPGDs with a size around a square metre came with new fabrication methods – the single-mask GEM, "bulk" Micromegas, and the novel Micromegas construction scheme with a "floating mesh". While in "bulk" Micromegas, the metallic mesh is integrated into the PCB read-out, in the "floating-mesh" scheme it is integrated in the panel containing drift electrodes and placed on pillars when the chamber is closed. The single-mask GEM technique overcomes the cumbersome practice of alignment of two masks between top and bottom films, which limits the achievable lateral size to 50 cm. This technology, together with the novel "self-stretching technique" for assembling GEMs without glue and spacers, simplifies the fabrication process to such an extent that, especially for large-volume production, the cost per unit area drops by orders of magnitude.

2022: MPGDs for High Luminosity LHC Upgrades

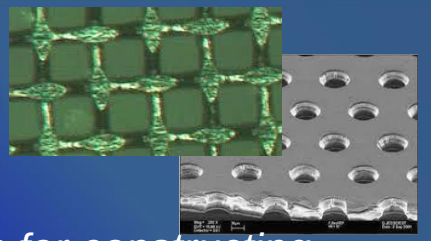

The successful implementation of MPGDs for relevant upgrades of CERN experiments indicates the degree of maturity of given detector technologies for constructing large-size detectors, the level of dissemination within the HEP community and their reliability

ATLAS NSW MicroMegas

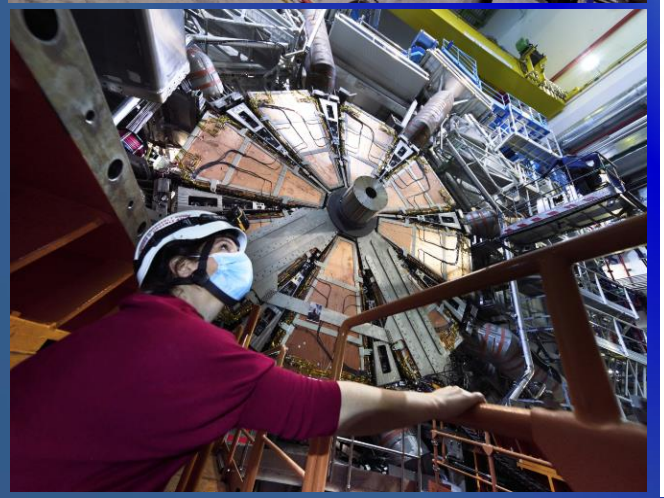

https://ep-news.web.cern.ch/content/atlas-new-small-wheel-upgrade-advances-0

ALICE GEM-TPC

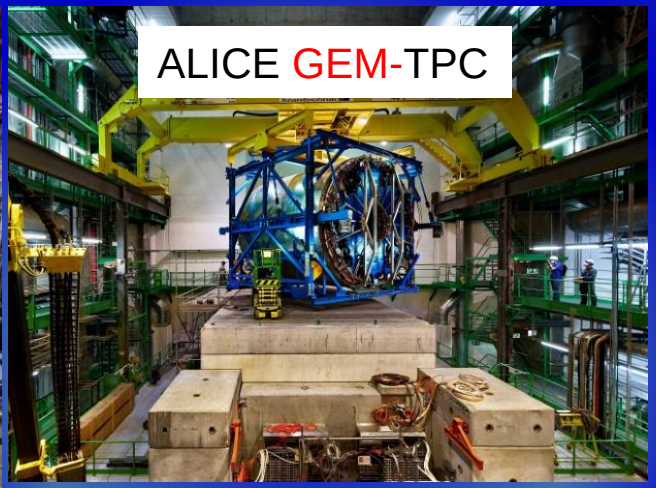

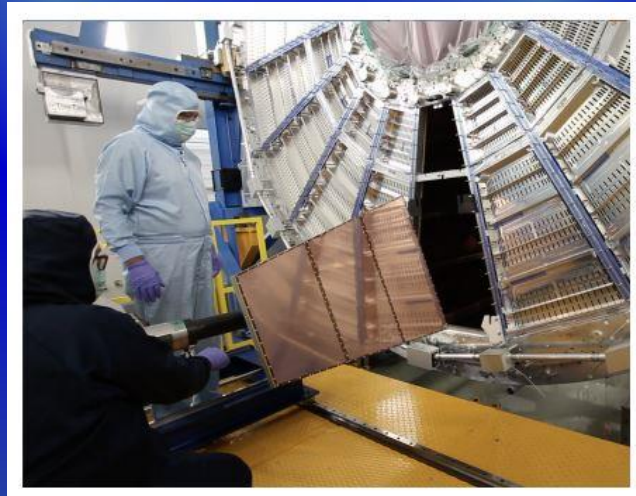

https://ep-news.web.cern.ch/upgraded-alice-tpc

CMS GEM muon endcaps

https://ep-news.web.cern.ch/content/demonstrating-capabilities-new-gem

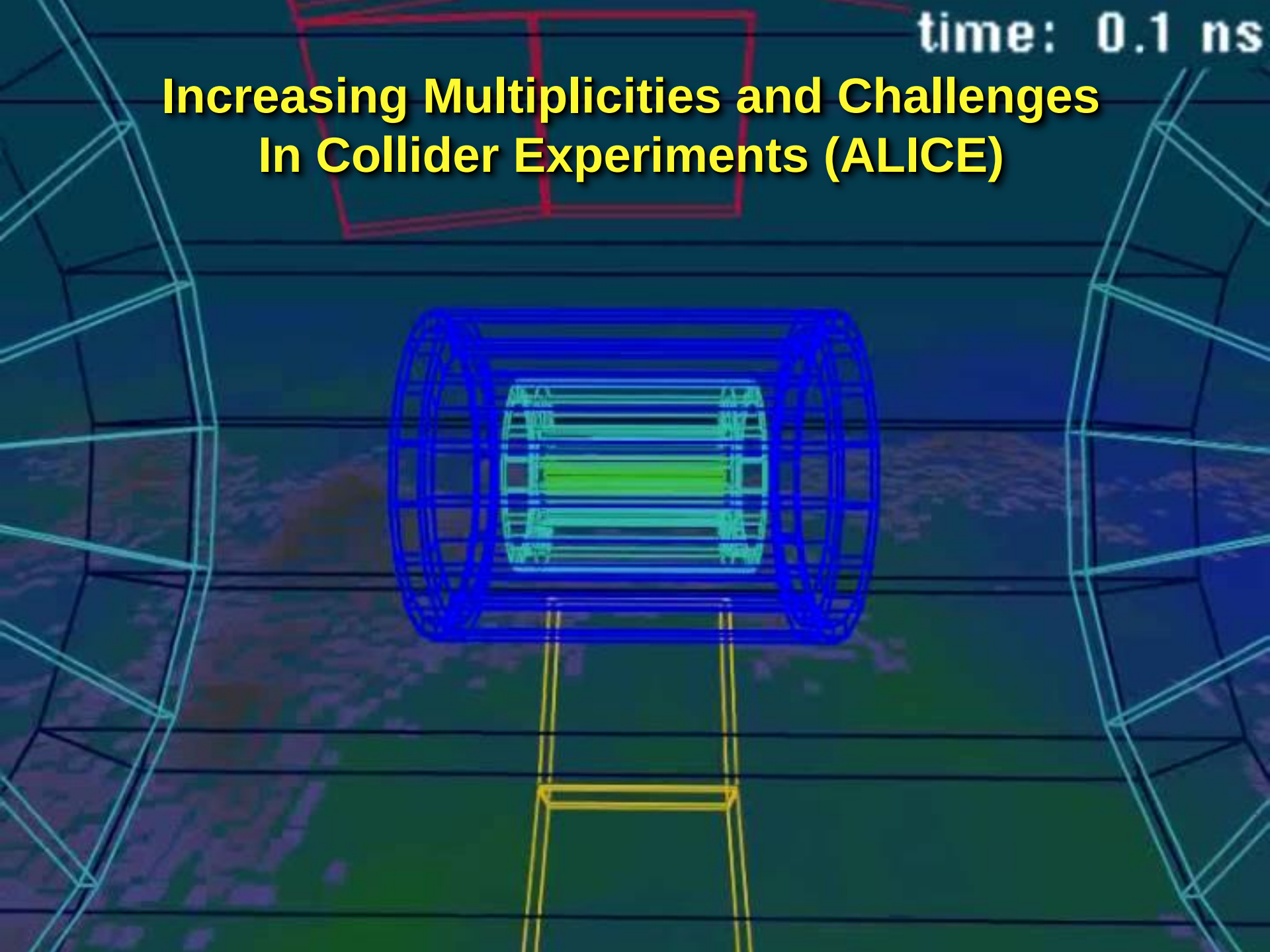

Increasing Multiplicities and Challenges In Collider Experiments (ALICE)

Tracking Detectors: History and Trends

- **Cloud Chambers, Nuclear Emulsions + Geiger-Müller tubes**
  → dominated until the early 1950s: Cloud Chambers now very popular in public exhibitions related to particle physics
- **Bubble Chambers had their peak time between 1960 and 1985**
  → last big bubble chamber was BEBC at CERN
- **Since 1970s: Wire Chambers (MWPCs and drift chambers) started to dominate; recently being replaced by Micro-Pattern Gas Detectors (MPGD)**
- **Since late 1980s: Solid state detectors are in common use**
  → started as small sized vertex detectors (at LEP and SLC)
  → now ~200 m^2 Si-surface in CMS tracker
- **Most recent trend: silicon strips & hybrid detectors, 3D-sensors, CMOS Monolithic Active Pixel Sensors (MAPS)** → See Frank Hartmann lectures

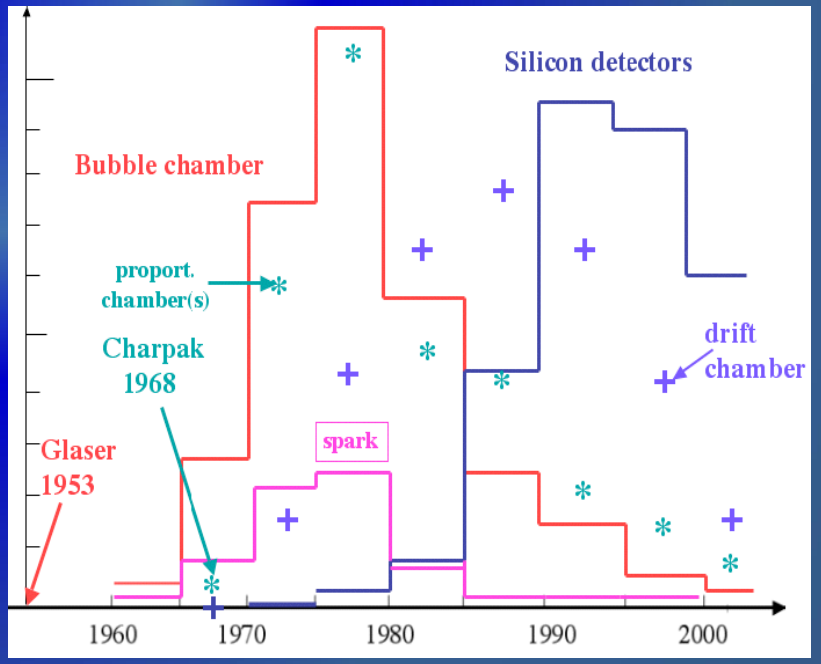

State-of-the-Art in Tracking and Vertex Detectors

Today's 3 major technologies of Tracking Detectors:

Silicon (strips, pixels, 3D, CMOS, monolithic):
→ electron – hole pairs in solid state material

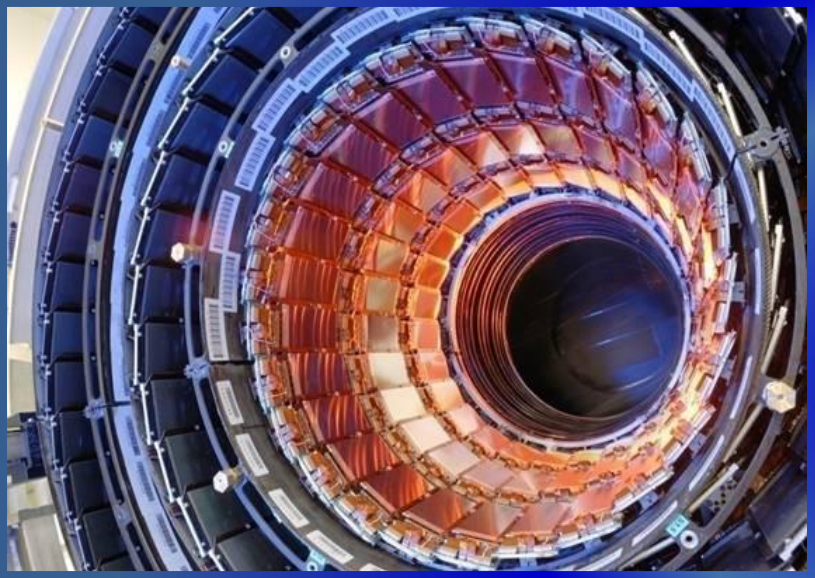

Gaseous (MWPC, TPC, RPC, MPGDs):
→ ionization in gas

Fiber Trackers: → scintillation light detected with photon detectors (sensitive to single electrons)

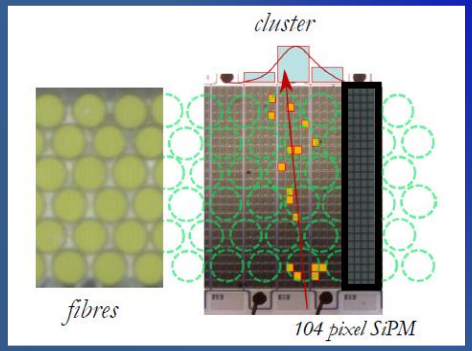

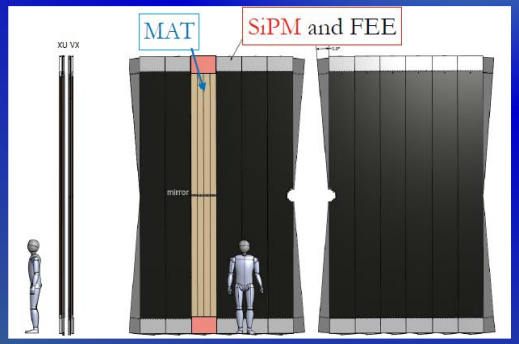

LHCb Tracker Upgrade (Sci-fibers with SiPM readout):

JINST

PUBLISHED BY IOP PUBLISHING FOR SISSA MEDIALAB

RECEIVED: June 12, 2020
ACCEPTED: June 28, 2020
PUBLISHED: October 22, 2020

INTERNATIONAL CONFERENCE ON INSTRUMENTATION FOR COLLIDING BEAM PHYSICS
NOVOSIBIRSK, RUSSIA
24–28 FEBRUARY, 2020

M. Titov, JINST15 C10023 (2020)

Next frontiers in particle physics detectors: INSTR2020 summary and a look into the future

M. Titov

Commissariat à l'Énergie Atomique et Énergies Alternatives (CEA) Saclay, DRF/IRFU/DPHP, 91191 Gif sur Yvette Cedex, France

E-mail: maxim.titov@cea.fr

Gaseous Detectors: Working Principle

- ✓ a charged particle passing through the gas ionizes a few gas molecules;
- ✓ the electric field in the gas volume transports the ionisation electrons and provokes multiplication;
- ✓ the movement of electrons and ions leads to induced currents in electrodes;
- ✓ the signals are processed and recorded.

Example:

- 10 GeV muon crossing
- Gas mixture: Ar/CO2 (80:20) %
- Electron are shown every 100 collisions, but have been tracked rigorously.
- Ions are not shown.

At the 100 µm – 1 mm scale:

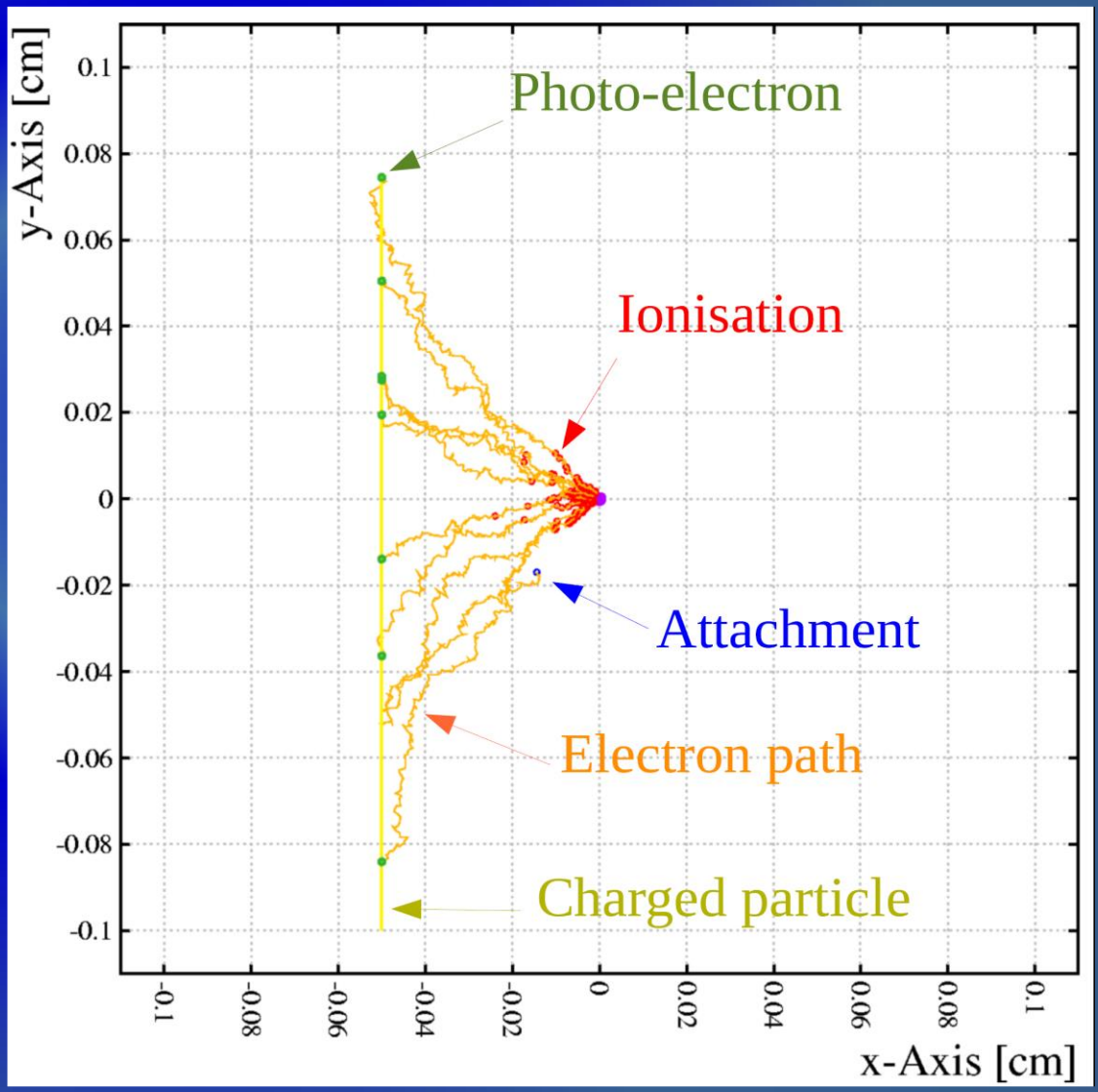

Gas Detectors: Why Use Gas as a Medium for Ionization ?

- ✓ Effectively quite light in terms of gm/cm^2, requirement for reducing multiple scattering in particle physics
- ✓ Few other technologies can easily realize detectors with as large a sensitive area as gas-filled devices
- ✓ Gas-filled detectors are relatively cheap in terms of $ per unit area/volume
- ✓ There are optimized gas mixtures for **charged particles detection** (high energy and nuclear physics), **X-rays** (synchrotron physics, astronomy) **and neutrons** (neutron scattering, national security)
- ✓ **Electron transport characteristics** are favorable and well characterized
- ✓ **Gas gain, *M*** (electron multiplication factor), can be achieved, over many orders of magnitude **(large dynamic range)**
- ✓ **Ionization collection or fluorescence** emission can **form the signal**

Gaseous Detectors: Signal Generation

- ✓ **Ionization statistics in gas**
- ✓ **Charge transport in gas**
  - a) Diffusion
  - b) Electron and ion mobility
  - c) Drift velocity
- ✓ **Loss of Electrons / Attachment**
- ✓ **Charge multiplication / Gas Amplification**

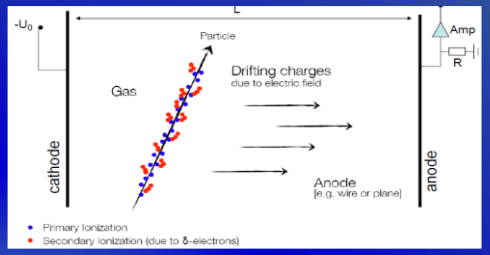

Gas	Density, mg cm^{-3}	E_x eV	E_I eV	W_I eV	$dE/dx\|_{min}$ keV cm^{-1}	N_P cm^{-1}	N_T cm^{-1}
H_2	0.084	10.8	13.6	37	0.34	5.2	9.2
He	0.179	19.8	24.6	41.3	0.32	3.5	8
Ne	0.839	16.7	21.6	37	1.45	13	40
Ar	1.66	11.6	15.7	26	2.53	25	97
Xe	5.495	8.4	12.1	22	6.87	41	312
CH_4	0.667	8.8	12.6	30	1.61	28	54
C_2H_6	1.26	8.2	11.5	26	2.91	48	112
iC_4H_{10}	2.49	6.5	10.6	26	5.67	90	220
CO_2	1.84	7.0	13.8	34	3.35	35	100
CF_4	3.78	10.0	16.0	35-52	6.38	52-63	120

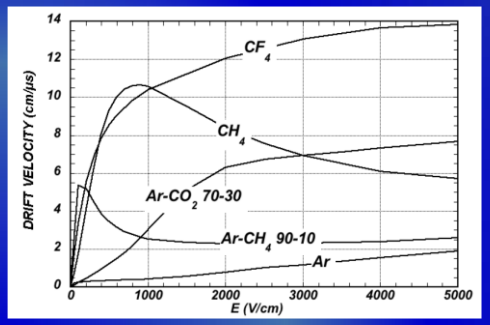

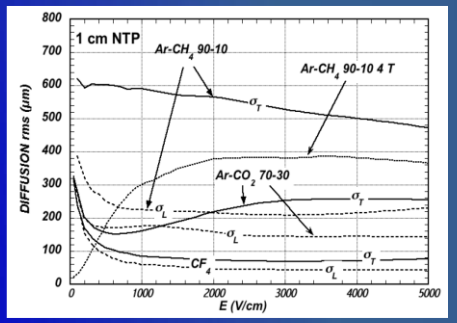

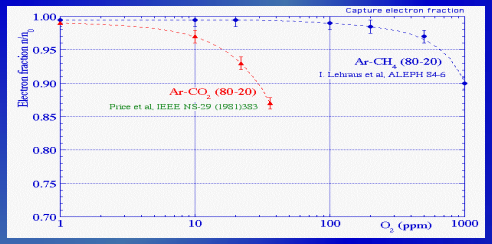

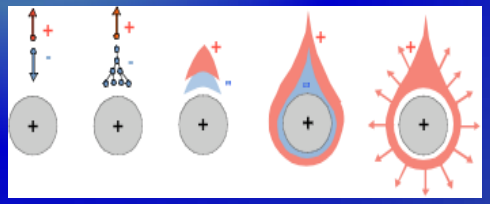

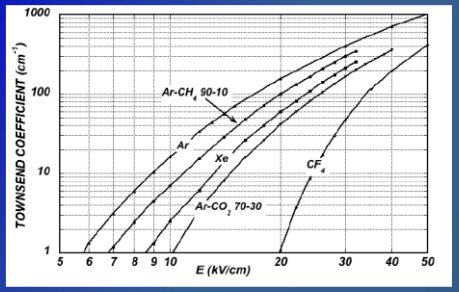

Efficient Gaseous Detector development *(energy deposit, electric fields, drift velocity & diffusion, attachment and amplification)* is today possible with *existing precise and reliable simulation tools*

Gaseous Detectors: Ionization Statistics (I)

TOTAL IONIZATION:

- Primary electron-ion pairs
  → Coulomb interactions of charged particles with molecules
  → typically ~ 30 primary ionization clusters /cm in gas at 1 bar
- Secondary ionization: clusters and delta-electrons → on average 90 electrons/cm in gas at 1 bar

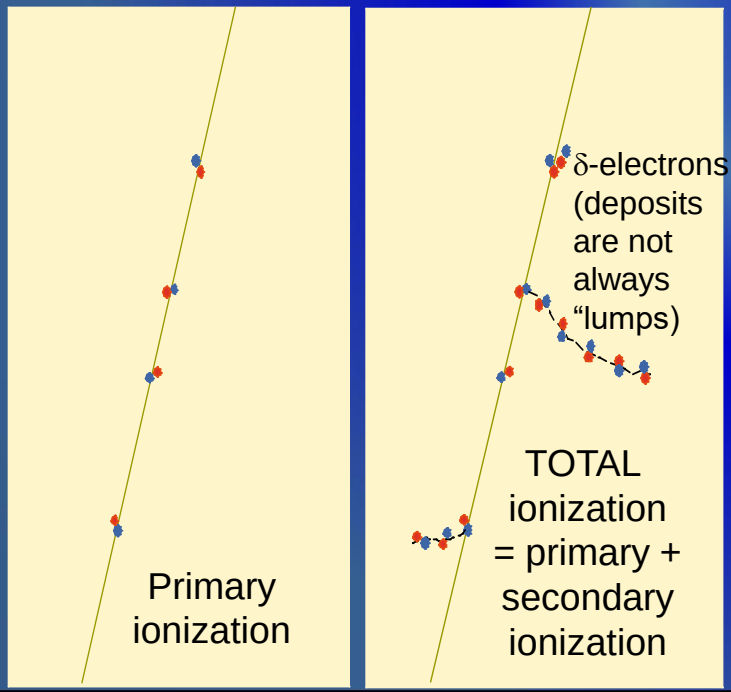

The actual number of primary electron/ion pairs (n_p) is Poisson distributed:

$$P(n_p, \langle n_p \rangle) = \frac{\langle n_p \rangle^{n_p} e^{-\langle n_p \rangle}}{n_p!}$$

σ_I : Ionization x-Section
n_e : Electron density
L : Thickness

$$\langle n_p \rangle = L/\lambda \qquad \lambda = 1/(n_e \sigma_I)$$

Number of primary electron/ion pairs in frequently used gases:

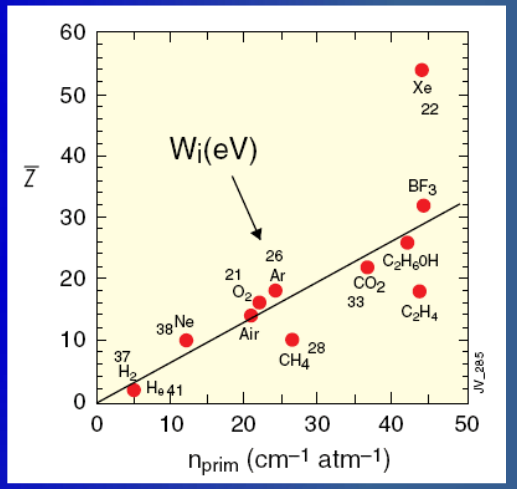

Detection efficiency of a perfect detector is limited to:

→ for thin (L) layers ε can be significantly lower than 1

$$\varepsilon = 1 - e^{-n_p}$$

$$\langle n_p \rangle = L/\lambda$$

GAS (STP)	thickness	ε (%)
Helium	1 mm	45
	2 mm	70
Argon	1 mm	91.8
	2 mm	99.3

Gaseous Detectors: Ionization Statistics (II)

Primary ionization

$$X + p \rightarrow X^+ + p + e^-$$

p = charge particle traversing the gas
X = gas atom
e^- = delta-electron (δ)

Secondary ionization

if E_δ is high enough ($E_\delta > E_i$)

$$X + e^- \rightarrow X^+ + e^- + e^-$$

Relevant Parameters
for gas detectors

Ionization energy	:	E_i
Average energy/ion pair	:	W_i
Average number of primary ion pairs [per cm]	:	n_p
Average number of ion pairs [per cm]	:	n_T

Differences due to δ-electrons

$$\langle n_T \rangle = \frac{L \cdot \langle \frac{dE}{dx} \rangle_i}{W_i}$$

[about 2-6 times n_p]
[L: layer thickness]

About 0:6% of released electrons in Ar have > 1keV energy → practical range is 70 um, contributing to coordinate meas. error

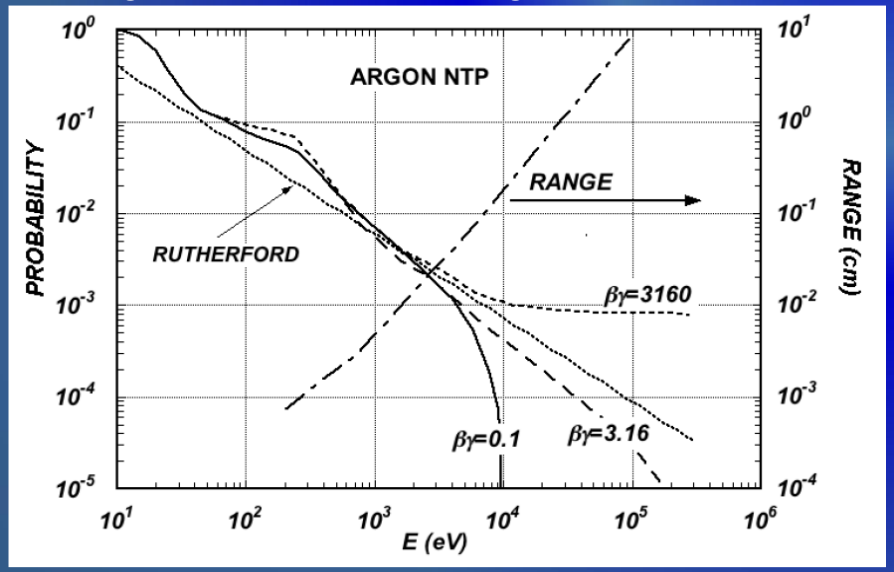

Total Ionization/Cluster Size Distribution:

Probabilities (%) to create N_{el} electrons (electrons are not evenly spaced, not even exponentially):

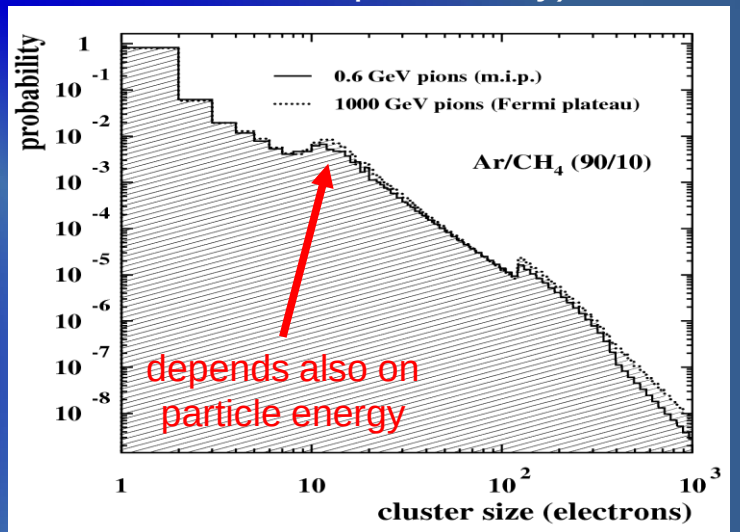

N_{el}	Ar	He
1	65.6	76.6
2	15.0	12.5
3	6.4	4.6
4	3.5	2.0
5	2.25	1.2
6	1.55	0.75
7	1.05	0.50
8	0.81	0.36
9	0.61	0.25
10	0.49	0.19

single el. →

multi el. cluster →

less multi-electron clusters at Helium (better!)

Ionization Statistics: Importance of PAI Model

- Every ionization process is a quantum mechanical transition initiated by the Coulomb field of the particle and the field created by neighbouring polarizable atoms; the average energy losses are described by the Bethe-Bloch formula with Sternheimer's density effect corrections;

- The fluctuations caused by Rutherford scattering on quasi-free electrons follow a Landau distribution and the influence of atomic shells is described by the photoabsorption ionization (PAI) model, which allows simulation of each energy transfer, with relaxation cascades and simulation of delta-electrons;

- Heed: a photo-absorption & ionization model:

Energy loss fluctuations
2 GeV protons on an (only !) 5 cm thick Ar gas layer:

Core formulae PAI model


Wade Allison


John Cobb

▶ Key: photo-absorption cross section $\sigma_\gamma(E)$

$$\frac{\beta^2\pi}{\alpha}\frac{d\sigma}{dE}=\frac{\sigma_\gamma(E)}{E}\log\left(\frac{1}{\sqrt{(1-\beta^2\epsilon_1)^2+\beta^4\epsilon_2^2}}\right)+$$ Relativistic rise

Cross section to transfer energy E

$$\frac{1}{N\hbar c}\left(\beta^2-\frac{\epsilon_1}{|\epsilon|^2}\right)\theta+$$ Черенков radiation

$$\frac{\sigma_\gamma(E)}{E}\log\left(\frac{2m_e c^2\beta^2}{E}\right)+$$ Resonance region

$$\frac{1}{E^2}\int_0^E\sigma_\gamma(E_1)\,dE_1$$ Rutherford scattering

With:

$$\epsilon_2(E)=\frac{N_e\hbar c}{EZ}\sigma_\gamma(E)$$

$$\epsilon_1(E)=1+\frac{2}{\pi}P\int_0^\infty\frac{x\,\epsilon_2(x)}{x^2-E^2}dx$$

$$\theta=\arg(1-\epsilon_1\beta^2+i\,\epsilon_2\beta^2)=\frac{\pi}{2}-\arctan\frac{1-\epsilon_1\beta^2}{\epsilon_2\beta^2}$$

Heed

▶ PAI model or absorption of real photons:

$Atom + \pi^- \rightarrow Ion^{+*} + \pi^- + e^-$	(photo-electric effect,
$Atom + \gamma \rightarrow Ion^{+*} + e^-$	real or virtual photon)

▶ Decay of excited states:

$Ion^{+*} \rightarrow Ion^{++} + e^-$	(Auger)
$Ion^{+*} \rightarrow Ion^{+} + \gamma$	(fluorescence)
$Ion^{+*} \rightarrow Ion^{+*}$	(Coster-Kronig)

▶ Processing of electrons:
- ▶ below ionisation energy — transport
- ▶ photo- & Auger-electrons — (clusters, "δ-electrons"):

$e^- + Atom \rightarrow Ion^+ + 2\,e^-$ (absorption of high-energy electrons)


Igor Smirnov

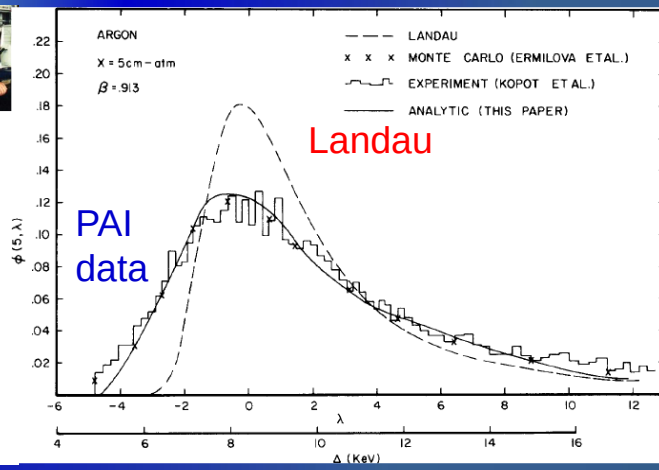

✓ Importance of PAI model (all terms in formula are important):
All electron orbitals (shells) participate:
→ outer shells: frequent interactions, few electrons;
→ inner shells: few interactions, many electrons.

Ionization Statistics: Table for Most Common Gases

F. Sauli, M. Titov,
Review of Particle Physics,
Particle Data Group (2022)

Table 35.1: Properties of noble and molecular gases at normal temperature and pressure (NTP: 20° C, one atm). E_X, E_I: first excitation, ionization energy; W_I: average energy for creation of ion pair; $dE/dx|_{\rm min}$, N_P, N_T: differential energy loss, primary and total number of electron-ion pairs per cm, for unit charge minimum ionizing particles. Values often differ, depending on the source, and those in the table should be taken only as approximate.

Gas	Density, mg cm^{-3}	E_x eV	E_I eV	W_I eV	$dE/dx\|_{\rm min}$ keV cm^{-1}	N_P cm^{-1}	N_T cm^{-1}
H_2	0.084	10.8	13.6	37	0.34	5.2	9.2
He	0.179	19.8	24.6	41.3	0.32	3.5	8
Ne	0.839	16.7	21.6	37	1.45	13	40
Ar	1.66	11.6	15.7	26	2.53	25	97
Xe	5.495	8.4	12.1	22	6.87	41	312
CH_4	0.667	8.8	12.6	30	1.61	28	54
C_2H_6	1.26	8.2	11.5	26	2.91	48	112
iC_4H_{10}	2.49	6.5	10.6	26	5.67	90	220
CO_2	1.84	7.0	13.8	34	3.35	35	100
CF_4	3.78	10.0	16.0	35-52	6.38	52-63	120

Ar/CO_2 (70/30):

$$N_P = 25 \cdot 0.7 + 35 \cdot 0.3 = 28 \frac{\text{pairs}}{\text{cm}}; \quad N_T = \frac{2530}{26} \cdot 0.7 + \frac{3350}{35} \cdot 0.3 \approx 97 \frac{\text{pairs}}{\text{cm}}.$$

N_T ~ 100 e-ion pairs during ionization process (typical number for 1 cm of gas) is not easy to detect → typical noise of modern pixel ASICs is ~ 100e- (ENC)

Need to increase number of e-ion pairs → … ☹ … how ??? → GAS AMPLIFICATION

Transport of Electrons in Gases: Drift Velocity

Electron transport theory =
BALANCE BETWEEN ENERGY ACQUIRED FROM THE FIELD AND COLLISION LOSSES

Electrons are completely 'randomized' in each collision. The actual drift velocity v along the electric field is quite different from the average velocity u of the electrons i.e. → about 100 times smaller.

The velocities v and u are determined by the atomic cross section $\sigma(\varepsilon)$ and the fractional energy loss $\Delta(\varepsilon)$ per collision (N is the gas density i.e. number of gas atoms/m^3, m is the electron mass.):

$$v = \sqrt{\frac{eE}{mN\sigma}}\sqrt{\frac{\Delta}{2}}$$

$$u = \sqrt{\frac{eE}{mN\sigma}}\sqrt{\frac{2}{\Delta}}$$

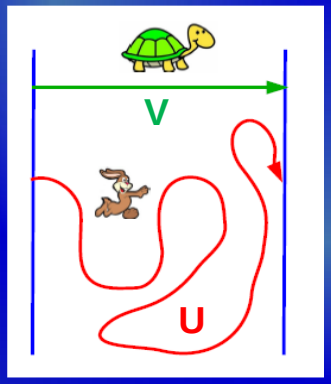

Because $\sigma(\varepsilon)$ und $\Delta(\varepsilon)$ show a strong dependence on the electron energy in the typical electric fields, the electron drift velocity v shows a strong and complex variation with the applied electric field.

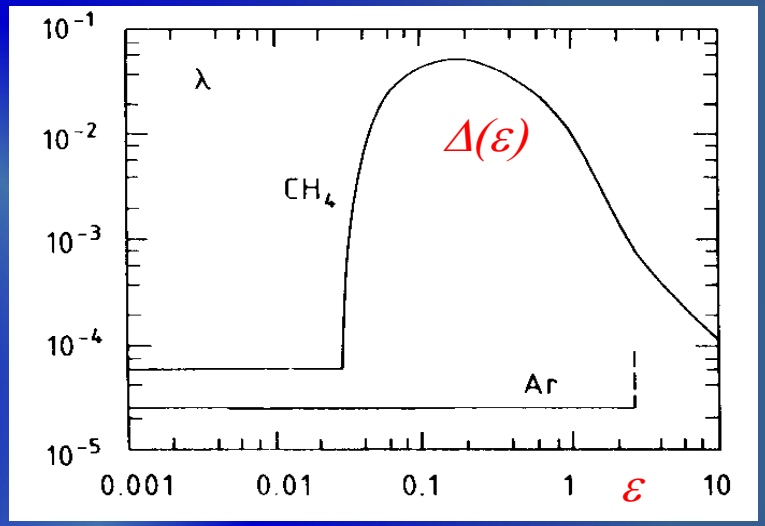

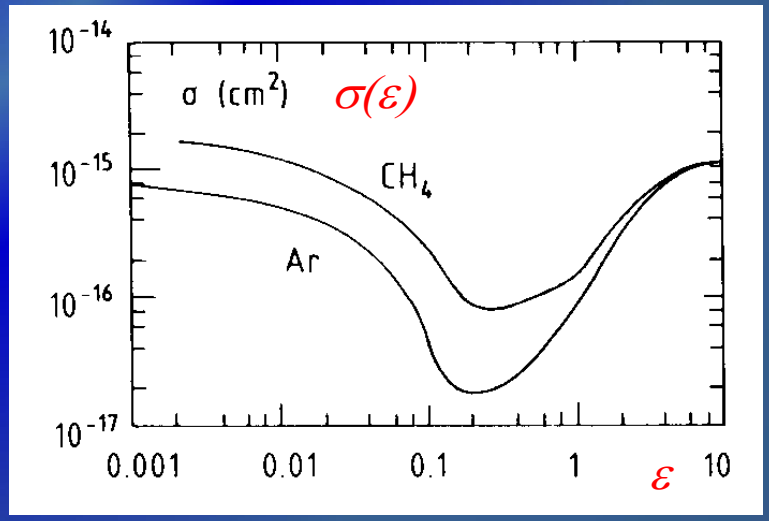

Transport of Electrons in Gases: Drift Velocity

CHARGE TRANSPORT DETERMINED BY ELECTRON-MOLECULE CROSS SECTION:

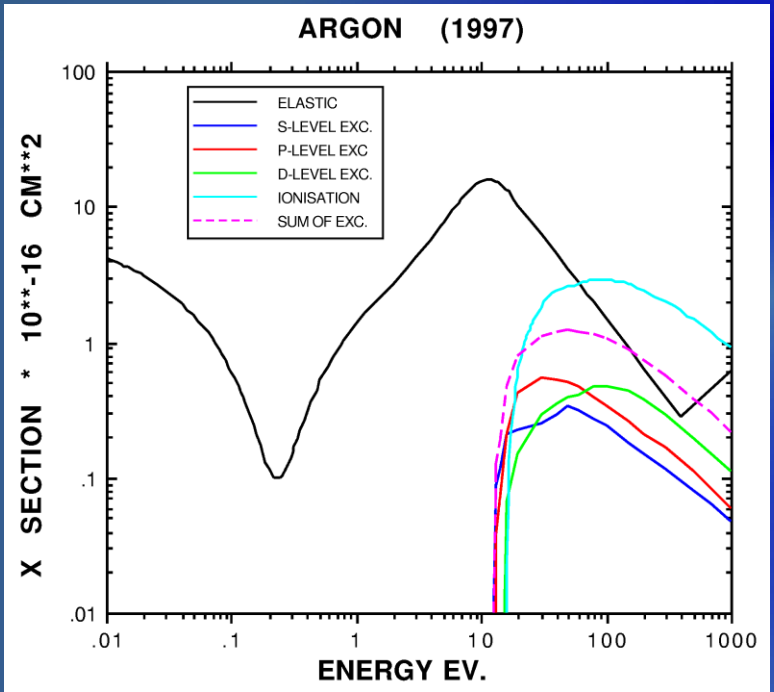

- CO_2 is linear:
  - O – C – O
- Vibration modes are numbered V(*ijk*)
  - *i*: symmetric,
  - *j*: bending,
  - *k*: anti-symmetric.

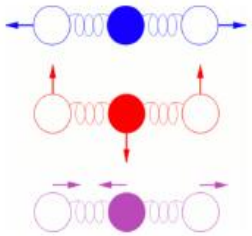

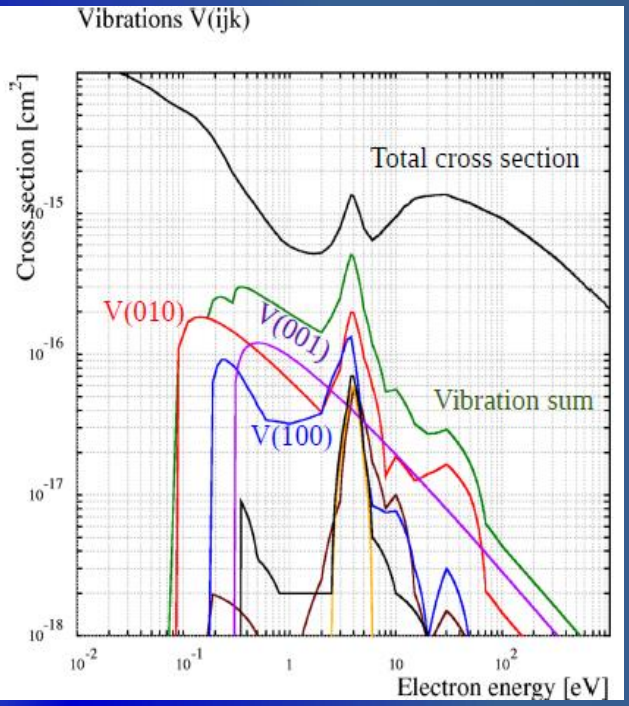

Magboltz: microscopic e⁻ transport

- A large number of cross sections for 60 molecules...
  - Numerous organic gases, additives, *e.g.* CO_2:
    - elastic scattering,
    - 44 inelastic cross sections (5 vibrations and 30 rotations + super-elastic and 9 polyads),
    - attachment,
    - 6 excited states and
    - 3 ionisations.
  - noble gases (He, Ne, Ar, Kr, Xe):
    - elastic scattering,
    - 44 excited states and
    - 7 ionisations.

LXcat (pronounced *elecscat*) is an open-access website for collecting, displaying, and downloading ELECtron SCATtering cross sections and swarm parameters (mobility, diffusion coefficient, reaction rates, etc.) required for modeling low temperature plasmas. [...]"

Lxcat:
http://www.lxcat.laplace.univ-tlse.fr/]

Magboltz:
S. Biagi, Nucl. Instr. and Meth. A421 (1999) 234
http://magboltz.web.cern.ch/magboltz/

Transport of Electrons in Gases: Drift Velocity

Large drift velocities are achieved by adding polyatomic gases (usually hydrocarbons, CO2, CF4) having large inelastic component at moderate energies of a few eV → electron ”cooling” into the energy range of the Ramsauer-Townsend minimum (at ~0.5 eV) of the elastic cross-section.

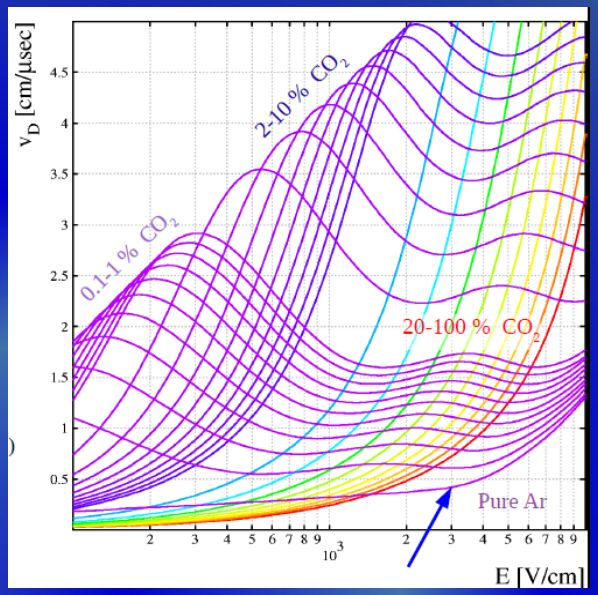

Even small addition of CO2 to Ar makes gas dramatically fster

Additives like CO2 & hydrocarbons are called “quenchers” or “admixtures”

Large range of drift velocities in gases: 1 .... 10 cm/μs; typical categories:

- ✓ “slow” gases, e.g. Ar/CO2 mixtures 1-2 cm/μs, almost linear dependence on E-field
- ✓ “fast” gases, e.g. Ar/CF4 mixtures ~10-15 cm/μs
- ✓ “saturated” gases, e.g. Ar/CH4; - e.g. Ar/CH4 (90/10) – drift velocity less sensitive to E-field variations and nearly constant (useful for drift chamber operation)

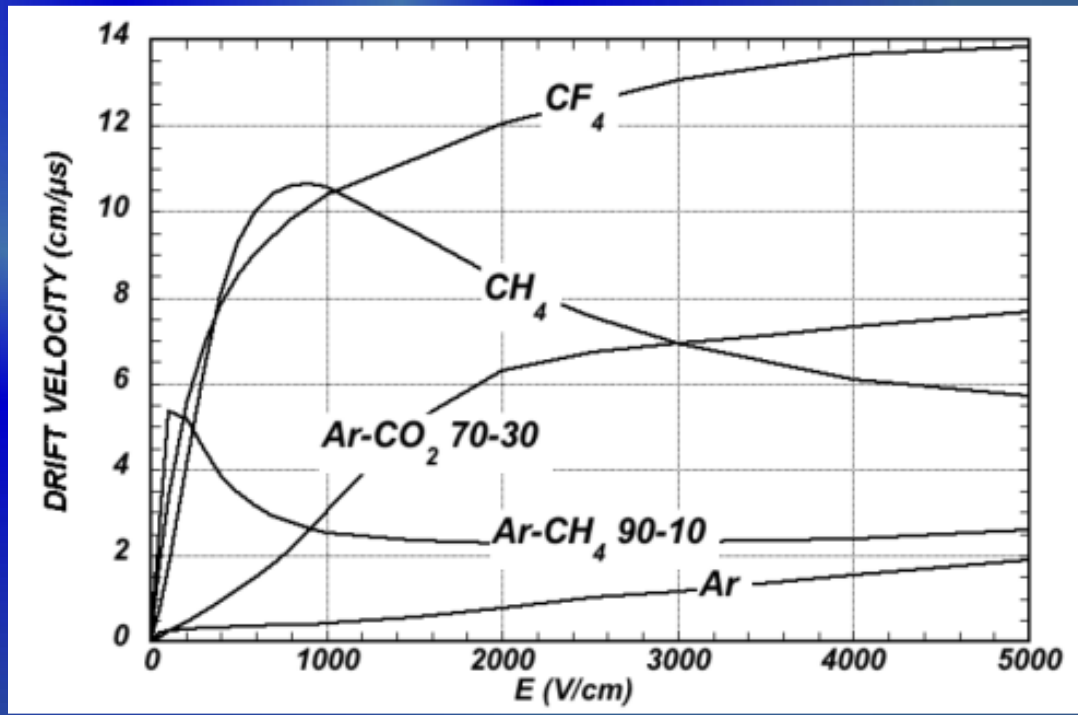

Selection of Gas Mixture: Quenching of Photons

- **Slight problem in gas avalanche**

→ Argon atoms can be ionized but also can be brought into excited states

→ Exited Argon atoms can only de-exite by emission of high-UV photons

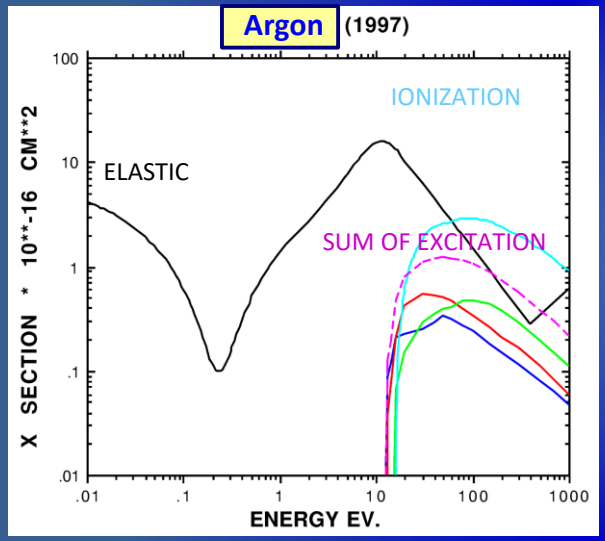

consequence: UV photons (>11.6 eV) hit surface of metals (cathode) and free new electrons, ionization energy of Cu = 7.7 eV

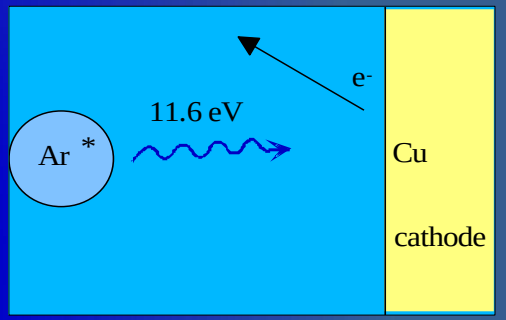

VERY unstable operation

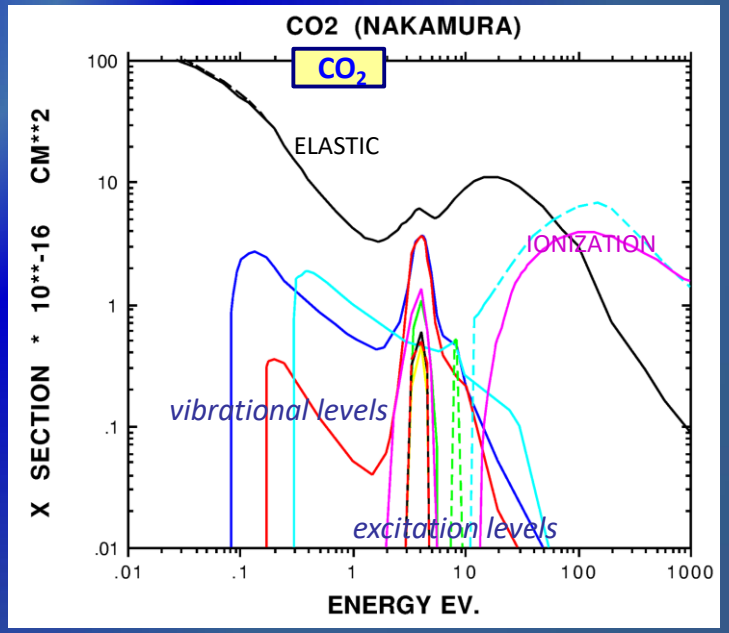

- **Solution**

→ Add gases with many vibrational and rotational energy levels: CO_2, CH_4

→ Absorption of UV photons over a wide energy range; dissipation by collisions or dissociation into smaller molecules (see aging effects)

Transport of Electrons in Gases: Diffusion

An initially point like cloud of electrons will 'diffuse' because of multiple collisions and assume a Gaussian shape. The diffusion depends on the average energy of the electrons. The variance σ^2 of the distribution grows linearly with time. In case of an applied electric field it grows linearly with the distance.

$$n(x) = \left(\frac{1}{\sqrt{4\pi Dt}}\right)^3 e^{\frac{-(x-v_D t)^2}{4Dt}}$$

$$v_D = \frac{\Delta s}{\Delta t} \qquad \sigma_x = \sqrt{2Dt} = \sqrt{2D\frac{s}{v_D}}$$

Solution of the diffusion equation (l=drift distance)

$$D = \frac{2}{3}\frac{v}{eE}\epsilon \qquad \sigma_x = \sqrt{\frac{4}{3}\frac{l}{eE}\epsilon}$$

'Cold' gases are close to the thermodynamic limit i.e. gases where the average microscopic energy ε=1/2mu2 is close to the thermal energy 3/2kT.

CH_4 has very large fractional energy loss → low ε → low diffusion.

Argon has small fractional energy loss/collision → large ε → large diffusion.

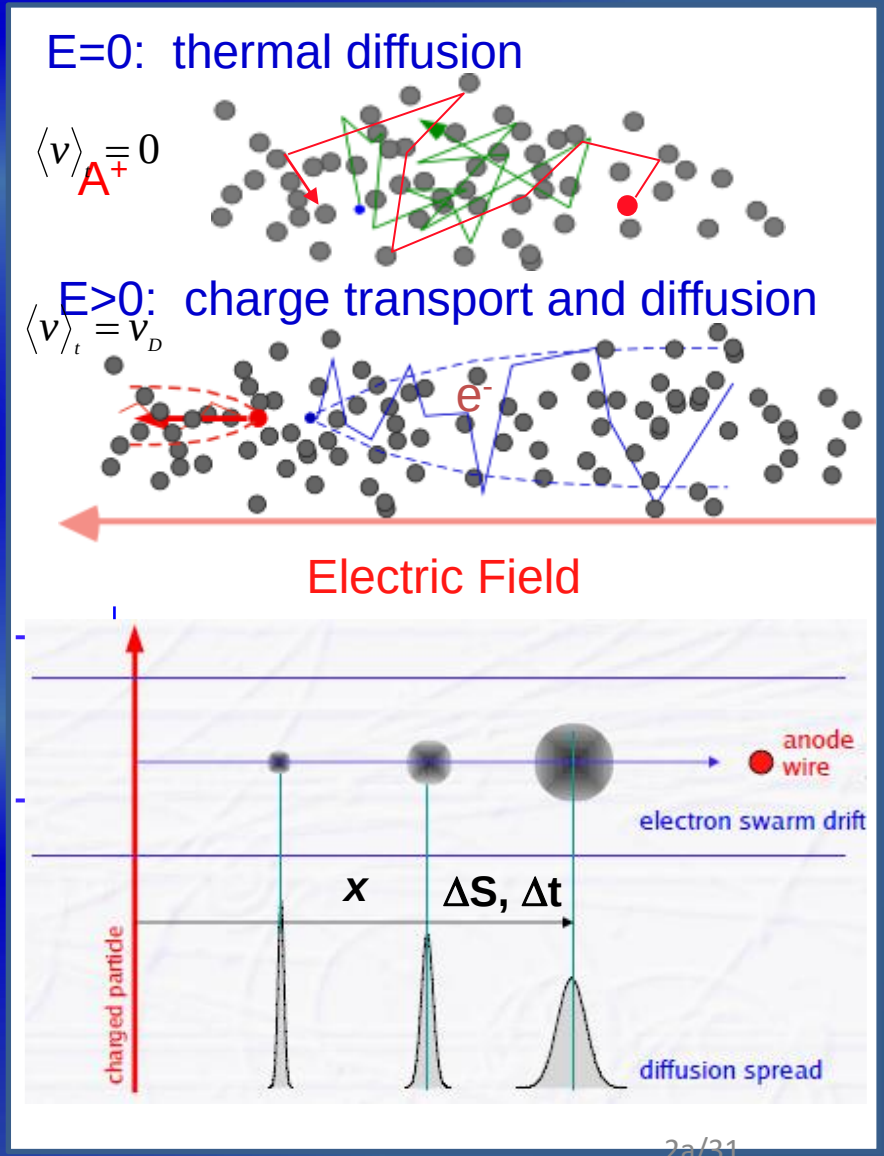

Transport of Electrons in Gases: Diffusion

Electric field alters the diffusion so that it is necessary to introduce two diffusion coefficients: longitudinal diffusion (σ_L) and transverse diffusion (σ_T)

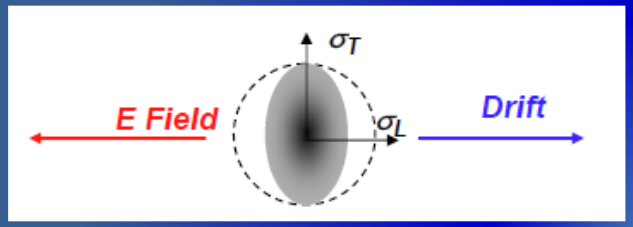

- ✓ CO_2 is much cooler gas than CH_4 at low electric fields → allows to optimize separately diffusion properties in the drift and multiplication regions (but, CH4 is much better quencher than CO2)

- ✓ CF4 has the largest drift velocity
- ✓ & lowest electron diffusion among known gases due to the sizeable Ramsauer-Townsend dip in the elastic cross-section which coincides with a very large vibrational modes (but, CF4 has a small quenching cross-section of excited Ar states and emits light from the far UV to the visible light)

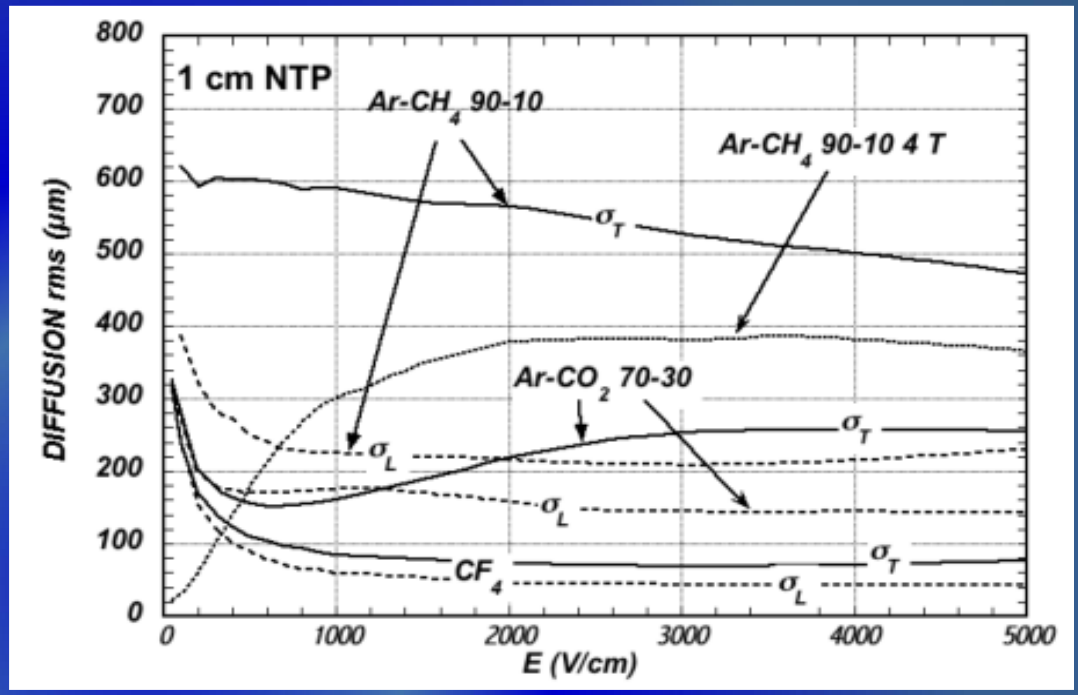

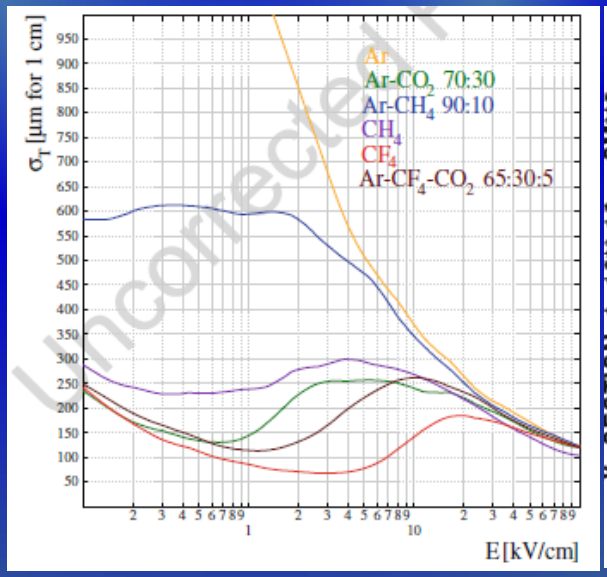

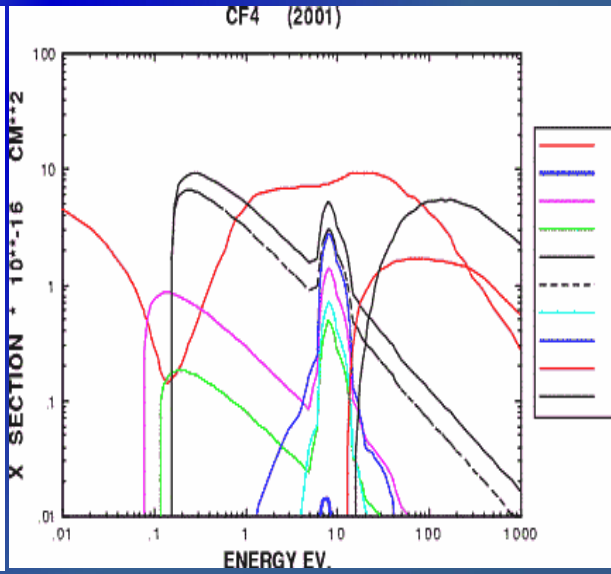

Electron Drift in Presence of Electric and Magnetic Fields

Equation of motion of free charge carriers in presence of E and B fields:

$$m\frac{d\vec{v}}{dt} = e\vec{E} + e(\vec{v}\times\vec{B}) + \vec{Q}(t)$$

where $\vec{Q}(t)$ stochastic force resulting from collisions

Time averaged solutions with assumptions: $\vec{v}_D = \langle\vec{v}\rangle = const.$ $< \vec{Q}(t) >= \frac{m}{\tau}\vec{v}_D$ friction force

$$\left\langle\frac{d\vec{v}}{dt}\right\rangle = 0 = e\vec{E} + e(\vec{v}_D\times\vec{B}) - \frac{m}{\tau}\vec{v}_D$$

τ mean time between collisions

$$\vec{v}_D = \frac{\mu|\vec{E}|}{1+\omega^2\tau^2}\left[\hat{E} + \omega\tau(\hat{E}\times\hat{B}) + \omega^2\tau^2(\hat{E}\cdot\hat{B})\hat{B}\right]$$

$\mu = \frac{e\tau}{m}$ mobility $\omega = \frac{eB}{m}$ cyclotron frequency

More precise calculation is available in Magboltz, which computes drift velocity by tracing electrons at the microscopic level through numerous collisions with gas molecules

$$\vec{E}\parallel\vec{B}\quad \sigma_L = \sigma_0 \quad \sigma_T = \frac{\sigma_0}{\sqrt{1+\omega^2\tau^2}}$$

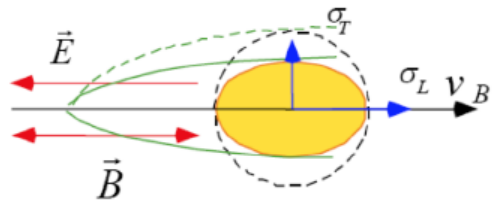

E.g.: $\omega\tau$ ~ 20 for Ar/CF4/iC4H10 (95:3:2)

This reduction iis exploited to substantially improve spatial resolution in the Drift and TPC Chambers

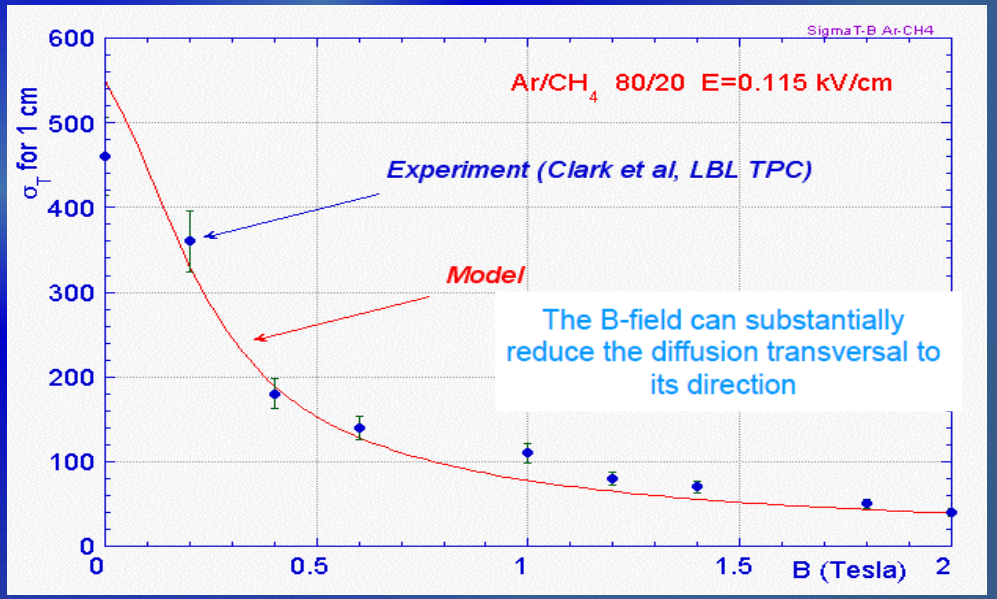

Electron Capture Losses for Electronegative Gases (Attachment)

- ✓ Some quencher gases can attach electrons
- ✓ Energy-momentum conservation: **3-body or dissociation**
- ✓ **The attachment cross section is energy-dependent**, therefore strongly depends on the gas composition and electric field

Attachmant coefficient of oxygen:

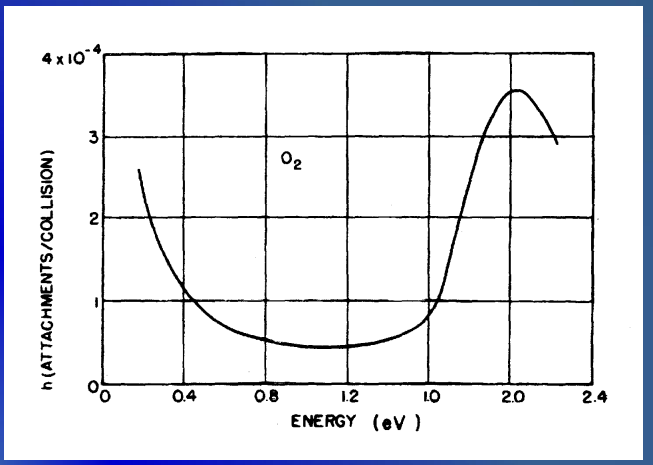

Examples:

- O_2: mostly 3-body O_2^- and at higher ϵ 2-body dissociative;
- H_2O: $[H_2O]_n$ has positive electron affinity, H_2O probably not;
- CF_4: mostly dissociative $F^- + CF_3$, $F + CF_3^-$ (below 10 eV);
- SF_6: $SF_6^{-*} < 0.1$ eV, $\sigma = 10^{-18}$ cm^2, then $F^- + SF_n^-$ (n=3, 4, 5)
- CS_2: negative ion TPC;
- CO_2: O^-, $[CO_2]_n^-$ but no CO_2^- (4 eV and 8.2 eV).

Electrons surviving after 20 cm drift (E = 200 V/cm):

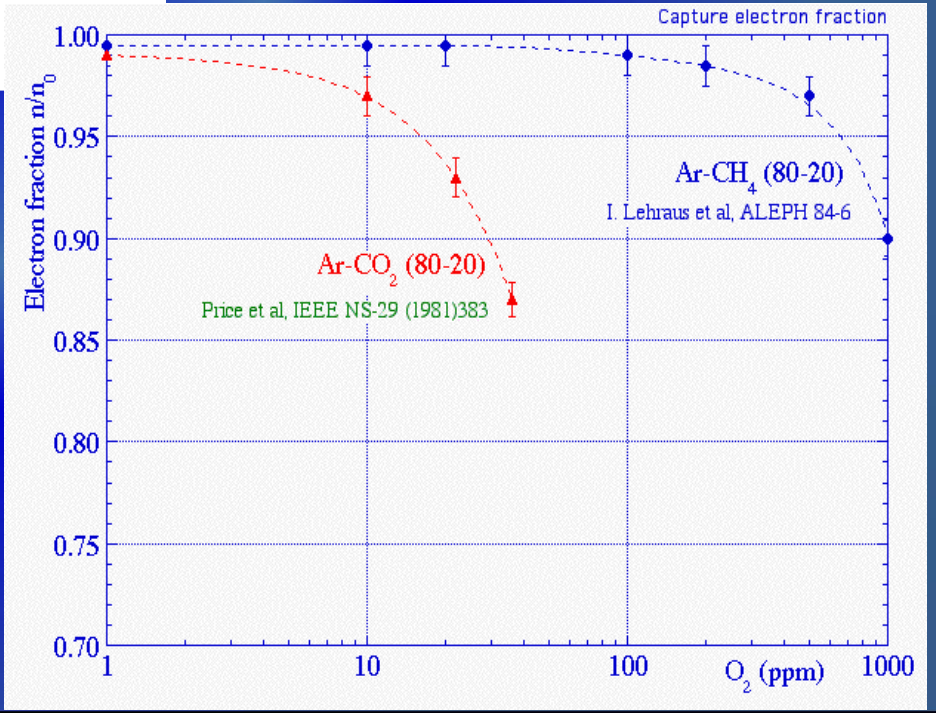

Certain quenchers as CO2 can significantly enhance the effect of oxygen → large uncrease in attachment

- CO_2 has a tiny attachment cross section at low energy.
- The 4 eV peak is linked to a short-lived $^2\Pi_u$ shape resonance which decays $e^- CO_2 \rightarrow CO + O^-$;

[A. Moradmand et al. (2013) 10.1103/PhysRevA.88.032703]

- The 8.2 eV peak is thought to be a Feshbach resonance.

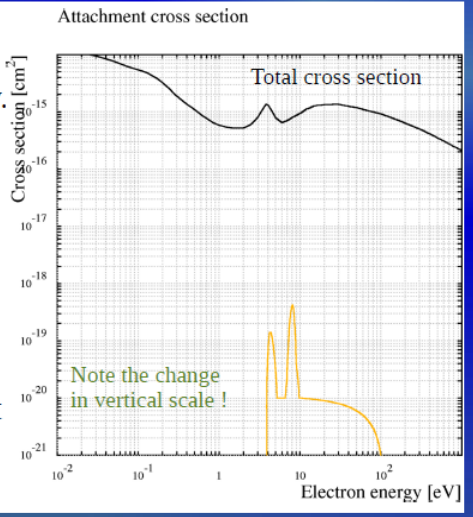

Transport of Ions in Gases: Drift and Diffusion

Signals in Wire Chambers, Micromegas are generated by ion movement

Drift velocity of ions

is almost linear function of E $v_D^{ion} = \mu^{ion} E$

Mobility: $\mu^{ion} = \frac{e\tau}{m}$ is

constant for given gas at fixed P and T, direct consequence of the fact that average energy of ion is unchanged up to very high E fields.

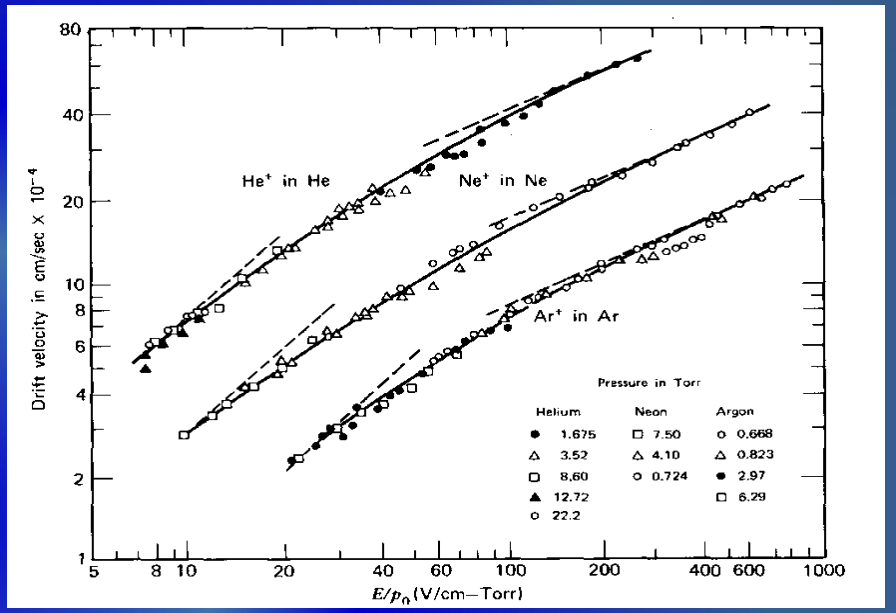

Diffusion of ions

IONS DIFFUSION (Einstein's law):

$\frac{D}{\mu} = \frac{KT}{e}$ $\sigma_x = \sqrt{2Dt}$ $\sigma_x = \sqrt{\frac{2KT}{e}\frac{x}{E}}$

Linear diffusion is independent of the nature of ions and gas → thermal limit (same for all gases)

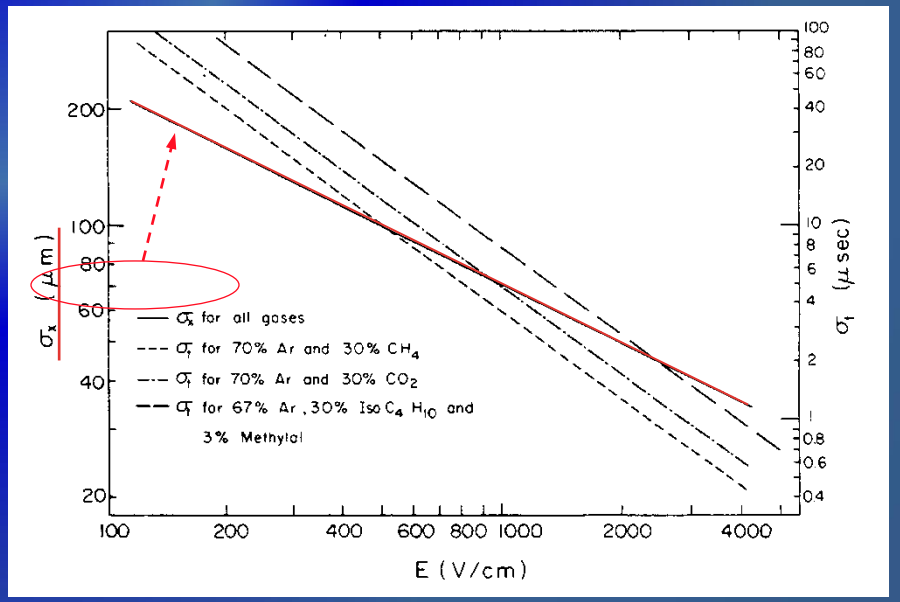

It has been historically assumed that, due to a very effective charge transfer mechanism, only ions with the lowest ionization potential survive after a short path in the mixture → NOT TRUE !!!

Transport of Ions in Gases: Drift and Diffusion

Recent experimental data suggests that the signal ions, in e.g. CO2-quenched mixtures of Ar and Ne are CO+2 · (CO2)*n* cluster ions, and not CO+2 or noble gas ions

Principal reactions involving CO_2

- Ar^+: charge exchange, $\tau \approx 0.85$ ns
  - $Ar^+ + CO_2 \rightarrow Ar + CO_2^+$
- Ne^+: charge transfer in 2-steps, $\tau \approx 8$ ns
  - $Ne^+ + CO_2 \rightarrow Ne + CO^+ + O$
  - $CO^+ + CO_2 \rightarrow CO + CO_2^+$
- CO_2: 3-body association, 7-20 ps
  - $CO_2^+ + 2CO_2 \rightarrow CO_2^+ \bullet CO_2 + CO_2$

Reaction dynamics in Ar CO_2

- Reactions:
  - $Ar^+ + CO_2 \rightarrow Ar + CO_2^+$
  - $CO_2^+ + 2CO_2 \rightarrow CO_2^+ \bullet CO_2 + CO_2$
  - $Ar^+ + 2Ar \rightarrow Ar^+ \bullet Ar + Ar$
- Parameters:
  - p = 1 bar
  - mix: 90 % Ar + 10 % CO_2

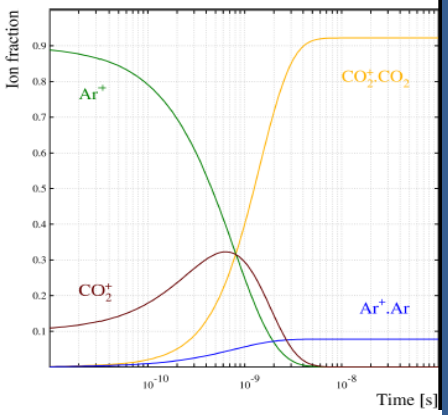

R. Veenhof, private communications
Y. Kalkan, JINST 10, 07, P07004 (2015)

Life cycle of $CO_2^+ \bullet (CO_2)_n$

- $CO_2^+ \bullet CO_2$ has a dissociation energy of 0.6 eV
  - far above thermal energies at 1 bar (35 meV);
  - it is a long-lived cluster – calculated lifetime = 5 ns.

  [B.M. Smirnov, "Cluster Ions and Van Der Waals Molecules," CRC press]
- This is much longer than the formation time τ = 7-20 ps via 3-body association in 10 % CO_2 with Ar + CO_2 as "helpers".
- Hence, any isolated CO_2^+ rapidly binds again.
- $CO_2^+ \bullet (CO_2)_n$ probably lives shorter but will recombine. The cluster size n will therefore fluctuate at the ns time scale.

Summary ions

- Avalanches ionise the constituent gases, and the initial ions undergo a staggering sequence of reactions.
  - In Ar-CO_2 and Ne-CO_2 mixtures, the signal ions are $CO_2^+ \bullet (CO_2)_n$ clusters, which are slower than CO_2^+;
  - water forms larger clusters, further reducing the mobility;
  - pure noble gases form dimers, Ar_2^+, Ne_2^+ which are faster than Ar^+ and Ne^+ due to resonant charge exchange;
  - Xe forms dimers, trimers and probably bigger objects;
  - alkanes combine to form heavier molecules.

Since the cluster ions are slower than the initial ions, the signals induced by ion motion in Micromegas or TPC might be altered (also lead to larger space-charge effect in gas vomule)

Gaseous Detectors: Software and Simulation Tools

Garfield, together with HEED, Degrad, Magboltz, SRIM, ANSYS, COMSOL, and neBEM software packages represent the core simulation tools for microscopic modelling of gaseous detector response.

Monte Carlo approach – a way out ?

- Analytic models are precious for the insight they afford.
- But the complexity of real gases and detectors make realistic models unwieldy:
  - inelastic collisions (vibrations, rotations, polyads);
  - excitations and Penning transfers;
  - ionisation;
  - attachment;
  - intricate, position-dependent *E* and *B* fields.
- Predictions for experiments are more practical using a Monte Carlo approach, here based on Magboltz.

- ✓ ***HEED** – energy loss, a photo-absorption and ionization model*
- ✓ ***DEGRAD** – electron transport, cluster size distribution*
- ✓ ***Magboltz** – electron transport properties: drift, diffusion, multiplication, attachment*
- ✓ ***ANSYS, COMSOL, neBEM** – electric field maps in 2D / 3D*
- ✓ ***Garfield** – fiedls, drift properties, signals (interfaced to above)*

Some recent highlights:

- ***Garfield++ et al.** (new development and maintenance of codes, documentation, examples)*
- *Garfield++ and delayed weighting fields in the calculation of the induced signal (resistive electrodes)*
- ***Greenhouse gases***
- ***Improving accuracy of the modelling and the detector physics understanding:** Penning transfer, Non equilibrium effect in gaseous detectors, Ions and cluster ions*

Electric Fields: (nearly) Exact Boundary Element Method

*, **neBEM** Field Solver (that solves the Poisson equation to obtain electric field throughout the device volume) is an integrated part of device simulation. One such Green function based solver (nearly exact Boundary Element Method), is integrated to GARFIELD since 2009.*

Merits of neBEM:

- Analytic integration of influence of charge distributed over small rectangular / triangular boundary elements (new formulation). Very precise potential and electric field values are obtained for any 2D / 3D geometry.
- Competitively accurate w.r.t any other commercial FEM / BEM package.
- Primitive geometry modeling.
- Parallelized using OpenMP.
- Field maps and reduced order modeling crudely implemented.
- Preliminary implementation of space charge and charging up simulations.

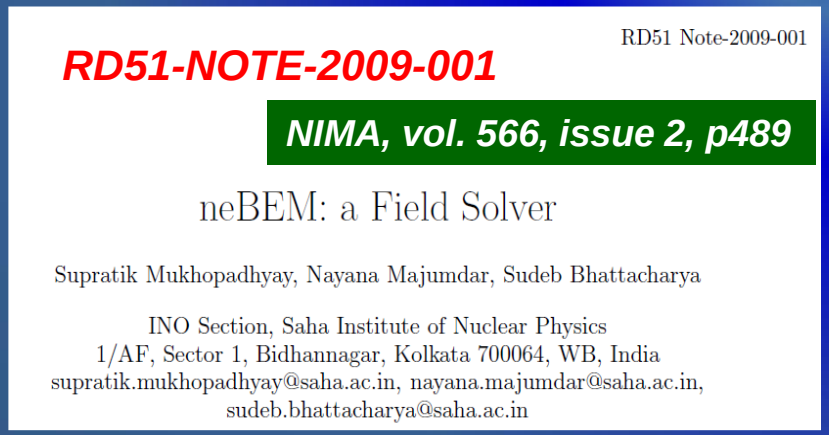
RD51 Note-2009-001

RD51-NOTE-2009-001

NIMA, vol. 566, issue 2, p489

neBEM: a Field Solver

Supratik Mukhopadhyay, Nayana Majumdar, Sudeb Bhattacharya

INO Section, Saha Institute of Nuclear Physics
1/AF, Sector 1, Bidhannagar, Kolkata 700064, WB, India
supratik.mukhopadhyay@saha.ac.in, nayana.majumdar@saha.ac.in,
sudeb.bhattacharya@saha.ac.in

http://nebem.web.cern.ch/nebem

(Supratik Mukhopadhay, Nayana Majumdar)

Maintained and updated by SINP (independent release till 05 Mar 2019, version 1.9.04; Since 2019, released along with Garfield++)

Future projects for neBEM:

- Orders of magnitude improvement in speed is possible:
  - FMM / GMRES or similar algorithms.
  - Better parallelization (OpenMP, GPU)
  - Smaller data storage and faster flow.
- Improvements in geometry modeler, surface mesh generation, adaptive mesh.
- Space charge and charging up simulation to be improved significantly. Charge transport through dielectrics is another important area to be explored.
- Graphical user interface.

Garfield ++ Package: Software Simulation and Tools

Garfield++ Installation Examples Documentation

Garfield++

Heinrich Schindler, Rob Veenhof

About

Garfield++ is a toolkit for the detailed simulation of particle detectors based on ionisation measurement in gases and semiconductors. The main
with the Garfield program. The main differences are the more up-to-date treatment of electron transport, the possibility to simulate silicon sens

More...

Support of Garfield++ package (maintenance and new developments)- *a unique software package for microscopic modeling of small-scale structures -*

Getting started

- Installation
- Examples
- Documentation (User Guide, Doxygen, FAQ)

Support

- If you have any questions, please send a mail to garfield-support@cern.ch (or contact Heinrich Schindler or Rob Veenhof directly).
- To receive (infrequent) announcements about updates of the code, please subscribe to the mailing list garfield-users@cern.ch on E-Gr
- Issues can be reported on JIRA or GitLab.

Related calculations

- Modelling of avalanches and streamers with COMSOL.

Examples

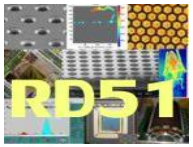

Tutorials

First steps

- Simulating a drift tube: gas tables, analytic fields, Runge-Kutta-Fehlberg integration of drift lines, signals
- Simulating a GEM: finite element model, microscopic tracking of electrons
- Simulating a silicon sensor: user-parameterized fields, strip/pixel weighting fields, Monte Carlo integration of drift lines, signals
- Simulating a Resistive Plate Chamber

Primary ionization

- Simulating charged-particle tracks using Heed.
- ing ion tracks using tables computed with SRIM or the TRIM interface.

Transport properties

- Generating gas tables and dealing with gas files.
- Penning transfer.
- Cross-sections used by Magboltz.

Electric fields

- Importing finite-element field maps calculated using
  - Elmer and Gmsh,
  - ANSYS, for two-dimensional and three-dimensional problems,
  - COMSOL,
  - CST.
- Importing TCAD field maps.
- Computation of electric fields using the nearly exact Boundary Element Method (neBEM).

Signals

- Weighting fields and induced currents

Applications

Micropattern gas detectors

- Movies of avalanches in a single GEM
- of avalanches in a triple GEM
- in a triple GEM
- ging up of a GEM
- on detection with a Thick GEM
- energy pion detection with a Micromegas
- facing with Geant4

ambers

lation of the ALICE TPC

IS

troluminescence

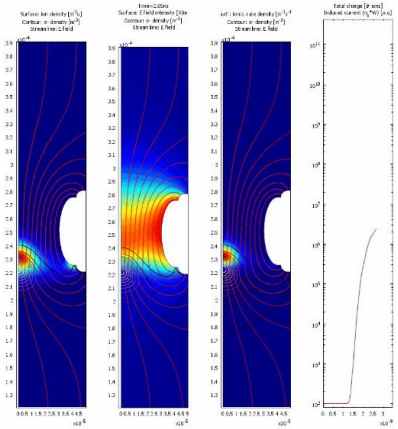

Gas properties

- Paschen curves

Gitlab Repository

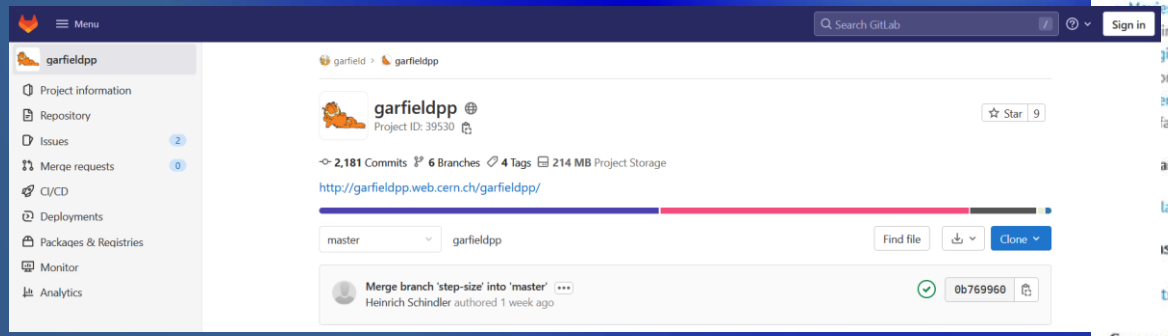

https://gitlab.cern.ch/garfield/garfieldpp

Signal Formation in Detectors with Resistive Elements

RD51 supports *ongoing efforts on* ***interfacing between different modeling tools –*** *to address properly involved processes at the microscopic level -* ***extending present simulation framework to other gaseous & Si-detectors***

EP R&D SEMINAR, Signal formation in detectors with resistive elements by **Djunes Janssens:** https://indico.cern.ch/event/1167590/contributions/4903447/attachments/2460899/4219187/EPSeminar_DjunesJanssens.pdf

Garfield++ and COMSOL to model the signal formation in detectors with resistive elements by applying an extended form of the Ramo-Shockley theorem

Gaseous (MPGD, RPC,..)

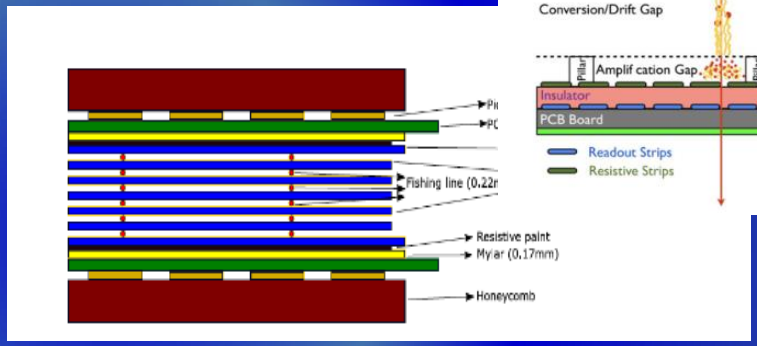

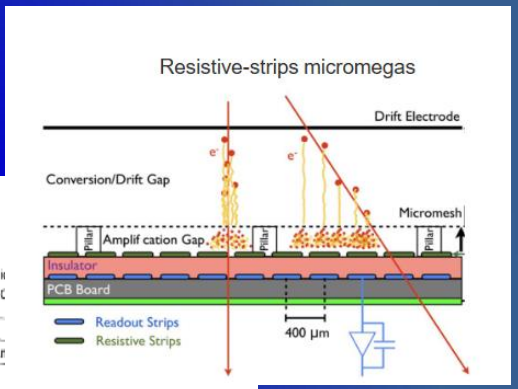

Solid State (Silicon, Diamond,..)

Ramo-Shockley theorem extension for conducting media

The time-dependent weighting potential is comprised of a static *prompt* and a dynamic *delayed* component:

$$\psi_i(\mathbf{x},t) \doteq \psi_i^P(\mathbf{x}) + \psi_i^d(\mathbf{x},t) \quad \text{where} \quad \psi_i^d(\mathbf{x},0) = 0 \ .$$

The current induced by a point particle q is given by:

$$I_i(t) = -\frac{q}{V_w}\int_0^t dt' \, \mathbf{H}_i\left[\mathbf{x}_q(t'), t-t'\right] \cdot \dot{\mathbf{x}}_q(t')$$

$$\mathbf{H}_i(\mathbf{x},t) \doteq -\nabla\frac{\partial\psi_i(\mathbf{x},t)}{\partial t} = -\nabla\psi_i^P(\mathbf{x})\delta(t) - \nabla\frac{\partial\psi_i^d(\mathbf{x},t)}{\partial t}\Theta(t)$$

Direct induction — Reaction from resistive material

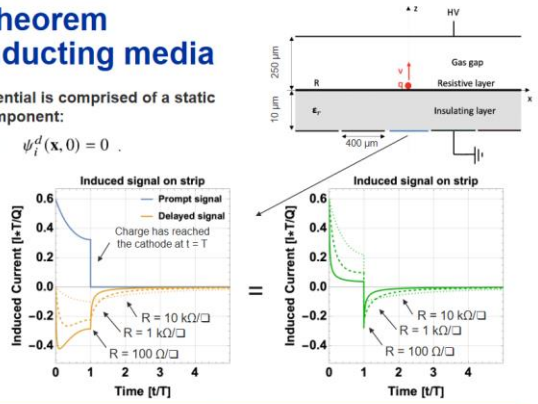

Examples of systems of which the weighting potential is analytically obtainable see W. Riegler, JINST **11** (2016) no.11, P11002.
Further reading: W. Riegler, P. Windischhofer, Nucl. Instrum. Meth. A 980 (2020)

Signal formation in AC-Coupled LGAD

In collaboration with INFN Torino group of N. Cartiglia, we are currently looking at simulating the currents induced in the AC-Coupled Low Gain Avalanche Diode (LGAD) geometry.

When successfully benchmarked, it can be use

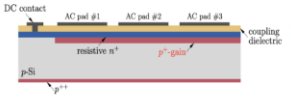

Diamond 3D Pixel Detector

A 3D geometry with thin columnar resistive electrodes orthogonal to the diamond surface, is expected to provide significantly better time resolution with respect to the extensively studied planar diamond sensors.

With the team of the INFN TimeSpot project, we are exploring the modelling of signal induction on the readout columns.

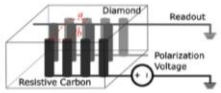

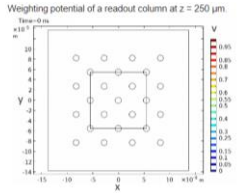

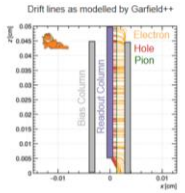

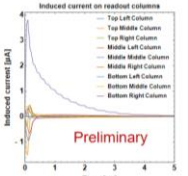

Anderlini L. et al., Frontiers in Physics 8 (2020)
For timing measurements and first modelling results see talk by M. Veltri: "A 4D diamond detector for HL-LHC and beyond".

Single Wire Proportional Counter: Avalanche Development

Thin anode wire (20 – 50 um) coaxial with cathode

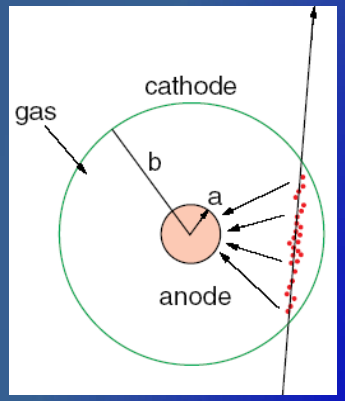

Electric field:

$$E(r) = \frac{CV_0}{2\pi\varepsilon_0}\frac{1}{r}$$

$$C = \frac{2\pi\varepsilon_0}{\ln(b/a)}$$

Avalanche development in the high electric field around a thin wire (multiplication region ~< 50 um):

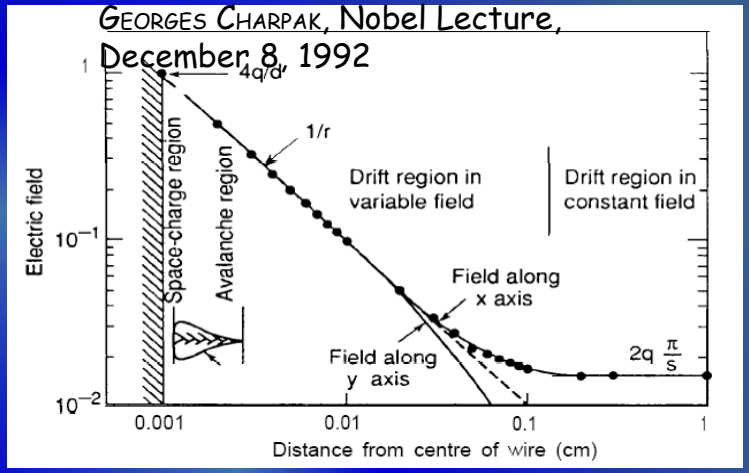

- *Strong increase of E-field close to the wire*
  - → ***electron gains more and more energy***
- *Above some threshold (>10 kV/cm)*
  - → *electron energy high enough to ionize other gas molecules*
  - → *newly created electrons also start ionizing*
- *Avalanche effect: exponential increase of electrons (and ions)*
- *Measurable signal on wire*
  - → *organic substances responsible for "quenching" (stopping) the discharge*

Different stages in the gas amplification process next to the anode wire.

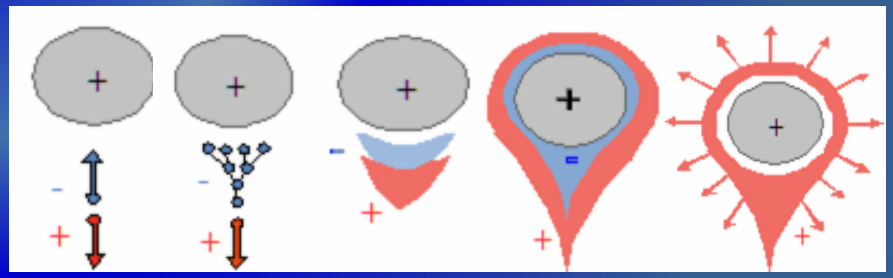

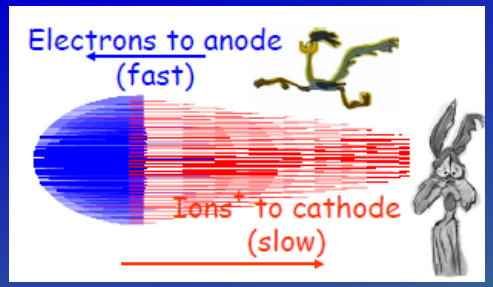

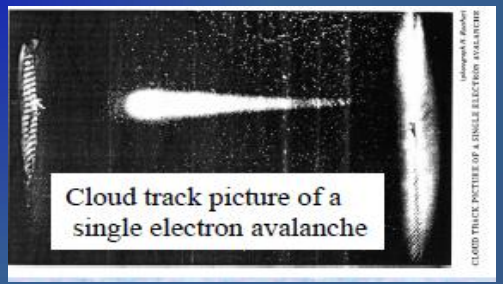

Ionization Cross Section: Townsend Coefficient

Multiplication of ionization is described by the first Townsend coefficient -α(E)

$dn = n\alpha dx$ $\quad \alpha = \frac{1}{\lambda}$ λ – mean free path

$$n = n_0 e^{\alpha(E)x} \quad \text{or} \quad n = n_0 e^{\alpha(r)x}$$

- ✓ α(E) is determined by the excitation and ionization cross sections of the electrons in the gas.
- ✓ It depends also on various and complex energy transfer mechanisms between gas molecules.
- ✓ There is no fundamental expression for α(E) → it has to be measured for every mixture.

$$M = \frac{n}{n_0} = \exp\left[\int_a^{r_C} \alpha(r)dr\right]$$

Amplification factor or Gain

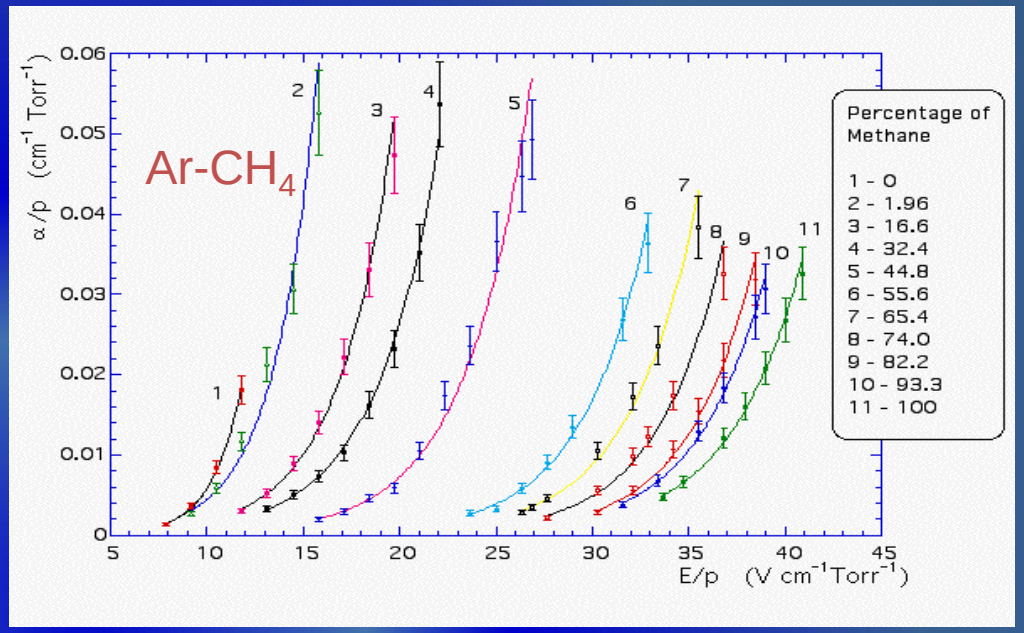

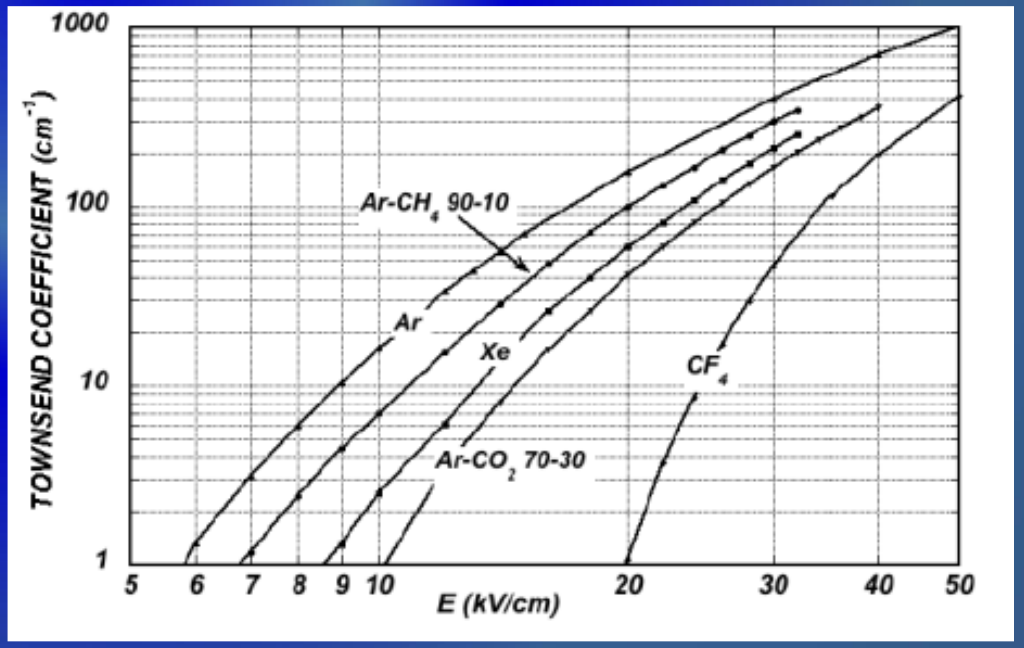

Ionization Cross Section: Penning Effects

- ✓ *Additional ionizing energy transfer mechanisms due to the excited noble gas atoms, called collisional Penning energy transfers, occur when the excitation energy of a noble gas is higher than the ionization potential of an admixture gas.*
- ✓ *The energy transfer rate, probability that an excited atom ionizes a quenching agent, is a priori not known for a mixture but can be extracted from the fits of the experimental gas gain data using the Magboltz simulations*
- ✓ *For example, the impact of the Penning effect on gas gain is roughly a factor 10 in Ar-CO2 mixtures and exceeding a factor of 100 in Ar-C2H2 mixtures*

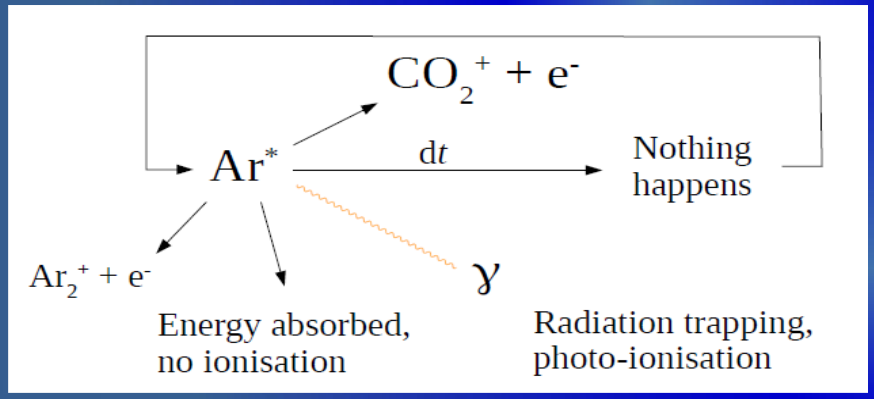

- The Penning transfer rate r_P is measured by finding the fraction of the excitations to be added to α so that the measured gain is reproduced:

$$G = \exp \int \alpha \left(1 + r_P \frac{\nu_{exc}}{\nu_{ion}}\right)$$

- r_P depends on gas choice, quencher fraction and density.

Ar/CO2 transfer rates:

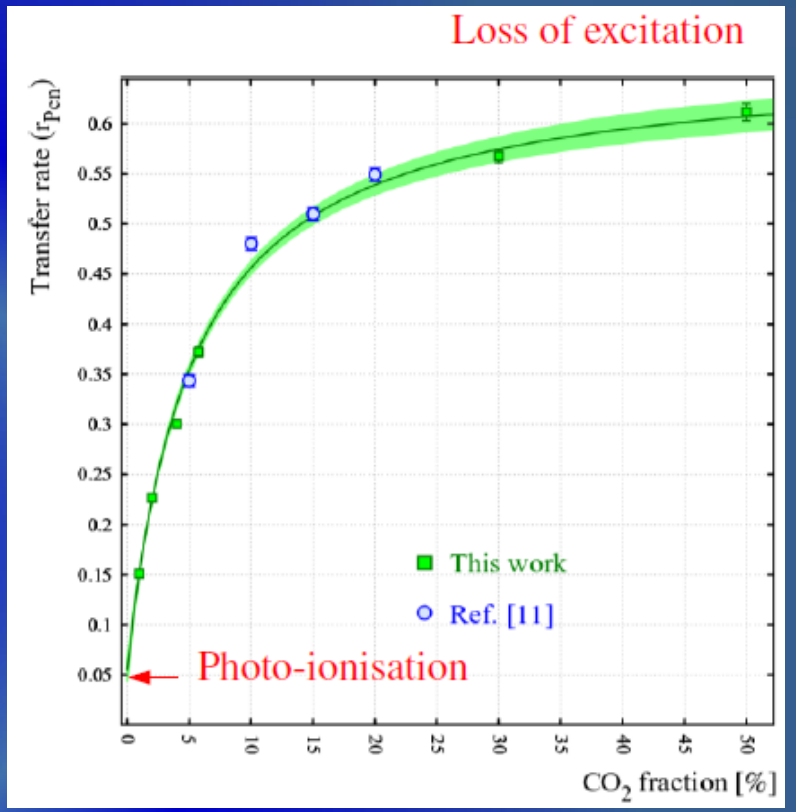

- ✓ *Collisional energy transfer mostly scales linearly with the gas pressure and the fraction of quenching gas in the mixture, while ionization by photons emitted from excitations is independent of the medium.*
- ✓ *In addition, collisional Penning transfers of some higher excited states can occur before they decay at atmopheric pressure and are not restricted to metastable states of the excited noble gas.*

Operation Modes of Gas Detector: Gain-Voltage Characteristics

- ✓ ***Ionization mode (II):***
  - → *full charge collection, but no multiplication – gain = 1*
- ✓ ***Proportional mode (IIIA):***
  - → *Multiplication of ionization starts; detected signal proportional to original ionization → possible energy measurement (dE/dx)*
  - → *proportional region (gain ~ 10^3 – 10^4)*
  - → *semi-proportional region (gain ~ 10^4 – 10^5), space charge effects*
  - → *secondary avalanches need quenching*
- ✓ ***Limited proportional mode (saturated, streamer) (IIIB):***
  - → *saturation (gain > 10^6), independent of number of primary electrons*
  - → *streamer (gain > 10^7), avalanche along the particle track*
- ✓ ***Geiger mode (IV):***
  - → *Limited Geiger region: avalanche propogated by UV photons;*
  - → *Geiger region (gain > 10^9), avalanche along the entire wire*

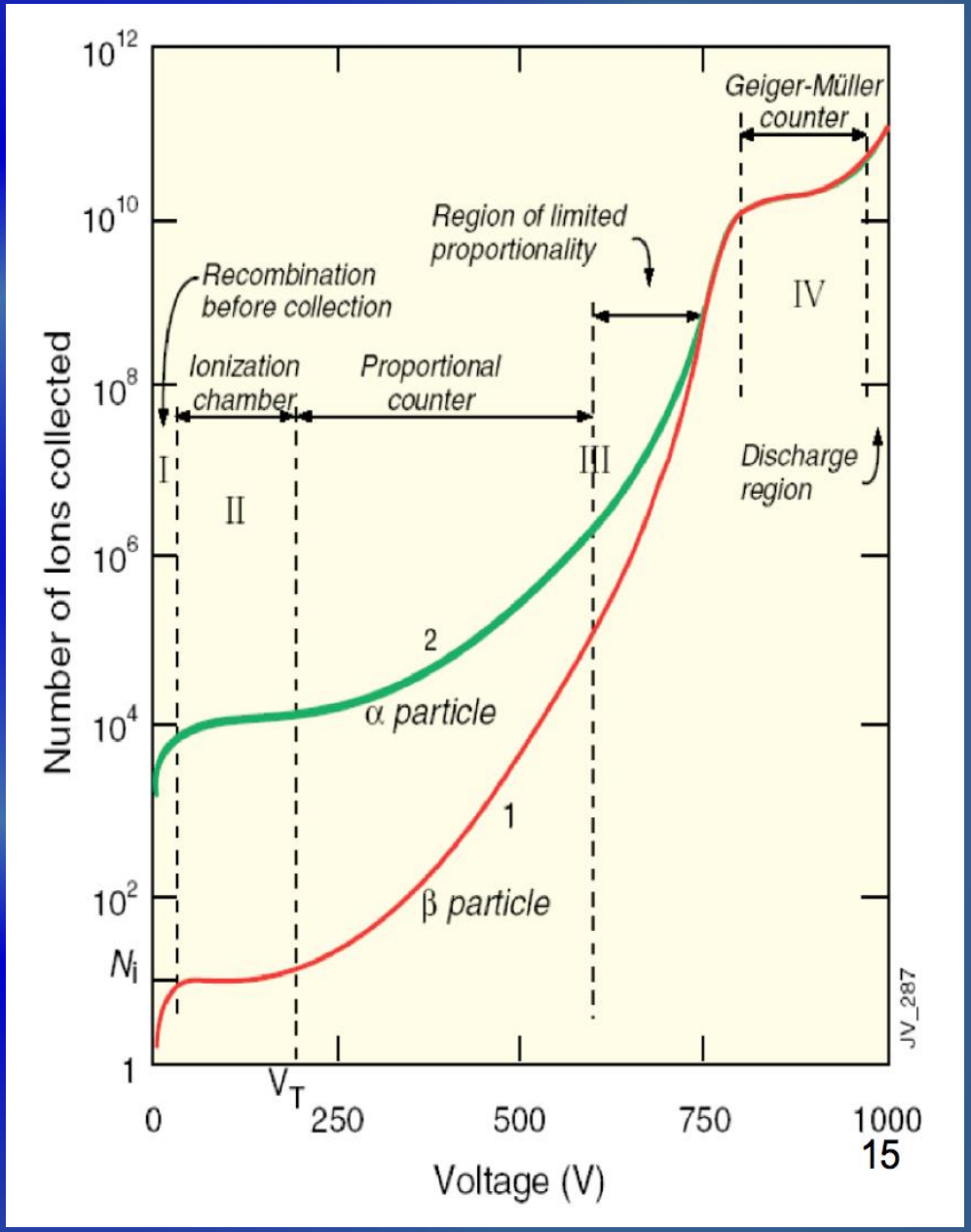

Wire Proportional Counter: Signal Development

Incremental charge induced by Q moving through dV:

$$dQ = \frac{Q}{V_0} dV = \frac{Q}{V_0} \frac{dV}{dr} dr$$

Assuming that the total charge of the avalanche Q is produced at a (small) distance l from the anode, the electron and ion contributions to the induced charge are:

$$q^- = \frac{Q}{V_0} \int_a^{a+\lambda} \frac{dV}{dr} dr = -\frac{QC}{2\pi\varepsilon_0} \ln\frac{a+\lambda}{a}$$

and

$$q^+ = \frac{Q}{V_0} \int_{a+\lambda}^{b} \frac{dV}{dr} dr = -\frac{QC}{2\pi\varepsilon_0} \ln\frac{b}{a+\lambda}$$

The total induced signal is

$$q = q^- + q^+ = -\frac{QC}{2\pi\varepsilon_0} \ln\frac{b}{a} = -Q$$

on the anode (+Q on the cathode)

The ratio of electron and ion contributions:

$$\frac{q^-}{q^+} = \frac{\ln(a+\lambda) - \ln a}{\ln b - \ln(a+\lambda)}$$

For a counter with a=10μm, b=10 m: q^-/q^+ ~1%

The electron-induced signal is negligible

Neglecting electrons, and assuming all ions leave from the wire surface:

$$q(t) = q^+(t) = -\int_0^t dq = -\frac{QC}{2\pi\varepsilon_0} \ln\frac{r(t)}{a}$$

$$\frac{dr}{dt} = \mu^+ E = \frac{\mu^+ C V_0}{2\pi\varepsilon_0} \frac{1}{r}$$

$$q(t) = -\frac{QC}{2\pi\varepsilon_0} \ln\left(1 + \frac{\mu^+ C V_0}{2\pi\varepsilon_0 a^2} t\right) = -\frac{QC}{2\pi\varepsilon_0} \ln\left(1 + \frac{t}{t_0}\right)$$

$$i(t) = -\frac{QC}{2\pi\varepsilon_0} \frac{1}{t_0 + t}$$

Total ions drift time:

$$T^+ = \frac{\pi\varepsilon_0 (b^2 - a^2)}{\mu^+ C V_0} \qquad q(T^+) = -Q$$

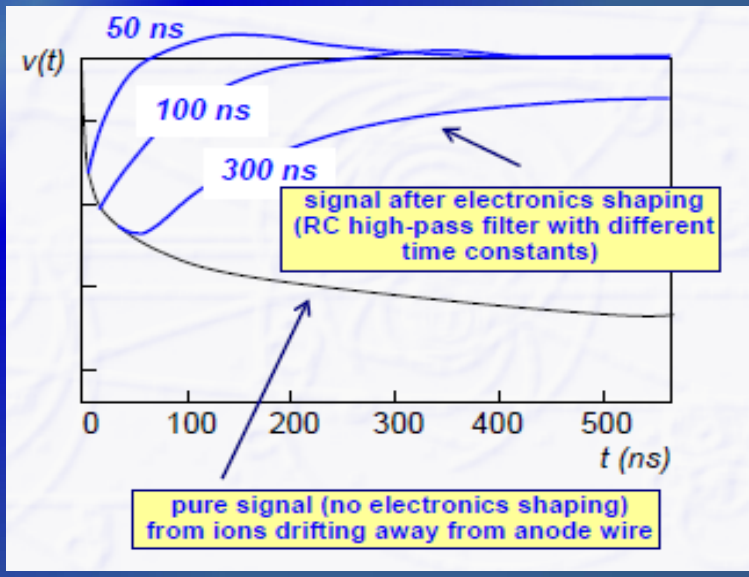

Useful Write-Ups on Gaseous Detectors

Wire & Drift Chamber Basics

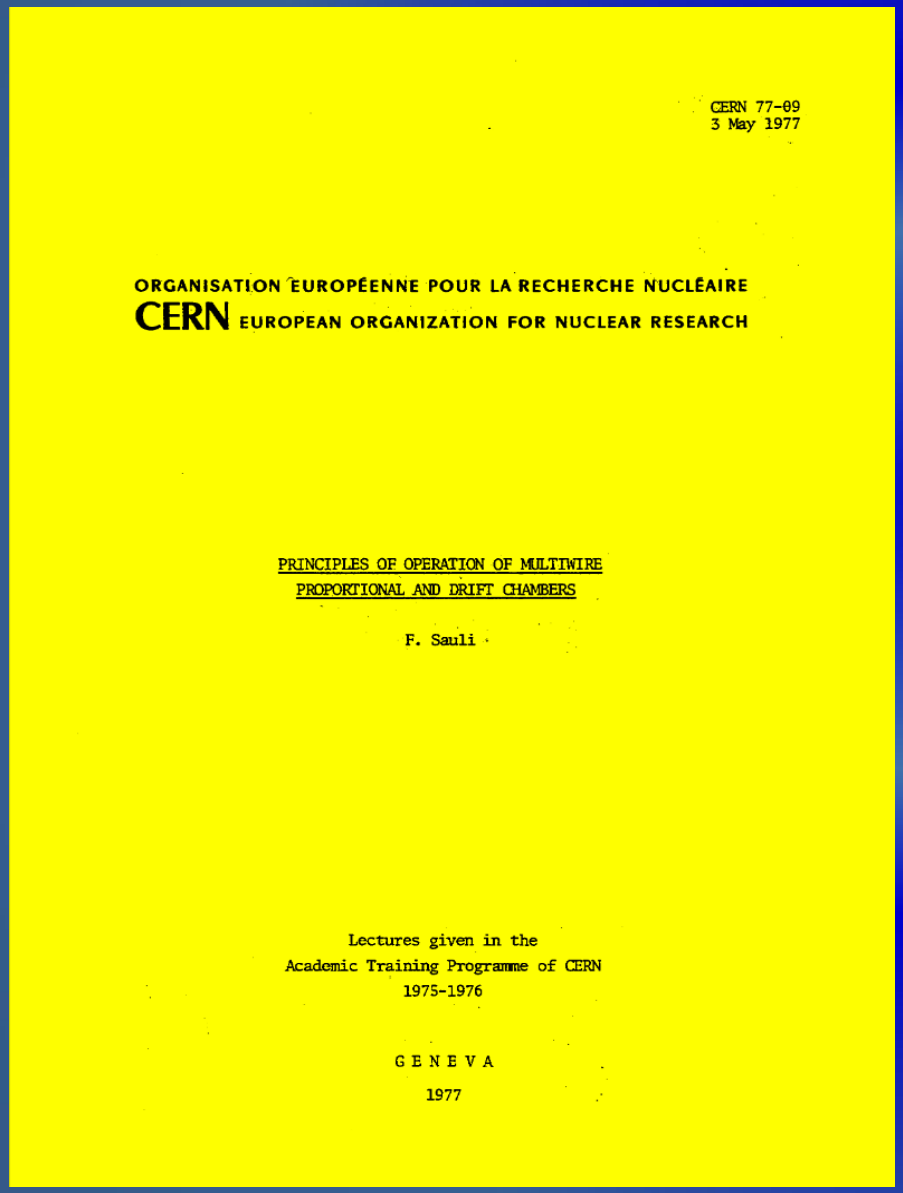

CERN 77-09
3 May 1977

ORGANISATION EUROPÉENNE POUR LA RECHERCHE NUCLÉAIRE
CERN EUROPEAN ORGANIZATION FOR NUCLEAR RESEARCH

PRINCIPLES OF OPERATION OF MULTIWIRE PROPORTIONAL AND DRIFT CHAMBERS

F. Sauli

Lectures given in the
Academic Training Programme of CERN
1975-1976

GENEVA
1977

More on signal theorems, readout electronics etc. can be found in:

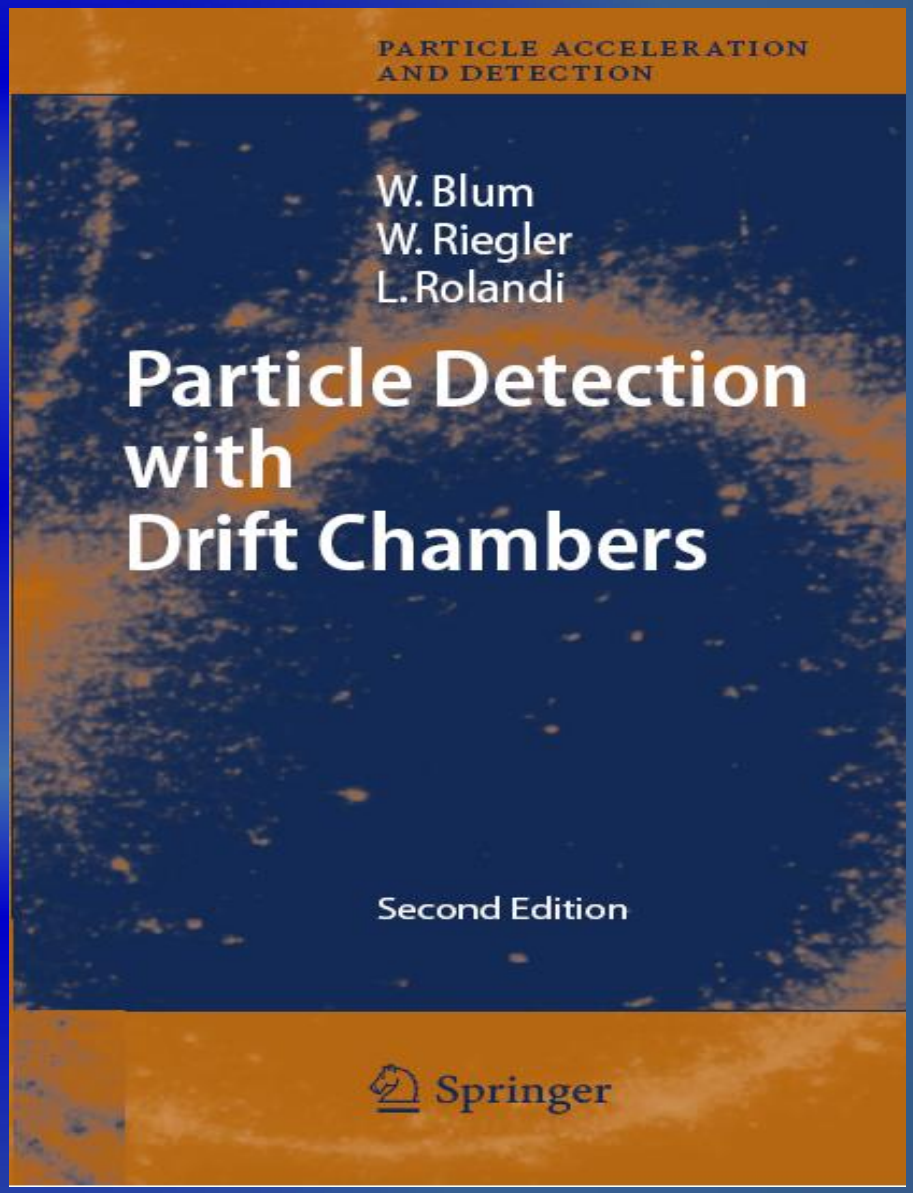

Multi-Wire Proportional Chamber (MWPC)

Simple idea to multiply SWPC cell → First electronic device allowing high statistics experiments !!

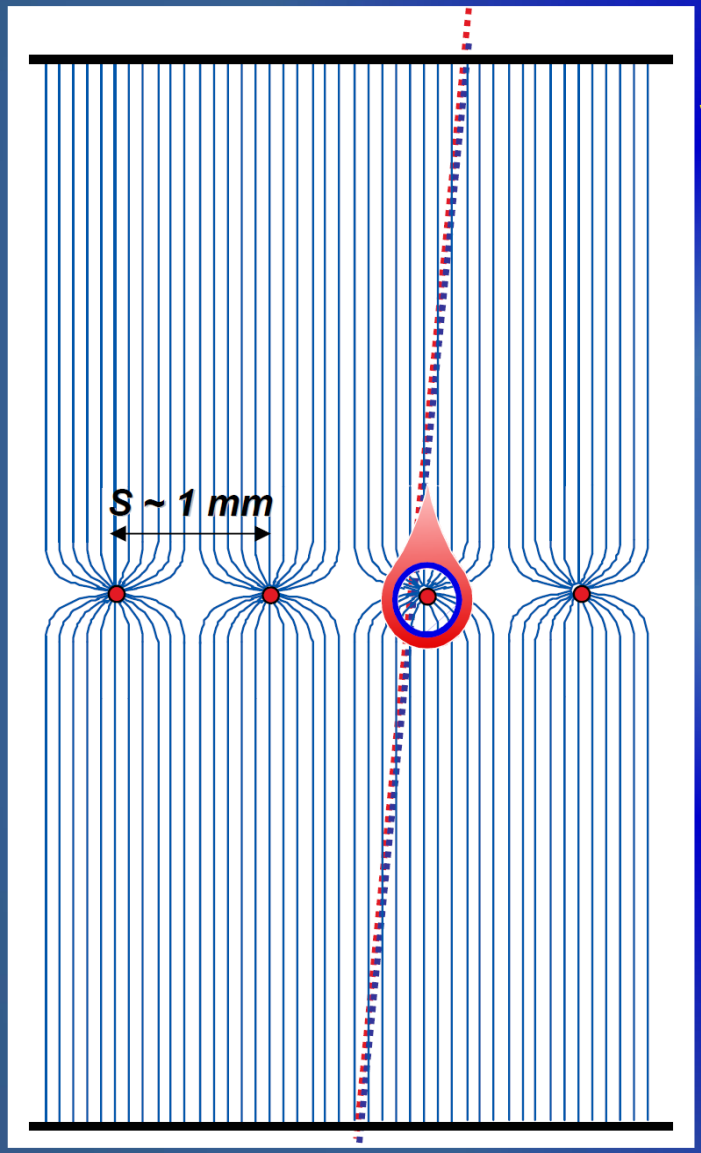

High-rate MWPC with digital readout:
Spatial resolution is limited to s_x ~ s/sqrt(12) ~ 300 μm

TWO-DIMENSIONAL MWPC READOUT CATHODE INDUCED CHARGE (Charpak and Sauli, 1973)

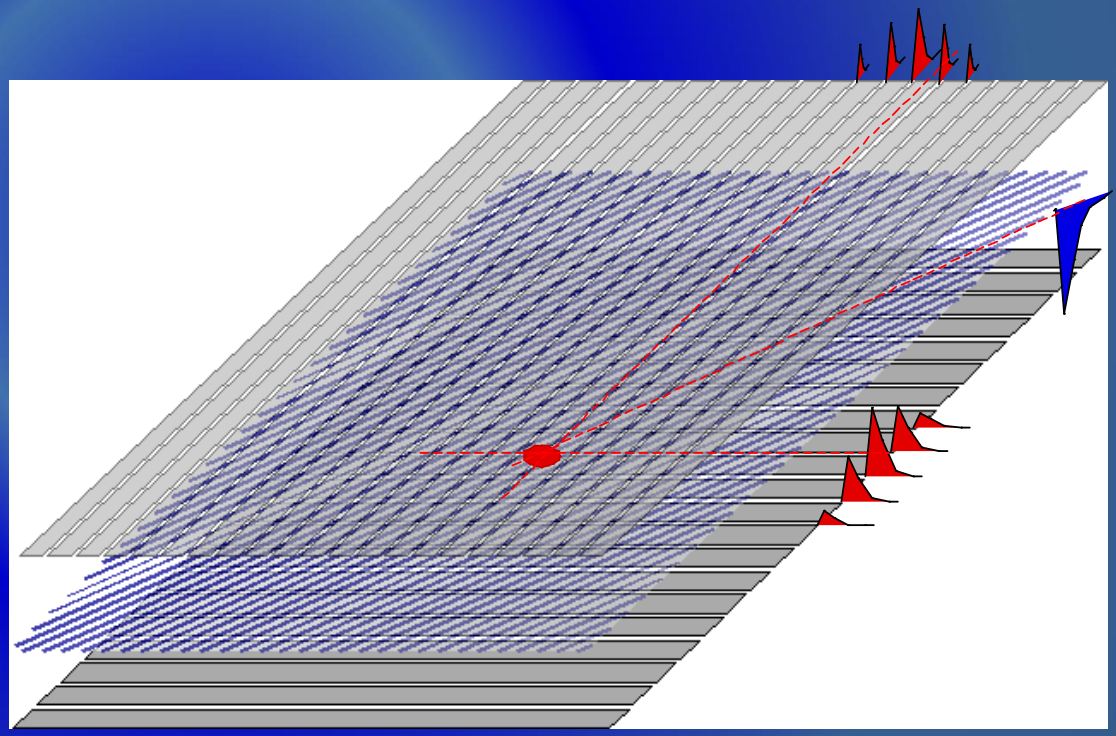

Spatial resolution determined by: Signal / Noise Ratio
Typical (i.e. 'very good') values: S ~ 20000 e: noise ~ 1000e
Space resolution < 100 μm

Multi-Wire Proportional Chamber (MWPC): Wire Displacements

Resolution of MWPCs limited by wire spacing
better resolution → shorter wire spacing → more (and more) wires...

- ✓ **Small wire displacements reduce field quality**

Table 35.1: Maximum tension T_M and stable unsupported length L_M for tungsten wires with spacing s, operated at $V_0 = 5$ kV. No safety factor is included.

Wire diameter (μm)	T_M (newton)	s (mm)	L_M (cm)
10	0.16	1	25
20	0.65	2	85

- ✓ **Need high mechanical precision both for geometry and wire tension ... (electrostatic and gravitation, wire sag …)**

- ✓ Several simplifying assumptions are made in analytical calculations: electrostatic force acting on the wire does not change during wire movements, or varies linearly with the displacement, the wire shape is parabolic; only one wire moves at a time.

- ✓ The advantage of numerical integrations using Garfield++ program is to simulate the collective movement of all wires, which are difficult analytically, and to consider all forces acting on a wire: forces between anode wire and other electrodes (wires, cathode) & gravitational force

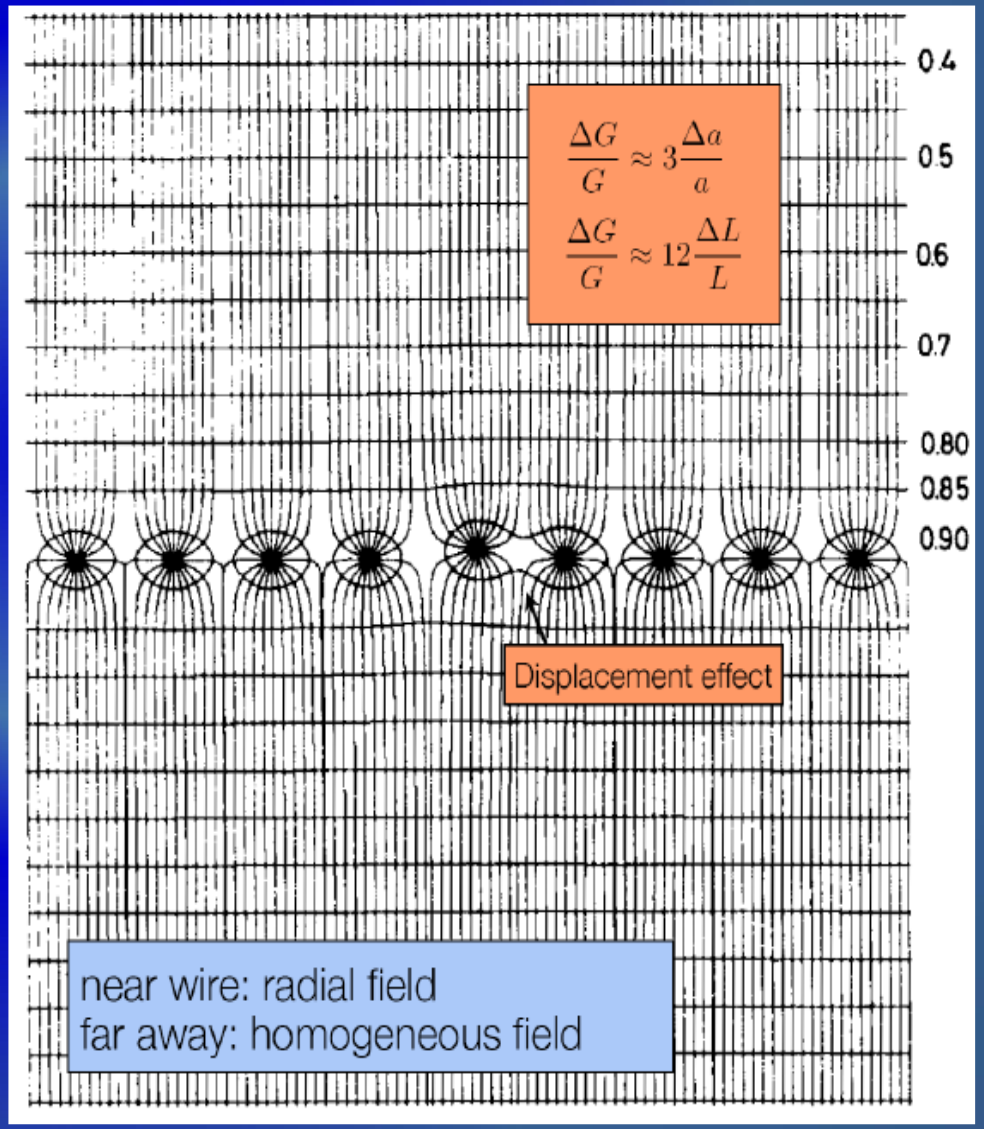

MWPC: First Presentation and First Large Experiment

colloque international sur l'électronique nucléaire

First presentation:

*

international symposium on nuclear electronics

VERSAILLES, 10-13 September 1968

Chambres à Etincelles

Spark chambers

Rapporteur Reporter	**M. CHARPAK** CERN - GENEVE (Suisse)
Secrétaire scientifique Scientific Secretary	**M. FEUVRAIS** Faculté des Sciences - Lyon (France)

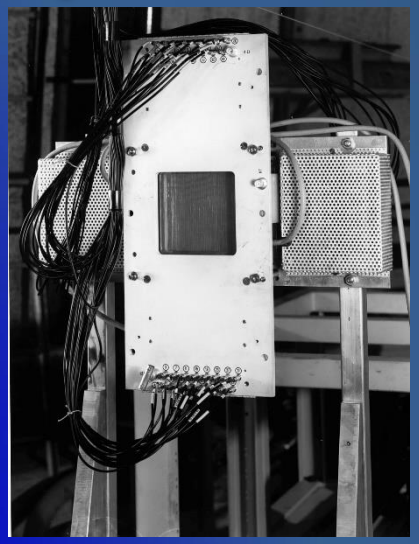

First Large Experiiment:

1972-1983:
SPLIT FIELD MAGNET DETECTOR: ~ 40 LARGE AREA MWPCs @ CERN ISR

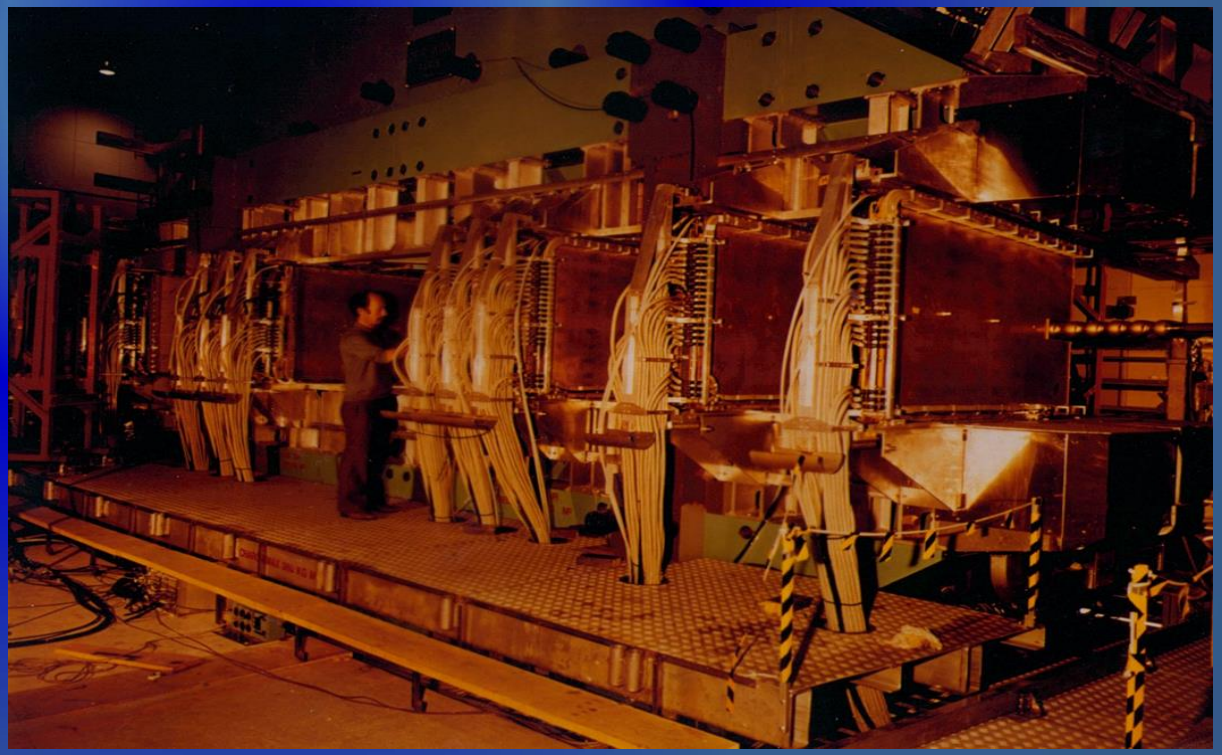

1968: Multi – Wire Proportional Chamber (MWPC)

NUCLEAR INSTRUMENTS AND METHODS 62 (1968) 262–268; © NORTH-HOLLAND PUBLISHING CO.

THE USE OF MULTIWIRE PROPORTIONAL COUNTERS TO SELECT AND LOCALIZE CHARGED PARTICLES

G. CHARPAK, R. BOUCLIER, T. BRESSANI, J. FAVIER and Č. ZUPANČIČ

CERN, Geneva, Switzerland

Received 27 February 1968

Properties of chambers made of planes of independent wires placed between two plane electrodes have been investigated. A direct voltage is applied to the wires. It has been checked that each wire works as an independent proportional counter down to separations of 0.1 cm between wires.

Counting rates of 10^5/wire are easily reached; time resolutions of the order of 100 nsec have been obtained in some gases; it is possible to measure the position of the tracks between the wires using the time delay of the pulses; energy resolution comparable to the one obtained with the best cylindrical chambers is observed; the chambers operate in strong magnetic fields.

1. Introduction

Proportional counters with electrodes consisting of many parallel wires connected in parallel [illegible] used for some years, for special application [illegible] investigated the properties of chambers ma[illegible] plane of independent wires placed between two plane electrodes. Our observations show that such chambers offer properties that can make them more advantageous than wire chambers or scintillation hodoscopes for many applications.

in cylindrical proportional chambers. It protects the wires against breakdown along the dielectrics. It is

G. Charpak et al,, NIMA62 (1968) 262

2. Construction

Wires of stainless steel, 4×10^{-3} cm in diameter, are stretched between two planes of stainless-steel mesh, made from wires of 5×10^{-3} cm diameter, 5×10^{-2} cm apart. The distance between the mesh and the wires is 0.75 cm. We studied the properties of chambers with wire separation $a = 0.1$, 0.2, 0.3 and 1.0 cm. A strip of metal placed at 0.1 cm from the wires, at the same potential (fig. 1), plays the same role as the guard rings

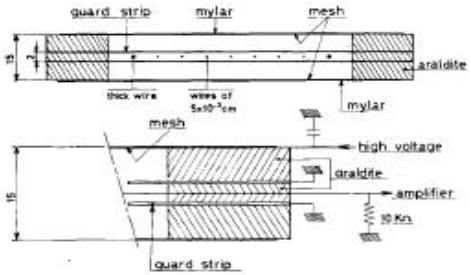

Fig. 1. Some details of the construction of the multiwire chambers.
A copper shield protects the wires at their output from the chamber and contains the solid state amplifiers.

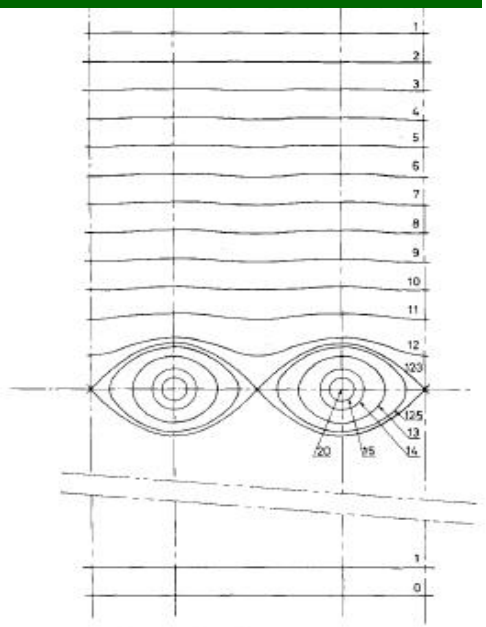

Fig. 2. Equipotentials in a chamber.
Wires of 4×10^{-3} cm diameter, 0.3 cm separation, and 1.5 cm total thickness. 20 V applied between the wires and the external mesh. Results from an analogic method.

ENERGY RESOLUTION ON 5.9 KeV:

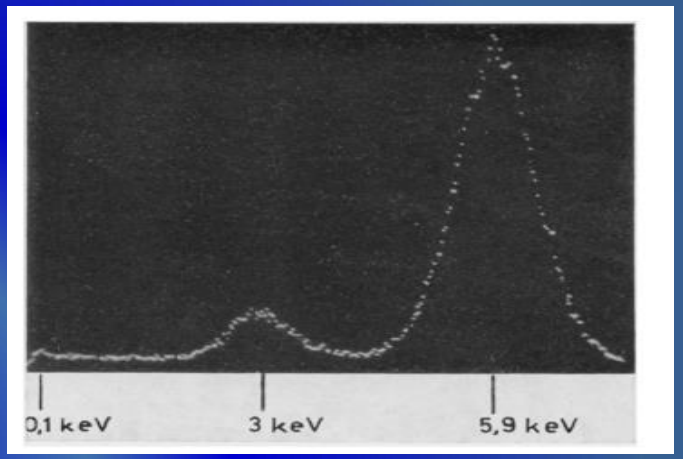

DEPENDENCE OF COLLECTION TIME FROM TRACK'S DISTANCE:

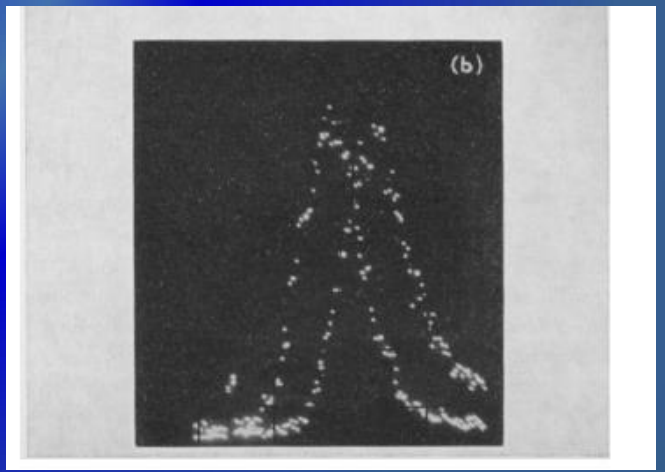

DRIFT CHAMBERS

Drift Chambers

FIRST DRIFT CHAMBER OPERATION (H. WALENTA ~ 1971);
HIGH ACCURACY DRIFT CHAMBERS (Charpak-Breskin-Sauli ~ 1973-75)

THE ELECTRONS DRIFT TIME PROVIDES THE DISTANCE OF THE TRACK FROM THE ANODE:

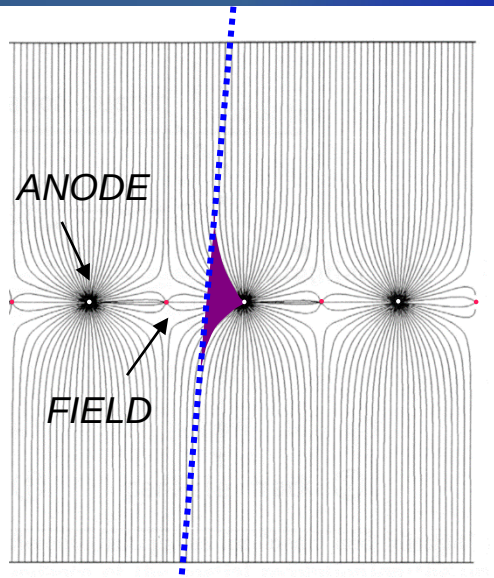

Choose drift gases with little dependence $v_D(E) \rightarrow$ linear space - time relation r(t)

Measure drift time t_D
[need to know t_0; fast scintillator, beam timing]

Determine location of original ionization:

$$x = x_0 \pm v_D \cdot t_D$$
$$y = y_0 \pm v_D \cdot t_D$$

If drift velocity changes along path:

$$x = \int_0^{t_D} v_D \, dt$$

In any case:
Need well-defined drift field ...

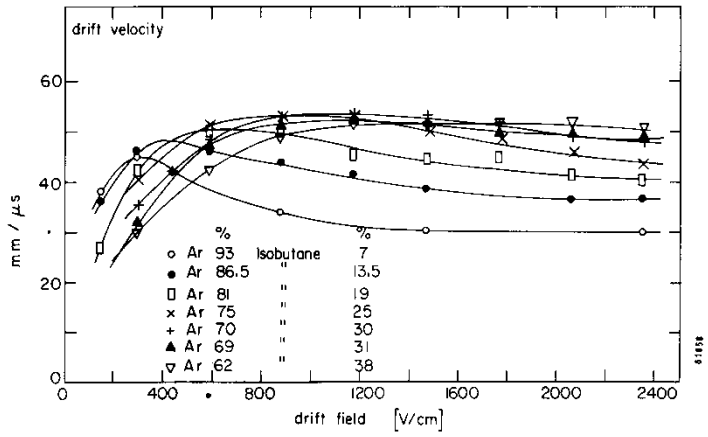

The spatial resolution is not limited to the cell size :

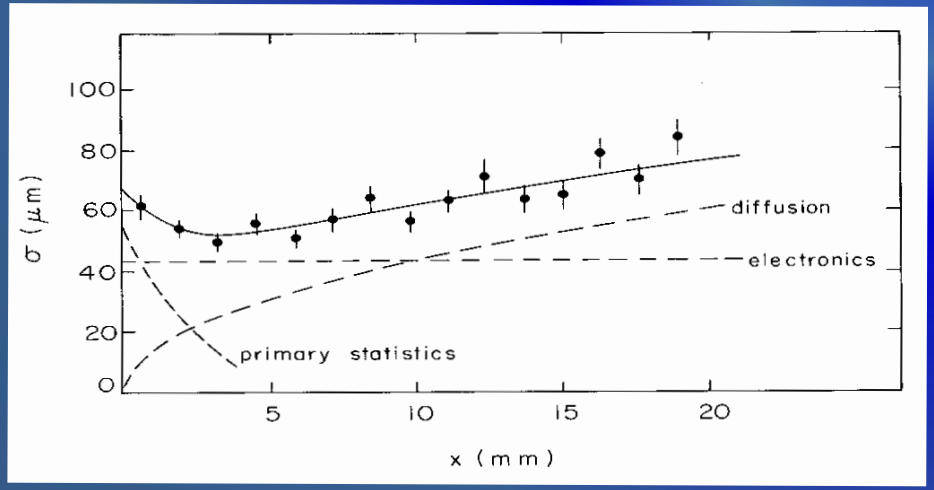

$$\sigma_x^2 = \underbrace{\left(\frac{1}{64N^2}\right) \cdot \frac{1}{x^2}}_{\text{1st ionization statistics}} + \underbrace{\frac{2D}{v_d} \cdot x}_{\text{diffusion}} + \underbrace{\sigma_{\text{const}}^2}_{\substack{\text{electronics} \\ \delta\text{-electrons}}}$$

Typical single point resolutions of drift chambers:
50...150 µm depends on length of the drift path

- ✓ *primary ionization statistics: how many ion pairs, ionization fluctuations dominates close to the wire*
- ✓ *diffusion of electrons in gas: dominates for large drift length*
- ✓ *electronics: noise, shaping characteristics constant contribution (drift length independent)*

Wire & Drift Chambers: Wide-Spread Tool in HEP for > 40 Years

Interior of OPAL drift chamber
Length: 4 m; R = 185 cm; 159 measurements per track
[$\sigma_{r\phi}$ = 135 µm, σ_z = 80 mm]

The Evolution of Drift Chambers and Future e+e- Colliders

past

SPEAR	MARK2	Drift Chamber
	MARK3	Drift Chamber
DORIS	PLUTO	MWPC
	ARGUS	Drift Chamber
CESR	CLEO1,2,3	Drift Chamber
VEPP2/4M	CMD-2	Drift Chamber
	KEDR	Drift Chamber
	NSD	Drift Chamber
PETRA	CELLO	MWPC + Drift Ch.
	JADE	Drift Chamber
	PLUTO	MWPC
	MARK-J	TEC + Drift Ch.
	TASSO	MWPC + Drift Ch.
TRISTAN	AMY	Drift Chamber
	VENUS	Drift Chamber
	TOPAZ	TPC

PEP	MARK2	Drift Chamber
	PEP-4	TPC
	MAC	Drift Chamber
	HRS	Drift Chamber
	DELCO	MWPC
BEPC	BES1,2	Drift Chamber
LEP	ALEPH	TPC
	DELPHI	TPC
	L3	Si + TEC
	OPAL	Drift Chamber
SLC	MARK2	Drift Chamber
	SLD	Drift Chamber
DAPHNE	KLOE	Drift Chamber
PEP2	BaBar	Drift Chamber
KEKB	Belle	Drift Chamber

present

VEPP2000	CMD-3	Drift Chamber
VEPP4	KEDR	Drift Chamber
BEPC2	BES3	Drift Chamber
S.KEKB	Belle2	Drift Chamber

future

ILC	ILD	TPC
	SiD	Si
CLIC	CLIC	Si
FCC-ee	CLD	Si
	IDEA	Drift Chamber
CEPC	Baseline	TPC / Si
	IDEA	Drift Chamber
SCTF	BINP	Drift Chamber
STCF	HIEPA	Drift Chamber

Lesson #1 - from "open" to "closed" cell

- closed
- closed
- the tra
- squar
- small

... but

- portion
- envelo
- small
- use of
- contrib
- some

Lesson #3 – small cells and He gas

- He radiation length 50× longer than Ar
- slower drift velocity implies smaller Lorenz angle for a given B-field
- He has a smaller cross section for low energy photons than Ar
- small size cells limit the electron diffusion contribution to spatial resolution
- small size cells provide high granularity (improving occupancy) and allow for a larger number of hits per track, improving spatial resolution

... but

- portions of active volume not sampled between the cylindrical envelope of axial wires and the hyperboloid envelope of stereo wires
- accumulation of trapped electrons and ions in a region of very low field
- longitudinal gain variation at boundaries between axial and stereo layers
- spatial resolution dominated by ionization statistics for short drift distances
- adding more quencher to compensate, mitigates the advantage of He

Lesson #4 – full stereo configuration

- no ga
- electro
- consta
- larger
- maxim
- two st

... but

- open t
- from th
- consta
- z (radi
- consta

Lesson #5 – summary

- the configuration offering the best performance in terms of **momentum resolution** is one with small, single sense wire closed cells, arranged in contiguous layers of opposite sign stereo angles, obtained with constant stereo angle transverse projection
- the gas mixture is based on helium with a small amount of quencher (90% He / 10% iC_4H_{10}, KLOE gas) which, besides low multiple scattering contribution, allows for the exploitation of the cluster timing technique, for improved spatial resolution, and of the cluster counting technique, for excellent particle identification
- suggested wire material is Ag coated Al, but lighter materials are under scrutiny (like metal coated carbon monofilaments)

An ultra-light drift chamber (IDEA concept) targetted for FCC-ee and CePC (100 km) was inspired by DAFNE KLOE Wire Chamber and by more recent version of it for MEG2 experiment

Original Gaseous Detectors (mostly wires/straws RPC) in LHC Experiments

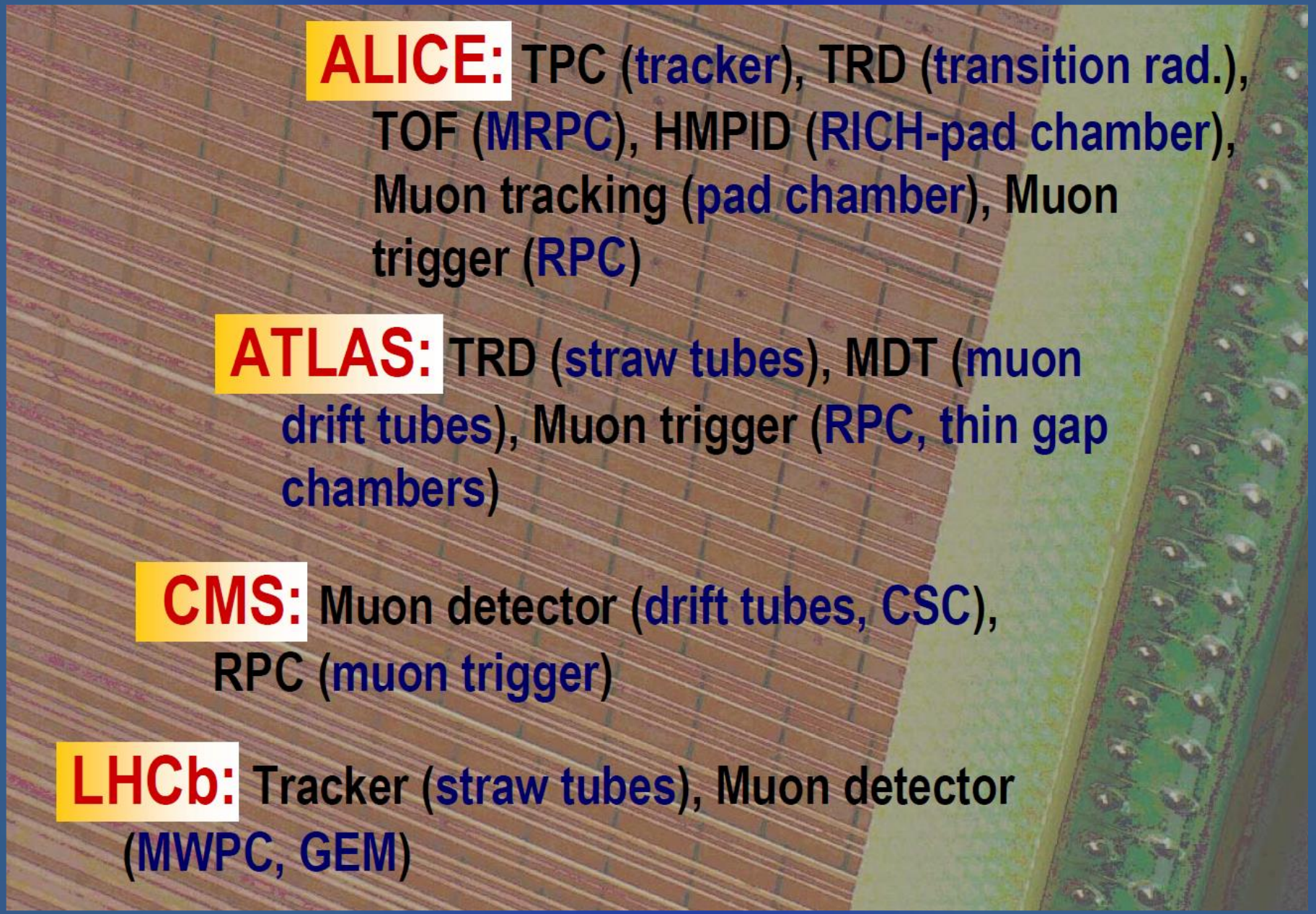

Original Gaseous Detectors in LHC Experiments

	Vertex	Inner Tracker	PID/ photo-detector	EM CALO	HAD CALO	MUON Track	MUON Trigger
ATLAS	-	TRD (straws)	-	-	-	MDT (drift tubes), CSC	RPC, TGC (thin gap chambers)
CMS ----- TOTEM	-	- -------- GEM	-	-	-	Drift tubes, CSC	RPC, CSC
LHCb	-	Straw Tubes	-	-	-	MWPC	MWPC, GEM
ALICE	-	TPC (MWPC)	TOF (MRPC), HPMID (RICH-pad chamber), TRD (MWPC)	-	-	Muon pad chambers	RPC

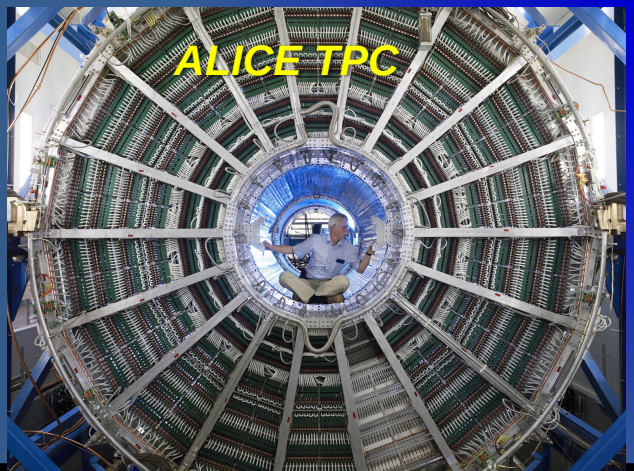

ALICE Time Projection Chamber (TPC)

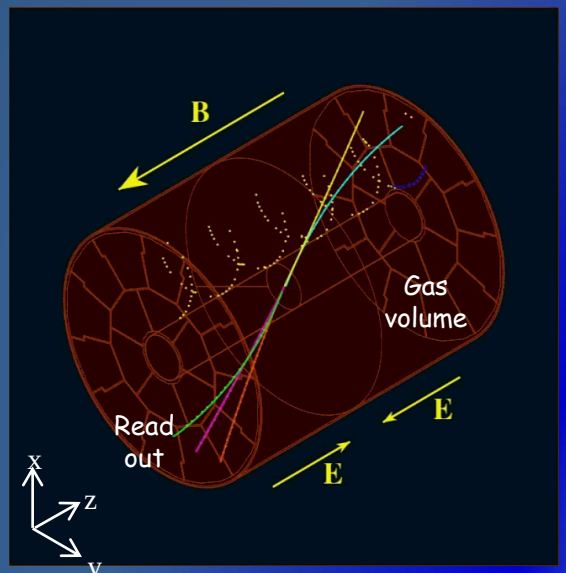

- Largest TPC:
  - Length 5m
  - Diameter 5m
  - Volume 88m^3
  - Detector area 32m^2
  - Channels ~570 000
- High Voltage:
  - Cathode -100kV
- Material X_0
  - Cylinder from composite materials from airplane industry (X_0= ~3%)

- ***Track point recorded in 3-D***

  (2-D channels in x-y) x (1-D channel in z = v_{drift} x t_{drift})

- ***Particle identification by dE/dx***

  long ionization track, segmented in 100-200 measurements

Precision in z: 250μm

End plates 250μm

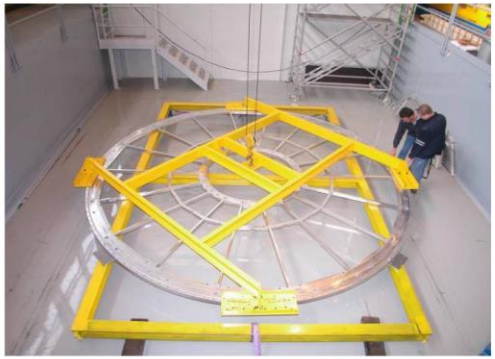

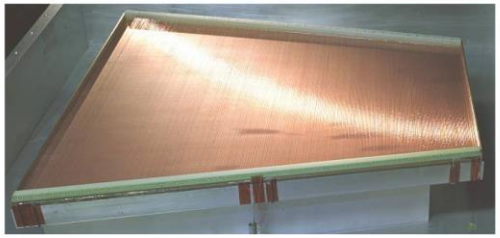

Wire chamber: 40μm

	STAR	ALICE	ILC
Inner radius (cm)	50	85	32
Outer radius (cm)	200	250	170
Length (cm)	2 * 210	2 * 250	2 * 250
Charge collection	wire	wire	MPGD
Pad size (mm)	2.8 * 11.5 6.2 * 19.5	4 * 7.5 6*10(15)	2 * 6
Total # pads	140000	560000	1200000
Magnetic field [T]	0.5	0.5	4
Gas Mixture	Ar/CH4 (90:10)	Ne/CO2 (90:10)	Ar/CH4/CO2 (93:5:2)
Drift Field [V/cm]	135	400	230
Total drift time (μs)	38	88	50
Diffusion σ_T(μm/$\sqrt{cm}$)	230	220	70
Diffusion σ_L(μm/$\sqrt{cm}$)	360	220	300
Resolution in rφ(μm)	500-2000	300-2000	70-150
Resolution in rz (μm)	1000-3000	600-2000	500-800
dE/dx resolution [%]	7	7	< 5
Tracking efficiency[%]	80	95	98

Gaseous Tracking @ LHC Experiments

- ✓ *Straw tubes (single-wire proportional counters) with xenon-based gas mixture*
- ✓ *4 mm in diameter, equipped with a 30 μm diameter gold-plated W-Re wire*

ATLAS TRT

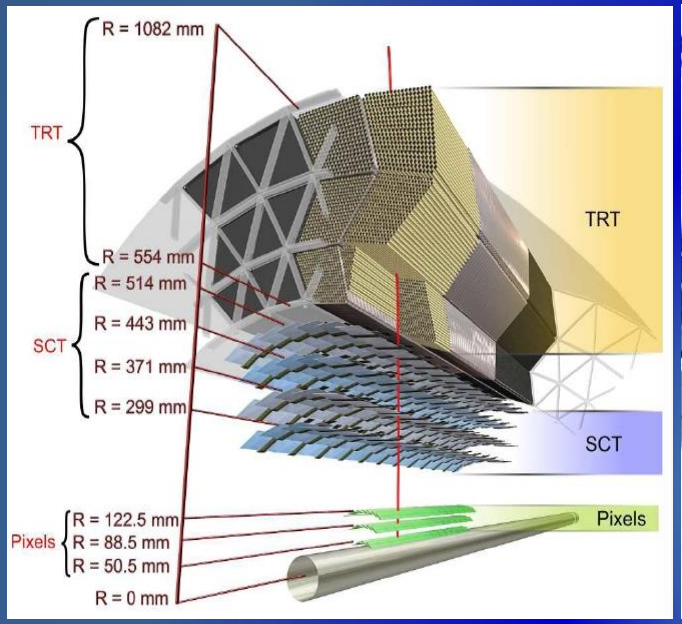

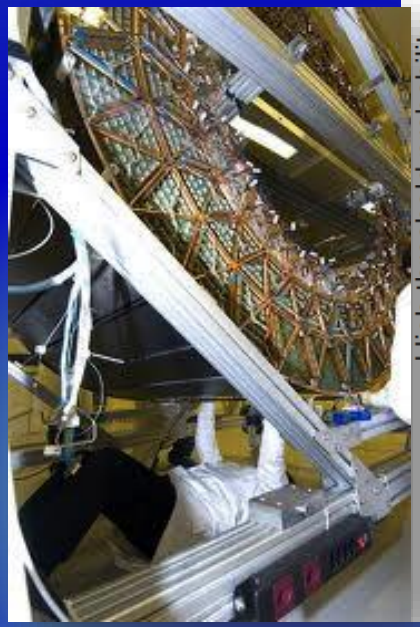

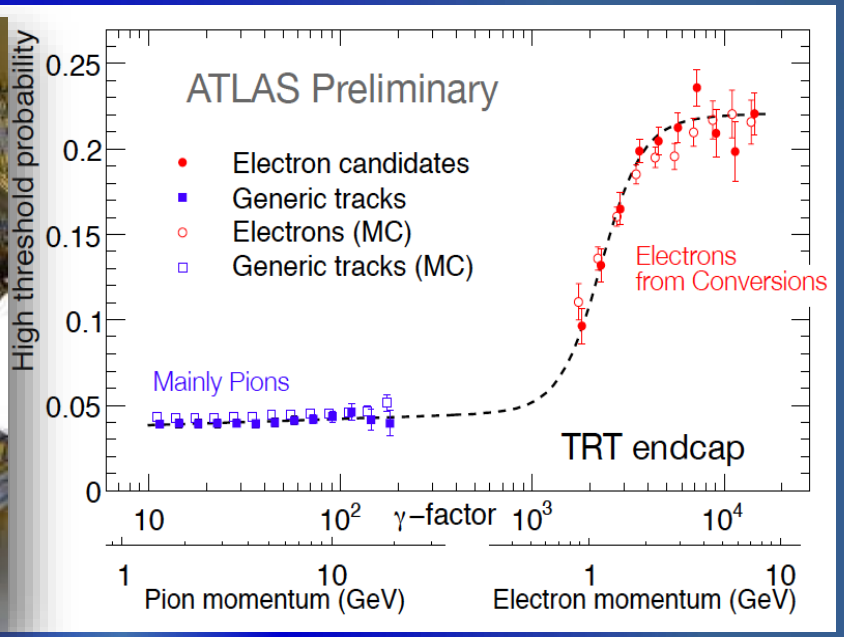

- ✓ *Stable operation at very high rates up to 12 MHz/cm²*
- ✓ *Achieved spatial (time) resolution: 135 um (7 ns) at high intensity 2* 10⁸ s⁻¹*

CMS/TOTEM GEM

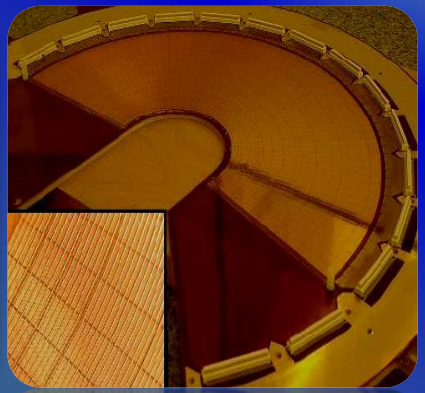

Muon Detectors: CMS Cathode Strip Chambers (CSC)

Muon detectors are tracking detectors (e.g. wire-based tubes):
→ they form the outer shell of the (LHC) detectors
→ they are not only sensitive to muons (but to all charged particles)!
→ just by "definition": if a particle has reached the muon detector (it's considered to be a muon); all other particles should have been absorbed in the calorimeters

Challenge for muon detectors:
- large surface to cover (outer shell); keep mechanical positioning stable over time
- also good knowledge of (inhomogeneous) magnetic field

CMS CSC: precise measurement of the second coordinate by interpolation of the signal induced on pads.

Closely spaced wires makes CSC fast detector.

CMS CSC

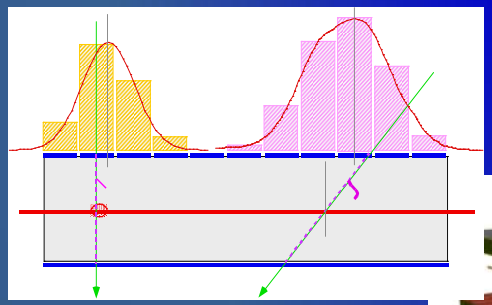

Space resolution

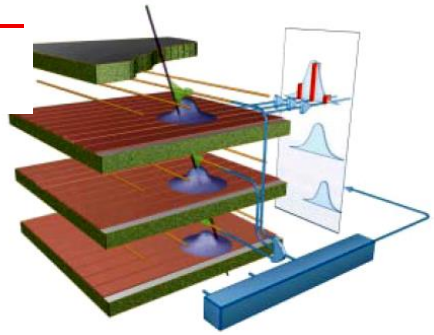

Center of gravity of induced signal method.

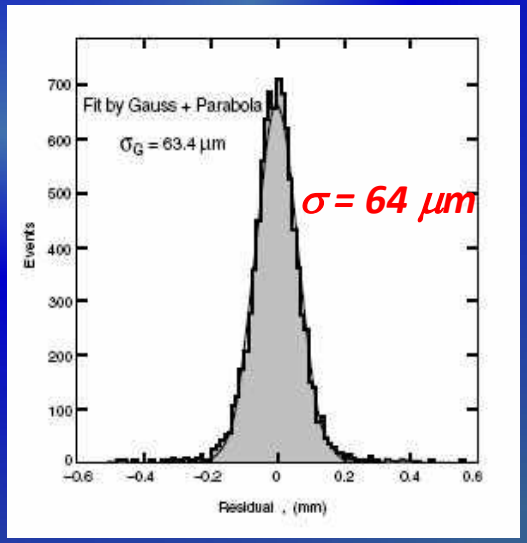

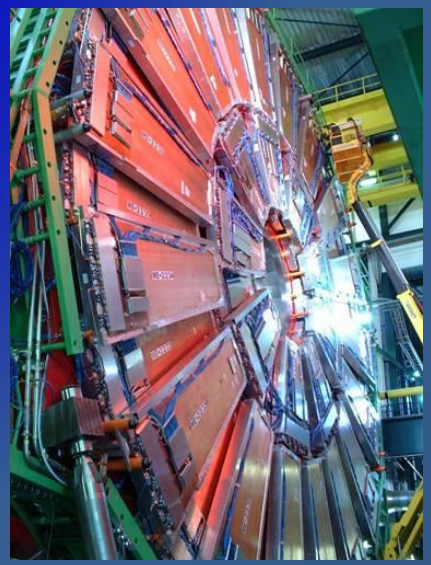

Muon Systems: Resistive Plate Chambers (RPC)

- *two resistive plates (~10^9 Ω cm) with a small gas gap (2 mm) and large high voltage (12 kV) on outside electrodes*
- *strong E-field: operation in "streamer mode"*
  - → gas avalanche starting in gas gap (no wires involved)
  - → developing of avalanche or "streamers" (blob with lots of charge)
  - → signal on external read-out strips via influence (segmented for position resolution)
  - → streamer/discharge is "self-quenching": stops when near-by resistive electrodes are locally discharged (E-field breaks down)

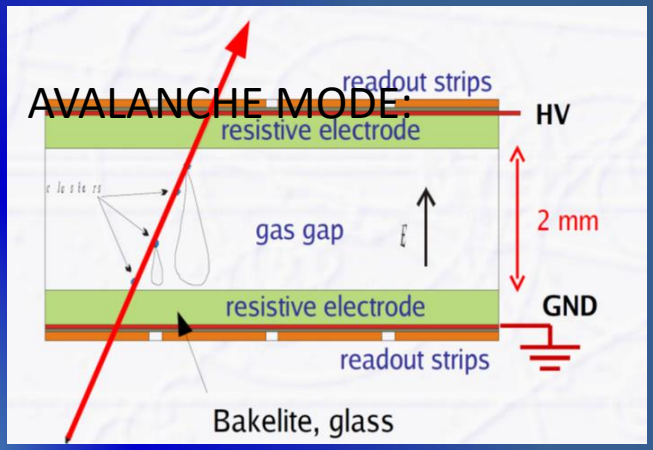

Experiment	Electrodes material & resistivity	Gas mixture	Operation mode; charge/track	Particle rates ; Accumulated charge
L3	Oiled bakelite $2*10^{11}$ Ωcm	$Ar/iC_4H_{10}/C_2H_2F_4$ (57:37:6)	Streamer	Consistent with cosmic rays
Belle	Float glass 10^{12} - 10^{13} Ωcm	$Ar/iC_4H_{10}/C_2H_2F_4$ (30:8:62)	Streamer	~10-20 Hz/cm^2;
BaBar	Oiled bakelite 10^{11} - 10^{12} Ωcm	$Ar/iC_4H_{10}/C_2H_2F_4$ (60.6:4.7:34.7)	Streamer 1000pC/track	~10-20 Hz/cm^2; <10 C/cm^2 (in 2010)
ATLAS	Oiled bakelite $2*10^{10}$ Ωcm	$C_2H_2F_4/iC_4H_{10}/SF_6$ (96.7:3:0.3)	Avalanche 30 pC/track	<0.1 kHz/cm^2; <0.3 C/cm^2
CMS barrel	Oiled bakelite: 10^{10} Ωcm	$C_2H_2F_4/iC_4H_{10}/SF_6$ (96:3.5:0.5)	Avalanche 30 pC/track	<0.1 kHz/cm^2; <0.3 C/cm^2
ALICE	Oiled bakelite $3*10^9$ Ωcm	$Ar/iC_4H_{10}/C_2H_2F_4/SF_6$ (49:40:7:1)	Streamer	<0.1 kHz/cm^2; <0.2 C/cm^2
LHC-b	Oiled bakelite $9*10^9$ Ωcm	$C_2H_2F_4/iC_4H_{10}/SF_6$ (95:4:1)	Avalanche 30 pC/track	0.25-0.75 kHz/cm^2 0.35-1.1 C/cm^2

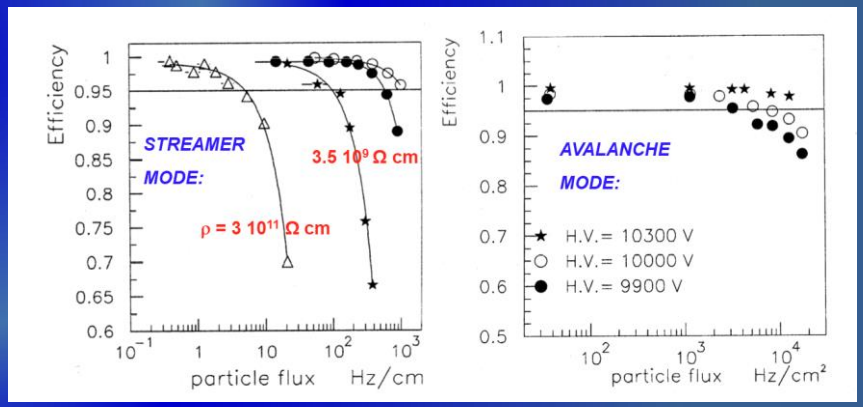

Advantages:

- → *simple device, good to cover large areas,*
- → *used as trigger devices in LHC experiments, BX trigger (25 ns)*

Disadvantages:

- → *Choice of resistive material + surface quality crucial, affects "dark" trigger rate*

ALICE Multi-Gap RPC: Timing Resolution

- *Relevant scale in HEP: t ~ L(m)/c ~ o(ns)*

$$T_1 - T_2 = \frac{L}{c}\left(\frac{1}{\beta_1} - \frac{1}{\beta_2}\right) = \frac{L}{c}\left(\sqrt{1 + m_1^2/p^2} - \sqrt{1 + m_2^2/p^2}\right) \cong (m_1^2 - m_2^2)L/2cp^2$$

- *Traditional technique:*
  - *Scintillator + PMT ~ o (100 psec)*
- *Breakthrough with a spark discharge in gas*
  - *Pestov counter → ALICE MRPC ~ 60psec*

ALICE-TOF has 10 gaps (two stacks of 5 gas gaps); each gap is 250 micron wide

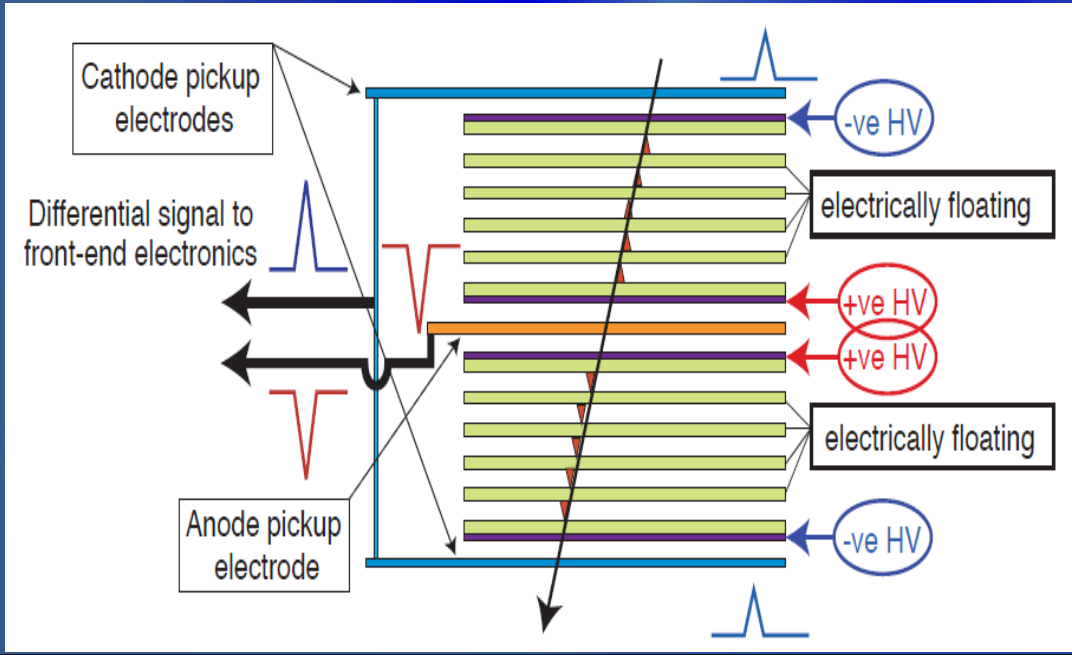

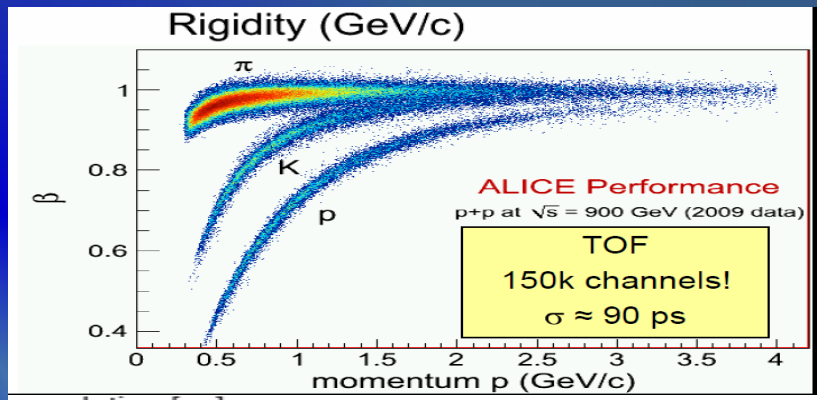

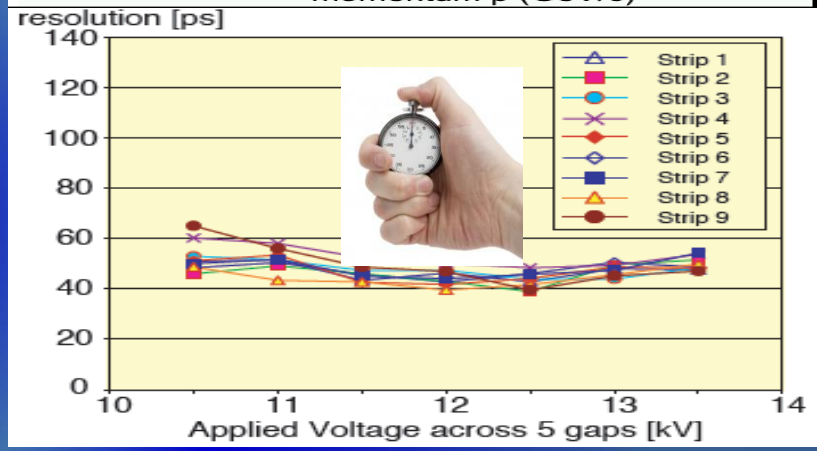

Technology	Time resolution
• Pestov Counter	30-50 ps
• RPC	~ 1-5 ns (MIP)
• MultiGap RPC	~ 50 ps (MIP)
• GEM	~ 1-2 ns (UV) ~ 5-10 ns (MIP)
• Micromegas	~ 700 ps (UV) ~ 5-10 ns (MIP)

ALICE MDT: Resolution Limits of High-Rate Wire Chambers

L3 Muon Spectrometer (LEP):

~ 40000 chan. ; σ (chamber) < 200 μm

ATLAS Muon Drift Tubes (LHC):

~ 1200 chambers, σ (chamber) ~ 50 μm

- *370000 tubes, 740000 end-plugs*
- *12000 CCD for optical alignment*

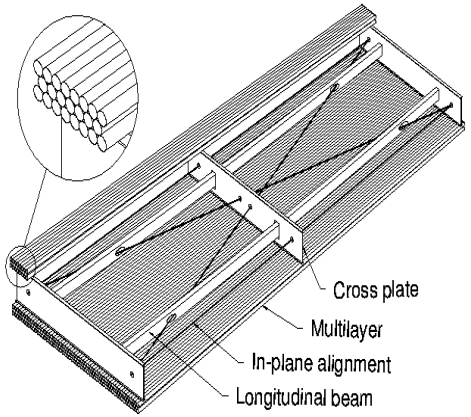

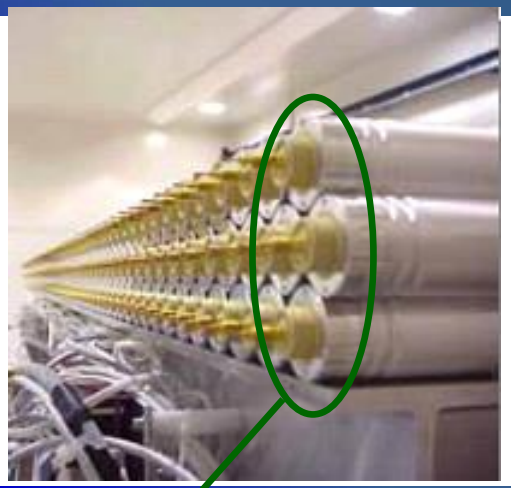

Intrinsic limitation of wire chambers:
(resolution degradation at high rates):

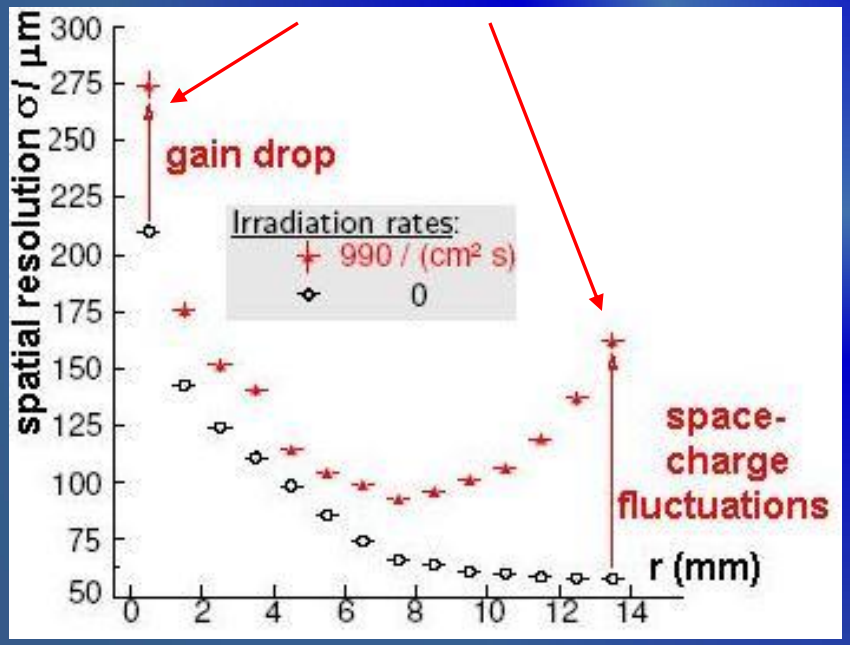

1 chamber → 2 layers of 3 drift tubes
Spatial resolution /chamber (2 layers of 3 drift tubes)

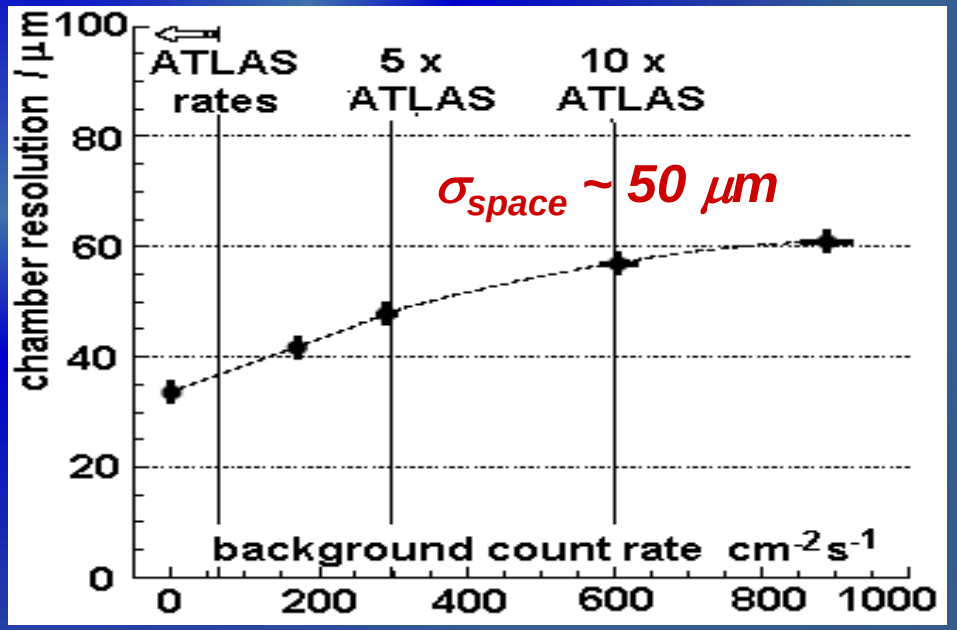

Micro-Pattern Gaseous Detectors: Bridging the Gap for Tracking between Wire Chambers and Silicon-based Devices

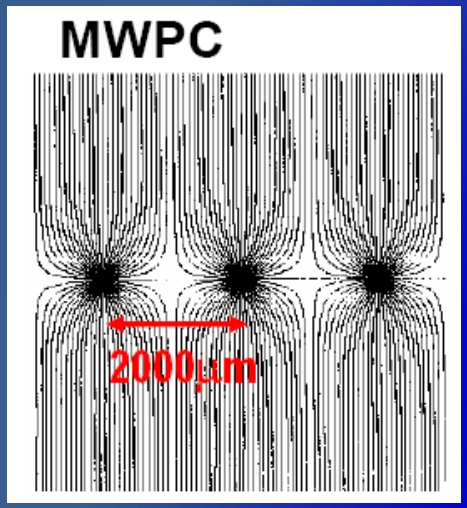

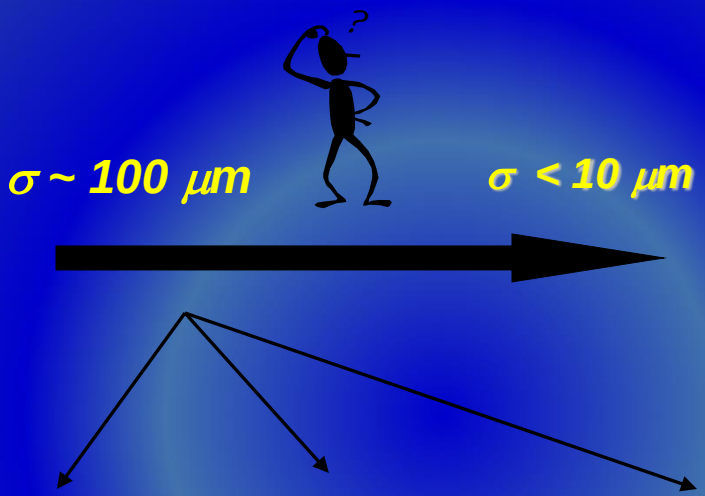

Pixel System:

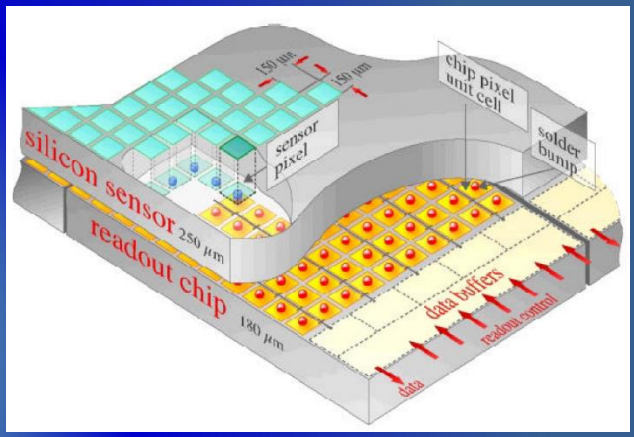

Advantages of gas detectors:

- *low radiation length*
- *large areas at low price*
- *flexible geometry*
- *spatial, energy resolution …*

Problem:

✓ *rate capability limited by space charge defined by the time of evacuation of positive ions*

Solution:

✓ ***reduction of the size*** *of the detecting cell (limitation of the length of the ion path)* ***using chemical etching and photo-lithographique techniques*** *developed for microelectronics and keeping at same time similar field shape.*

Micro-Strip Gas Chamber (MSGC): An Early MPGD

Multi-Wire Proportional Chamber (MWPC)

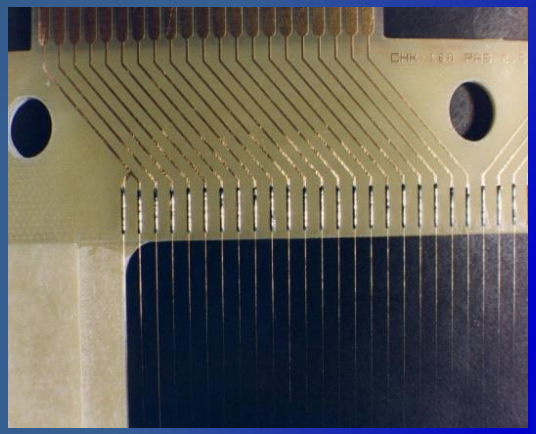

Typical distance between wires limited to ~1 mm due to mechanical and electrostatic forces

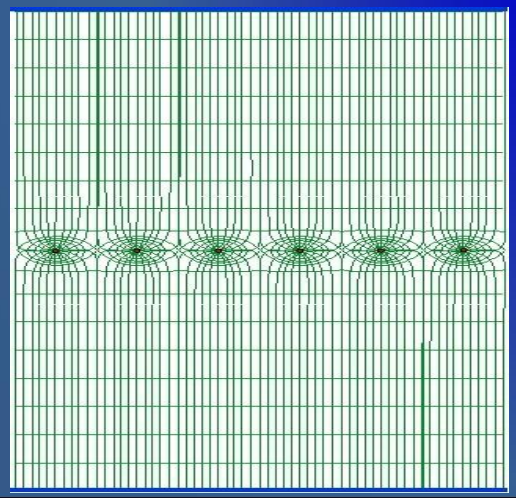

Micro-Strip Gas Chamber (MSGC)

A. Oed, NIMA263 (1988) 351

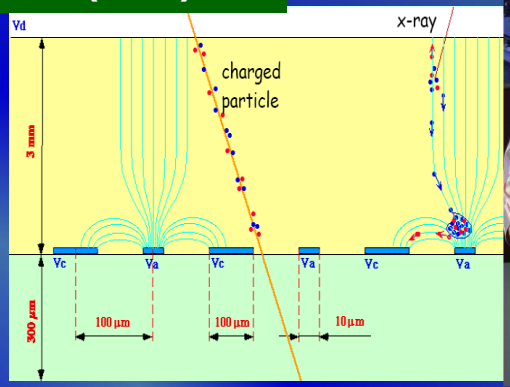

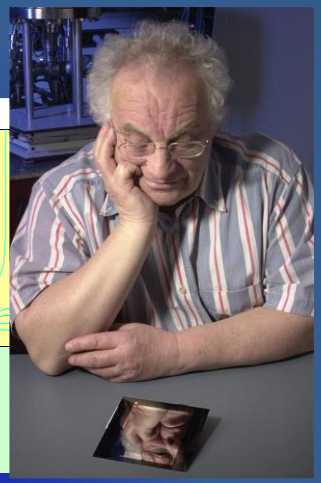

Excellent spatial resolution

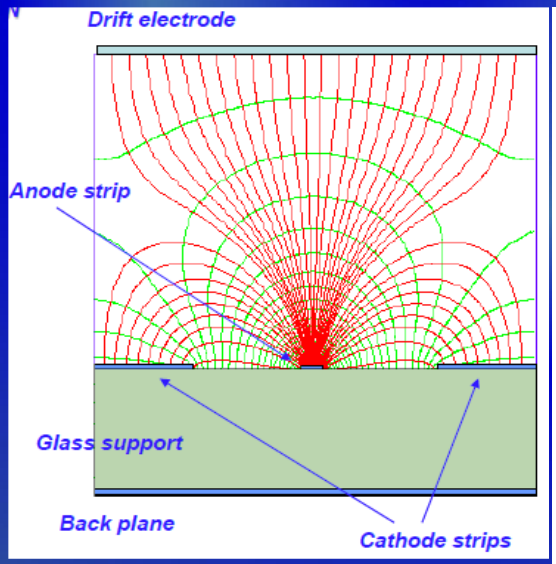

Typical distance between electrodes ~100 µm

MSGC significantly improves rate capability due to fast removal of positive ions

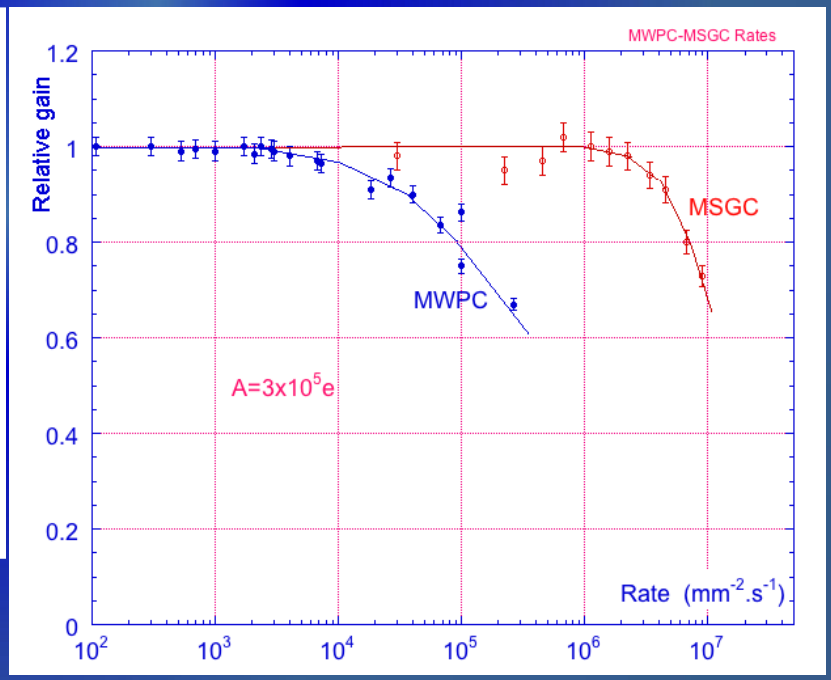

Micro-Strip Gas Chamber (MSGC): Discharge Problems

For efficient detection of minimum ionizing tracks a gain ~ 5000 is needed:

→ No discharges with X-rays and electrons;

→ Discharge probability is large ~ many per min (heavy ionizing particles)

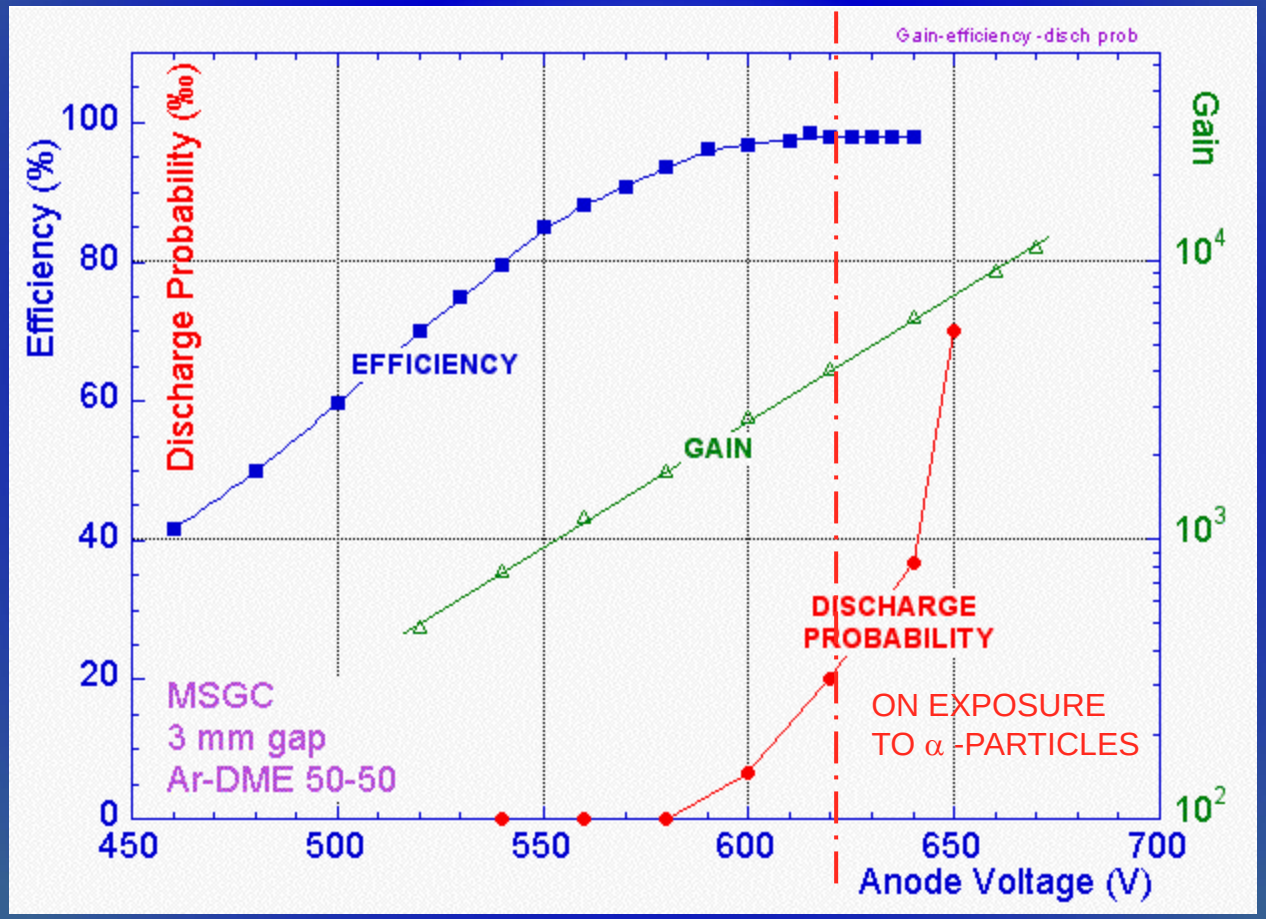

Induced discharges are intrinsic property of all single stage MPGDs in hadronic beams (MSGC turned out to be prone to irreversible damages)

Micro-Strip Gas Chamber (MSGC): Discharge Problems

Major processes leading at high rates to MSGC operating instabilities:

- ✓ **Substrate charging-up and time-dependent modification of the E field**
  → slightly conductive support

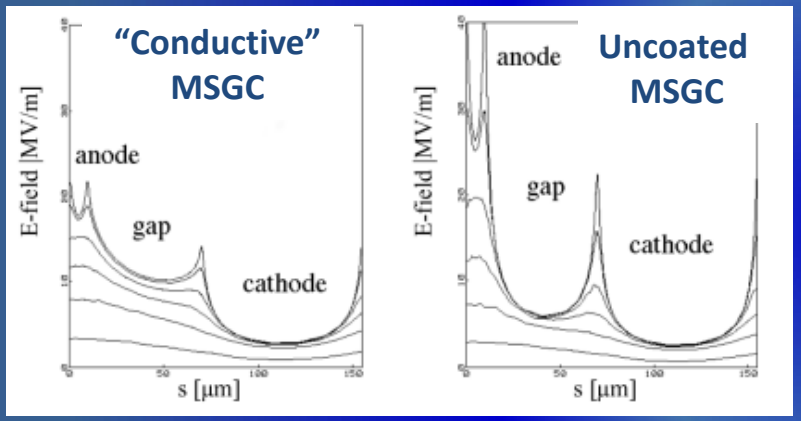

- ✓ **Deposition of polymers (aging)**
  → validation of gases, materials, gas systems

- ✓ **Discharges under exposure to highly ionizing particles**
  → multistage amplification, resistive anodes

FIELD EMISSION FROM CATHODE EDGE

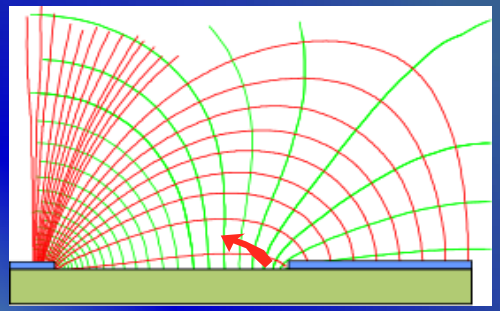

CHARGE PRE-AMPLIFICATION FOR IONIZATION RELEASED IN HIGH FIELD CLOSE TO CATHODE

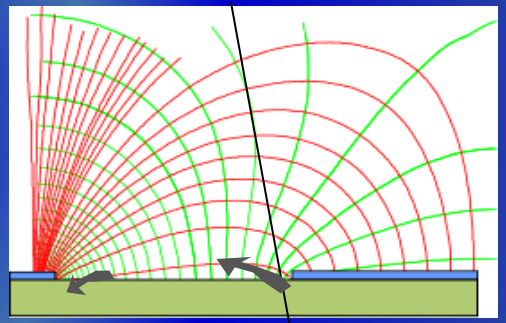

VERY HIGH IONIZATION RELEASE FROM HEAVILY IONIZING PARTICLES:

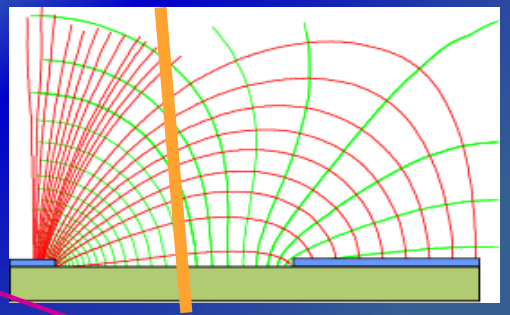

High Fields

Small Gap

Discharge

Valid for all micro-pattern detectors - Law of Nature!!!

MSGC Discharge Problems

Excellent spatial resolution, but poor resistance to discharges

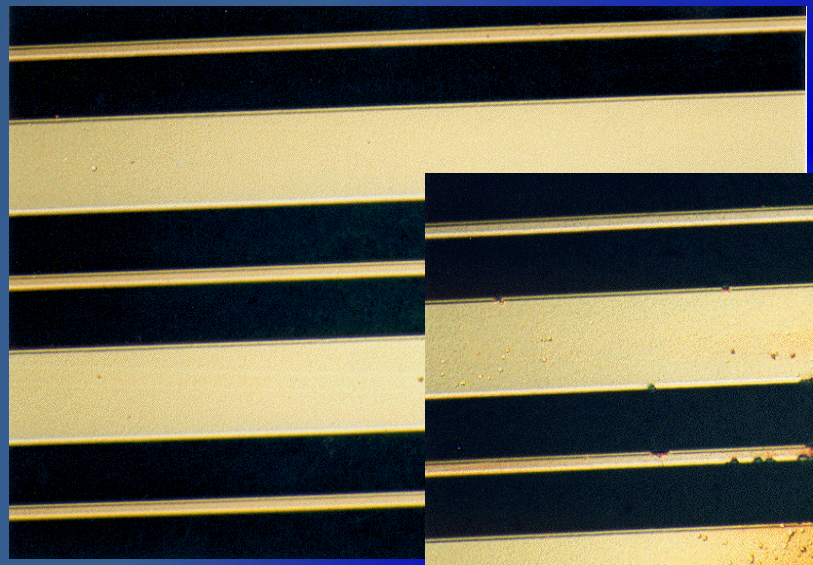

Discharge is very fast (~ns)
Difficult to predict or prevent

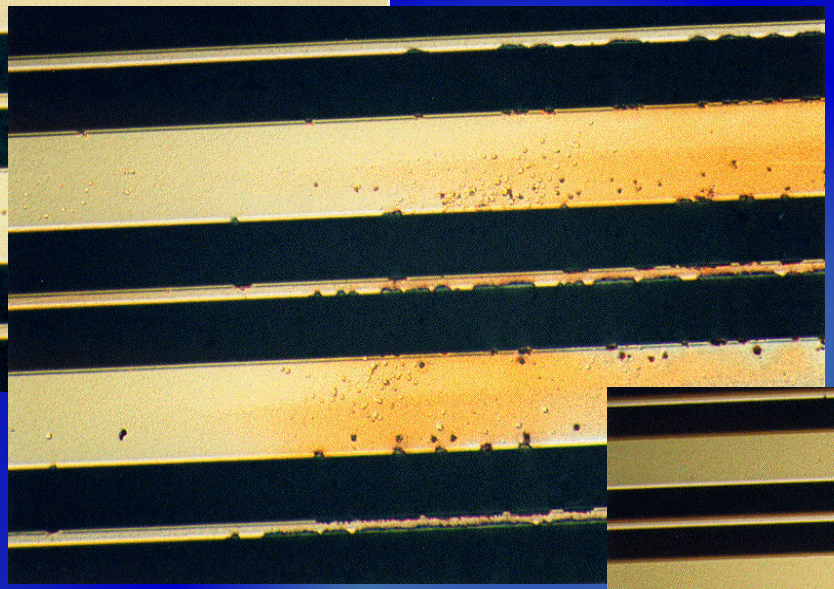

MICRODISCHARGES

Owing to very small distance between anode and cathode the transition from proportional mode to streamer can be followed by spark, discharge, if the avalanche size exceeds RAETHER'S LIMIT
$Q \sim 10^7 - 10^8$ electrons

FULL BREAKDOWN

MSGC In Experiments

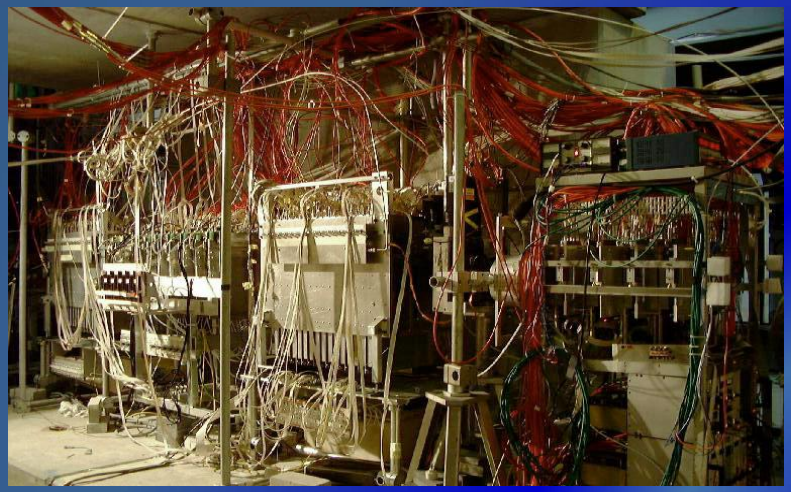

Telescope of 32 MSGCs
tested at PSI inNov99 (CMS Milestone)

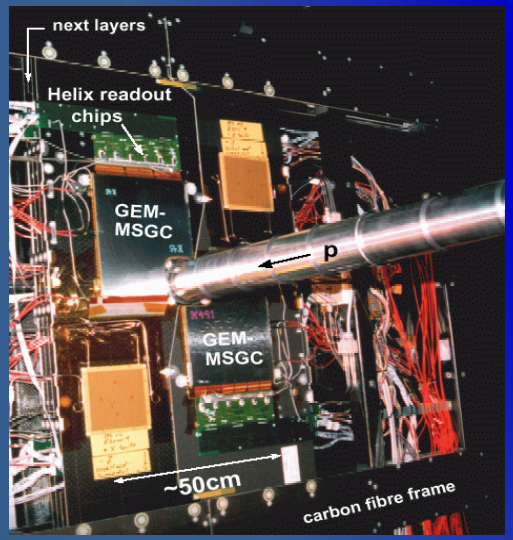

HERA-B Inner Tracker
MSGC-GEM detectors
R_{min} ~ 6 cm
$\Rightarrow 10^6$ particles/cm^2 s
300 um pitch
184 chambers: max 25x25 cm^2
~ 10 m^2; 140.000 channels

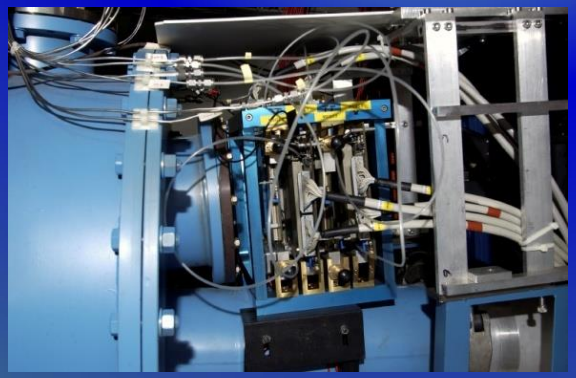

The D20 diffractometer MSGC is working since Sept 2000
1D localisation
48 MSGC plates (8 cm x 15 cm)
Substrate: Schott S8900
Angular coverage : 160° x 5,8°
Position resolution : 2.57 mm (0,1°)
5 cm gap; 1.2 bar CF4 + 2.8 bars 3He

DIRAC
4 planes MSGC-GEM
Planes 10x10 cm^2

Aging Phenomena in Wire Chambers

Avalanche formation close to wire can be considered as a micro plasma discharge ...and plasma chemistry not well understood in general:

black magic...

Whereas most ionization processes require electron energies > 10 eV, the breaking of chemical bonds and formation of free radicals requires ~ 3-4 eV

- ✓ dissociation of detector gas and pollutants
- ✓ formation of highly active radicals (many expected to have large dipole moments)
- ✓ polymerization of organic quenchers
- ✓ insulating deposits on anodes and cathodes

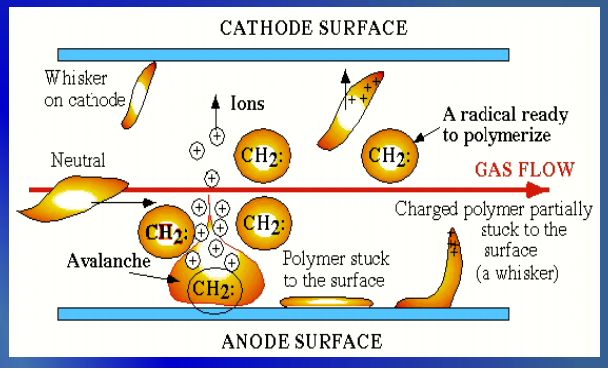

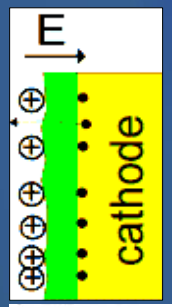

Anode: increase of wire diameter
reduced and variable E-field
variable gain and energy resolution

Cathode: (Malter Effect) ions on top of insulating layer cannot recombine built-up of strong E-field across insulating electron field emission and microdischarges

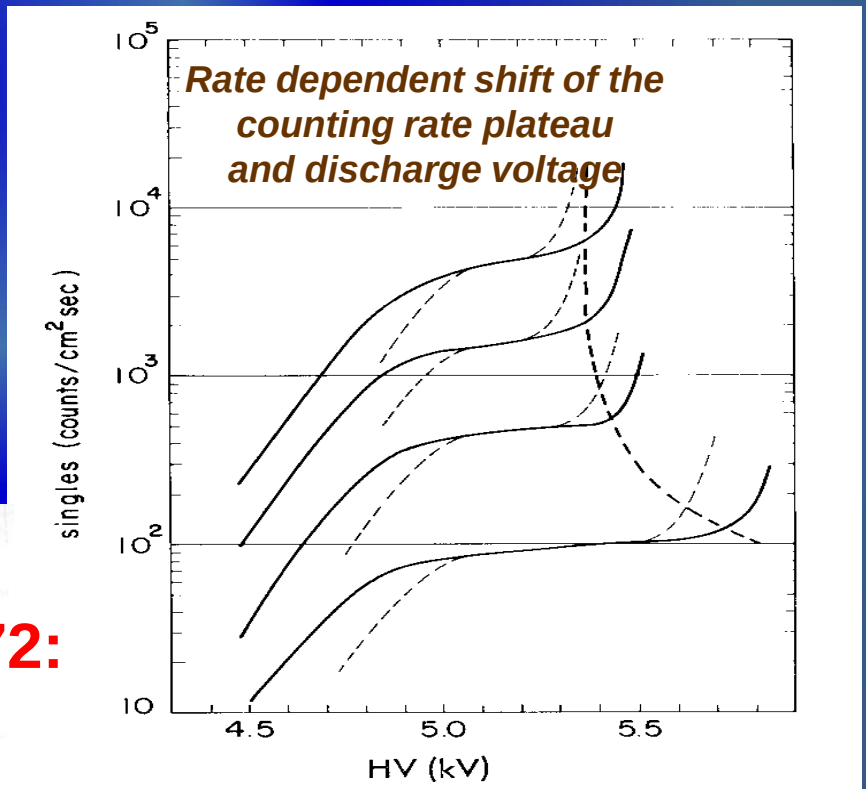

NUCLEAR INSTRUMENTS AND METHODS 99 (1972) 279–284; © NORTH-HOLLAND PUBLISHING CO.

TIME DEGENERACY OF MULTIWIRE PROPORTIONAL CHAMBERS

G. CHARPAK, H. G. FISHER, C. R. GRUHN, A. MINTEN, F. SAULI and G. PLCH
CERN, Geneva, Switzerland
and
G. FLÜGGE
II. Institut für Experimentalphysik, Hamburg, Germany

Received 28 May 1971

The deterioration with time of multiwire proportional chambers using isobutane as one component of the gas mixture is studied. It is shown that by addition of methylal among others, a long lifetime can be obtained without changing the properties of the gas mixture. Irradiation tests of 5×10^{10}/cm² have not shown any alteration in the chamber performance.

1972:

Aging Phenomena in Wire Chambers: 1st Workshop (1986)

First systematic attempts to summarize aging results and to provide remedies minimizing wire chamber aging

Proceedings of the
Workshop on Radiation Damage to
Wire Chambers

1986:

Lawrence Berkeley Laboratory, Berkeley, California

January 16-17, 1986

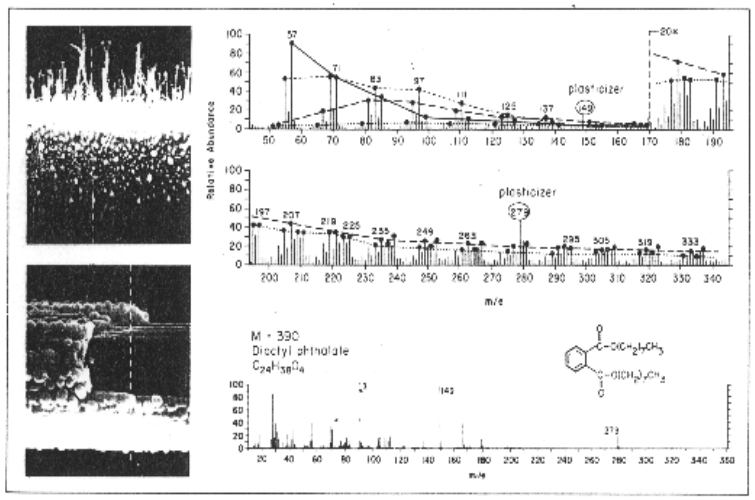

April 1986

Lawrence Berkeley Laboratory
University of California
Berkeley, California 94720

Nuclear Instruments and Methods in Physics Research A252 (1986) 547–563
North-Holland, Amsterdam

REVIEW OF WIRE CHAMBER AGING *

J. VA'VRA

Stanford Linear Accelerator Center, Stanford University, Stanford, California 94305, USA

This paper makes an overview of the wire chamber aging problems as a function of various chamber design parameters. It emphasizes the chemistry point of view and many examples are drawn from the plasma chemistry field as a guidance for a possible effort in the wire chamber field. The paper emphasizes the necessity of tuning of variables, the importance of purity of the wire chamber environment as well as it provides a practical list of presently known recommendations. In addition, several models of the wire chamber aging are qualitatively discussed. The paper is based on a summary talk given at the Wire Chamber Aging Workshop held at LBL, Berkeley on January 16-17, 1986. Presented also at Wire Chamber Conference, Vienna, February 25-28, 1986.

Nuclear Instruments and Methods in Physics Research A300 (1991) 436–479
North-Holland

Wire chamber aging *

John A. Kadyk

Lawrence Berkeley Laboratory, 1 Cyclotron Road, Berkeley, CA 94720, USA

Received 27 June 1990

An overview of wire chamber aging is presented. A history of wire aging studies and the manifestations of wire aging are reviewed. Fundamental chemical principles relating to wire chamber operation are presented, and the dependences of wire aging on certain wire chamber operating parameters are discussed. Aging results from experimental detectors and laboratory experiments are summarized. Techniques for analysis of wire deposits and compositions of such deposits are discussed. Some effects of wire material and gas additives on wire aging are interpreted in chemical terms. A chemical model of wire aging is developed, and similarities of wire chamber plasmas to low-pressure rf-discharge plasmas are suggested. Procedures recommended for reducing wire aging effects are summarized.

***Harmful are:* halogen or halocarbons, silicon compounds, oil, fats …**
CO_2 helps with water, and alcohol admixtures

Aging Phenomena in Gaseous Detectors: 2nd Workshop (2001)

IEEE TRANSACTIONS ON NUCLEAR SCIENCE, VOL. 49, NO. 4, AUGUST 2002 1609

Summary and Outlook of the International Workshop on Aging Phenomena in Gaseous Detectors (DESY, Hamburg, October 2001)

M. Titov, M. Hohlmann, C. Padilla, and N. Tesch

arXiv:physics/0403055 v1 9 March 2004

RADIATION DAMAGE AND LONG-TERM AGING IN GAS DETECTORS[1]

MAXIM TITOV

Institute of Physics, Albert-Ludwigs University of Freiburg, Hermann-Herder Str. 3, Freiburg, D79104, Germany and

Institute of Theoretical and Experimental Physics (ITEP), B. Cheremushkinskaya, 25, Moscow, 117259, Russia

International Workshop on

AGING PHENOMENA IN GASEOUS DETECTORS

DESY, Hamburg October 2-5, 2001

Topics will include:

- Coping with classical aging problems
- New aging effects
- Models and new insights from plasma chemistry
- Materials: Lessons for detectors and gas systems
- Experiences with large detector systems
- Recommendations for future detectors

Deadline for registration: August 1, 2001

Deadline for submission of abstracts: June 29, 2001

Proceedings to be published in Nuclear Instruments and Methods A

International Advisory Committee

M. Danilov (ITEP Moscow) — V. Peskov (Lund)
B. Dolgoshein (MEPHI Moscow) — F. Sauli (CERN)
D. Froidevaux (CERN) — I. Shipsey (Purdue)
J. Kadyk (LBL) — J. Va'vra (SLAC)
P. Krizan (Ljubljana) — A. Wagner (DESY)

Local Organizing Committee

M. Hohlmann (chair, DESY)
C. Padilla (DESY)
N. Tesch (DESY)
M. Titov (ITEP Moscow)
I. Kerkhoff, R. Matthee (secretaries)

Registration, Contact & Info

Register and submit abstracts online at
http://www.desy.de/agingworkshop
Contact: aging.workshop@desy.de
Tel.: +49 40 8998-4600
FAX: +49 40 8998-4900

- ✓ ***The HERA-B Experiment was the first high-rate experiment, which addressed SYSTEMATICALLY aging phenomena in gas detectors, followed later by ALL LHC experiments***
- ✓ ***Many ORIGINAL PROBLEMS in HIGH RATE GAS DETECTORS were due to CASUAL SELECTION of chamber designs, gas mixtures, materials and gas system components, which worked at "low rates", but failed in high-rate environments***

Table 1. Aging results with wire detector prototypes for the use at high energy physics facilities.

Experiment, Detector, Reference	Gas Mixture	Gain reduction/ etching	Cathode aging	Charge C/cm	Gas gain(G); Current density(I); Rate (R), Irradiated area (S)
HERA-B OTR [34]	$Ar/CF_4/CO_2$ (65:30:5)	No/Au damage	No	0.6	G~$3*10^4$; I~0.4-0.9μA/cm; 100MeV π-beam; S~50cm^2
HERA-B MUON [35]	$Ar/CF_4/CO_2$ (65:30:5)	No	No/F-film on Al cath.	0.7	G~10^4-10^5; I ~ 0.3μA/cm; R<10^6 Hz/cm^2; S~1200cm^2
HERA-B MUON[35]	Ar/CF_4 (70:30)	No	No	0.07	G~10^5; I ~ 0.15μA/cm; R~10^6 Hz/cm^2; S~150cm^2
ATLAS TRT [15,48]	$Xe/CF_4/CO_2$ (70:20:10)	No	No	20	G~ $3*10^4$; I ~ 0.7 μA/cm; S~24 cm^2
Straw R&D[45]	$Xe/CF_4/CO_2$ (70:20:	No/Au	No	9	G~$3*10^4$; I ~ 1.7μA/cm; m^2
Straw R&D[45]	$Ar/CF_4/$ (60:10:				;
CMS MUON [14]	$Ar/CF_4/$ (40:10:50)	cracks	on Cu cath.		R~$2*10^6$ Hz/cm^2; S~1cm^2
CMS MUON [46]	$Ar/CF_4/CO_2$ (40:10:50)	No	Si-F film on Cu cath.	0.4	G~10^5; I < 0.05 μA/cm; R~$2*10^6$ Hz/cm^2;S~21000cm^2
LHC-B MUON [52]	$Ar/CF_4/CO_2$ (40:10:50)	No	Etching of FR4 bars	0.25	G~10^5; I < 0.03 μA/cm; R~$3*10^6$ Hz/cm^2; S~1500cm^2
COMPASS Straws [53]	$Ar/CF_4/CO_2$ (74:20:6)	No/ Si-traces	No	1.1	G~$4*10^4$; I ~ 4 μA/cm; R~$2*10^6$ Hz/cm^2; S~3 cm^2
HERMES FD [47]	$Ar/CF_4/CO_2$ (90:5:5)	No	Al etching/ Cl deposits	9	G~$5*10^4$; I ~ 1 μA/cm; R~10^5 Hz/cm^2; S~7 cm^2
ATLAS TRT[16]	$Xe/CO_2/O_2$ (70:27:3)	No	No	11	G~ $3*10^4$; I ~ 1-3 μA/cm; S~1 cm^2
ATLAS TRT[16]	$Xe/CO_2/O_2$ (70:27:3)	No/Si-deposits	No	0.3	G~$3*10^4$; I ~ 0.1 μA/cm; S~1 cm^2
ATLAS MDT[55]	Ar/CO_2 (90:10)	No	No	0.7	I ~ 0.1μA/cm; R~$4*10^5$ Hz/cm^2;S~7500cm^2
ATLAS MDT[56]	Ar/CO_2 (93:7)	No	No	>1.5	G~$2*10^4$; I ~ 0.05-0.2μA/cm; R~$8*10^5$-10^6Hz/cm^2;S~90cm^2
ATLAS MDT[57]	Ar/CO_2 (93:7)	Yes/Si-deposits	No	0.2	G~$9*10^4$; I ~ 0.02μA/cm; R~$5*10^5$ Hz/cm^2;S~15000cm^2
CMS MUON[14]	Ar/CO_2 (30:70)	Yes/ Si-deposits	No	0.76	G~$6*10^4$; I ~ 2 μA/cm; R~$2*10^6$ Hz/cm^2; S~ 1 cm^2

Wire chambers

Table 2. Summary of aging experience with Micro-Pattern Gas Detectors.

Detector type	Mixture	Gain reduction Δ G/G	Charge m C/mm^2	Current density, nA/mm^2	Irradiate d area; Irradiation rate	Irrad. source
MSGC [65,104]	Ar/DME (90:10)	No	200	10	3 mm^2; 10^5 Hz/mm^2	6.4 keV X-rays;
MSGC [66]	Ar/DME (50:50)	No	40	63	0.3*0.8mm^2; $8*10^2$ Hz/mm^2	5.4 keV X-rays
MSGC [66]	Ar/DME (50:50)	Anode deposit	50	9	0.3*0.8mm^2; $2*10^2$ Hz/mm^2	5.4 keV X-rays
MSGC+GEM [66]	Ar/DME (90:10)	No	70	63	0.3*0.8mm^2; $2*10^2$ Hz/mm^2	5.4 keV X-rays
MSGC+GEM [51]	Ar/DME (50:50)	No	5	2	~ 113 mm^2; $2*10^2$ Hz/mm^2	8 keV X-rays
MSGC+GEM [51]	Ar/DME (50:50)	Yes	0.5	1	~ 900 mm^2; 10^2 Hz/mm^2	8 keV X-rays
MSGC+GEM [51]				2	350 mm^2 $2*10^2$ Hz/mm^2	8 keV X-rays
Double GEM [67]				6	2 mm^2; $7*10^2$ Hz/mm^2	5.4 keV X-rays
Triple GEM [68]				13	1.5 mm^2; $6*10^2$ Hz/mm^2	5.4 keV X-rays
Double GEM [69]	Ar/CO_2 (70:30)	No	12	4	200 mm^2; $5*10^2$ Hz/mm^2	6 keV X-rays
Triple GEM [70]	Ar/CO_2 (70:30)	No	11	10	1260 mm^2; $2*10^2$ Hz/mm^2	8.9 keV X-rays
Triple GEM [71,72]	$Ar/CF_4/CO_2$ (60:20:20)	< 5 %	230	270	1 mm^2; $5*10^2$ Hz/mm^2	5.9 keV X-rays
Triple GEM [72]	$Ar/CF_4/CO_2$ (45:40:15)	< 5 %	45	160	1 mm^2; $5*10^2$ Hz/mm^2	5.9 keV X-rays
Triple GEM [73]	$Ar/CF_4/CO_2$ (45:40:15)	Yes/ 55%	20	20	200*240 mm^2	25 kCi ^{90}Co
Triple GEM [72]	$Ar/CF_4/CH_{10}$ (65:28:7)	~ 10 %	110	160	1 mm^2; $5*10^2$ Hz/mm^2	5.9 keV X-rays
Triple GEM+ CsI [88]	CF_4 (100)	No	0.1	3	100 mm^2; 10^2 Hz/mm^2	Hg UV Lamp
Micromegas [74]	Ne/C_4H_{10} (91:9)	Yes/ 35 %	10	50	16 mm^2; 33Hz spark rate	5.3 MeV α's
Micromegas [75]	Ar/CF_4 (95:5)	No	2	10	--------	8 keV X-rays
Micromegas [76]	CF_4/C_4H_{10} (94:6)	No	1.6	25	20 mm^2; ~10^2 Hz/mm^2	8 keV X-rays
Micromegas [76]	Ar/C_4H_{10} (94:6)	No	18	20	20 mm^2; $2*10^2$ Hz/mm^2	8 keV X-rays
Micromegas+ GEM[77]	Ar/CO_2 (70:30)	No	23	17	3 mm^2	5.4 keV X-rays
MSGC+GEM DIRAC [64]	Ar/DME (60:40)	10 % eff. drop	0.01	0.05	100*100 mm^2; $3*10^2$ Hz/mm^2	24 GeV protons
3-GEM [78] COMPASS	Ar/CO_2 (70:30)	No	2.3	--	310*310 mm^2; $2*10^2$ Hz/mm^2	Compass Beam

MPGDs

Aging Phenomena in Gaseous Detectors

Implicit assumption: ***aging rate is proportional only to the total accumulated charge***

$$R = -(1/G)(dG/dQ) \quad (\%\ \text{per C/cm})$$ **(Kadyk'1985)**

Aging phenomena depends on many highly correlated parameters:

Microscopic parameters:

- ✓ Cross-sections
- ✓ Electron or photon energies
- ✓ Electron, ion, radical densities
- ✓ …

Macroscopic parameters:

- ✓ Gas mixture (nature of gas, trace contaminants)
- ✓ Gas flow & Pressure
- ✓ Geometry/material of electrodes & configuration of electric field

~1980

CLASSICAL AGING:

There are simply too many variables in the problem →

would be too naive to expect that one can express the aging rate using a single variable (C/cm)

- ✓ Construction materials
- ✓ Radiation intensity
- ✓ Gas gain, ionization density
- ✓ Size of irradiation area

'NEW AGING' EFFECTS:

~2000

Aging Phenomena in Gaseous Detectors

- ✓ *Early aging studies of MSGCs indicated that they are much more susceptible to aging than wire chambers, potentially due to the filigree nature of MSGC structures and catalytic effects on the MSGC substrate*
- ✓ *More robust detectors (GEM, Micromegas) are better suited for the high-rate environments than MSGC and Wire-type detectors*

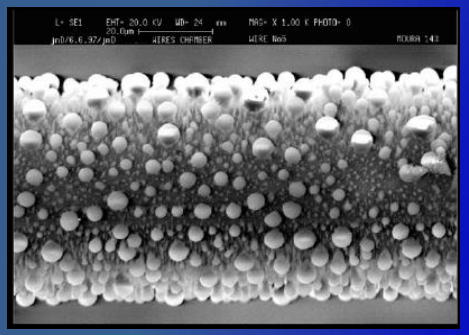

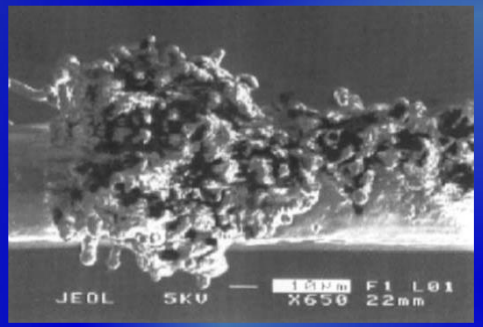

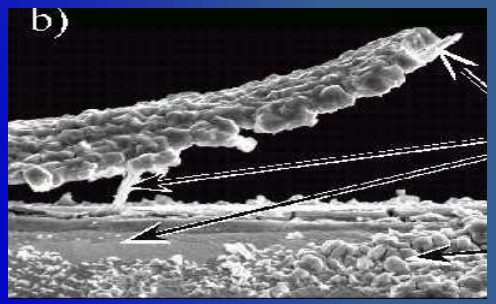

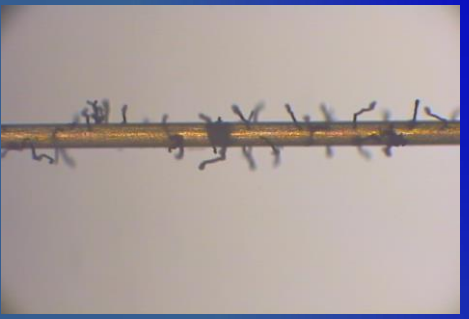

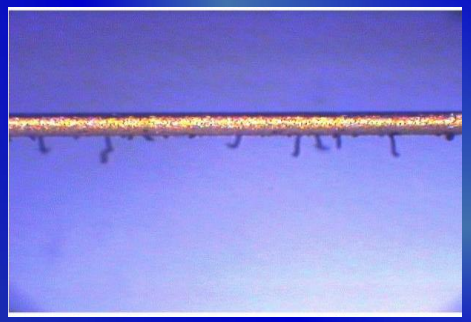

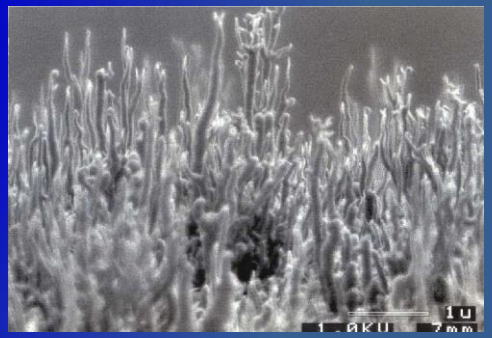

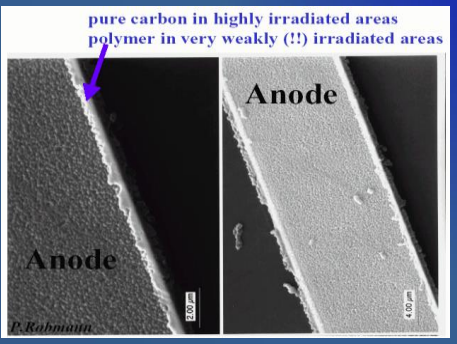

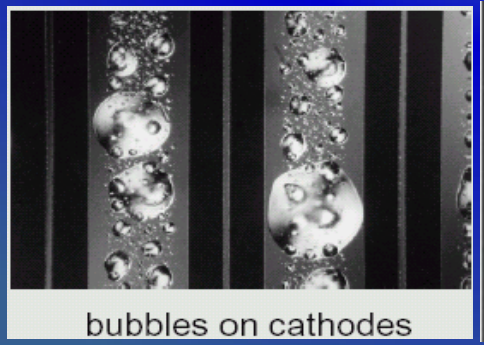

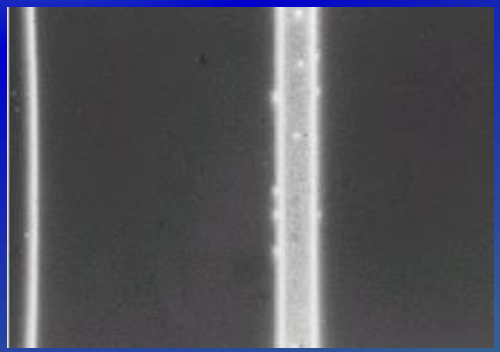

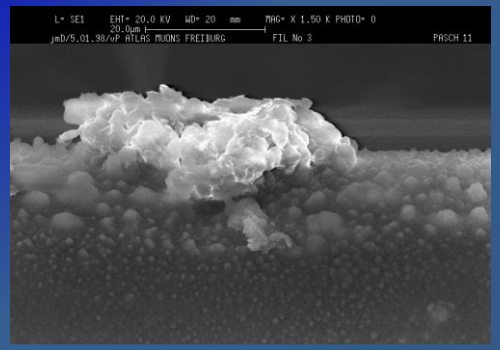

Building Radiation-Hard Gas Detector (2001): Rules of Thumb

- ✓ *Build a "full-size prototype" (the smallest independent element of your detector)*
- ✓ *Expose full detector area of to the real radiation profile (particle type, gas gain, ionization density)*
- ✓ *Choose your gas mixtures (hydrocarbons are not trustable) and materials very carefully*
- ✓ *Vary all parameters systematically (gas gain, irradiation intensity, gas flow, …) and verify your assumptions → make aging studies on several identical prototypes*
- ✓ *Do not extrapolate aging results for any given parameter by more than an order of magnitude*
- ✓ *If you observed unexpected result - understand the reason – and reproduce results …*

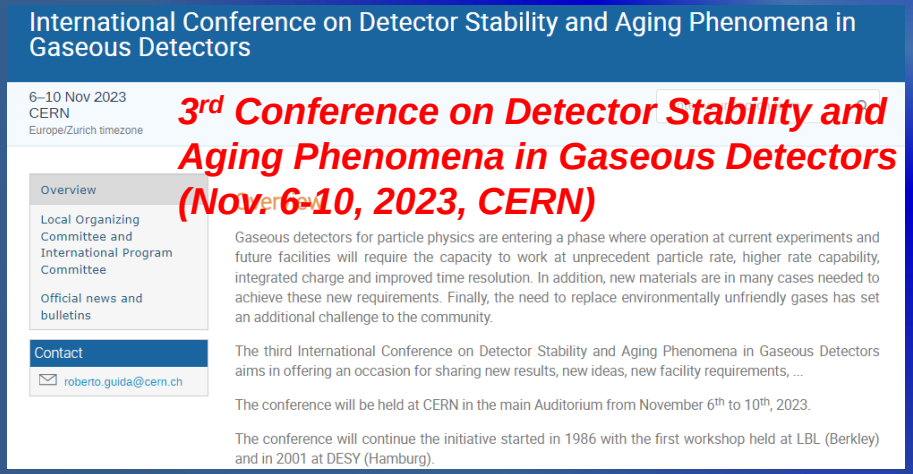

Micro-Pattern Gaseous Detector Technologies (MPGD)

- ✓ *Micromegas*
- ✓ *Gas Electron Multiplier (GEM)*
- ✓ *Thick-GEM (LEM), Hole-Type & RETGEM*
- ✓ *MPDG with CMOS pixel ASICs ("GridPix")*

- ✓ *Micro-Pixel Chamber (μ–PIC)*
- ✓ *μ–Resistive WELL (μ-RWELL)*
- ✓ *Resistive-Plate WELL (RPWELL)*

Rate Capability: MWPC vs GEM:

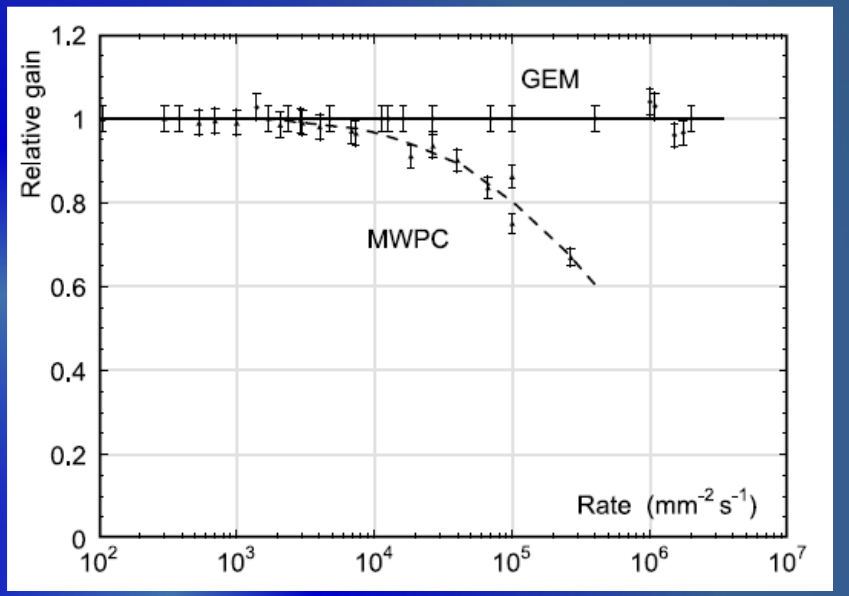

Micromegas ***GEM*** ***THGEM***

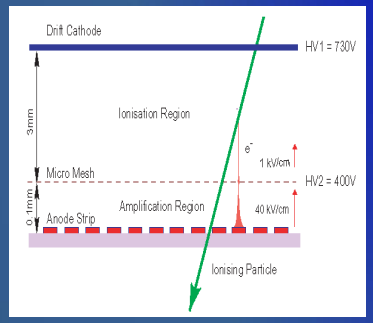

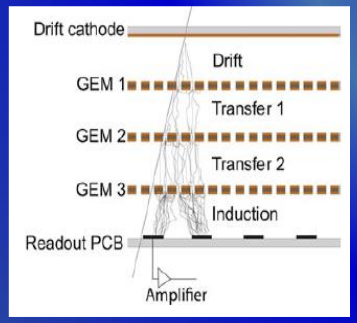

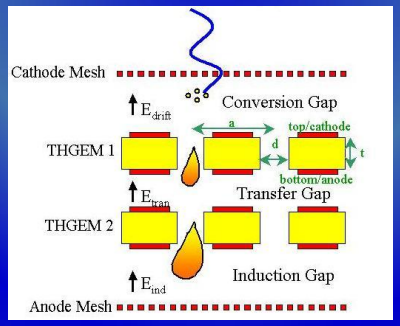

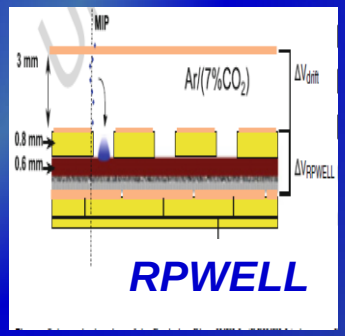

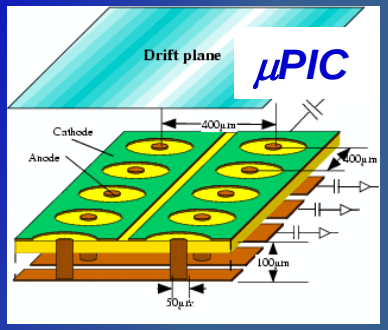

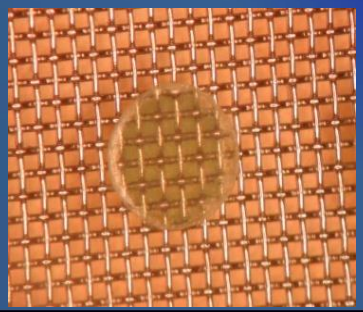

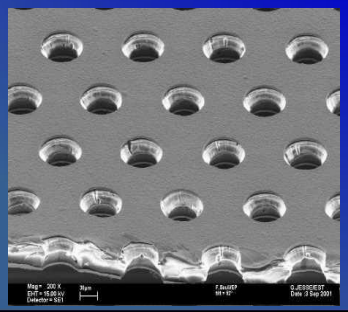

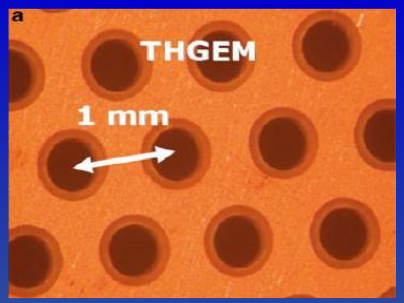

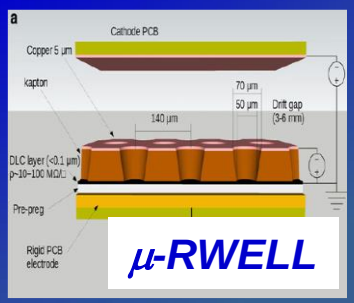

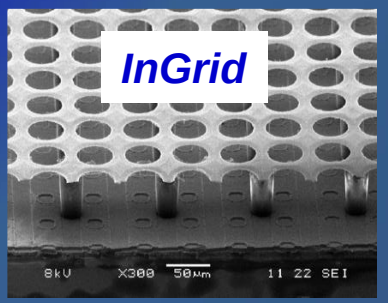

Gas Electron Multiplier (GEM)

Thin metal-coated polymer foil chemically pierced by a high density of holes

A difference of potentials of ~ 500V is applied between the two GEM electrodes.

→ the primary electrons released by the ionizing particle, drift towards the holes where the high electric field triggers the electron multiplication process.

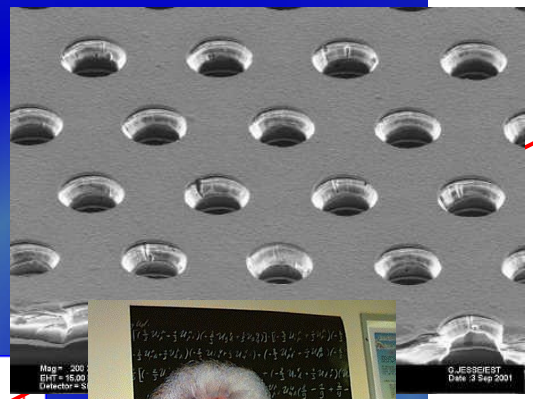

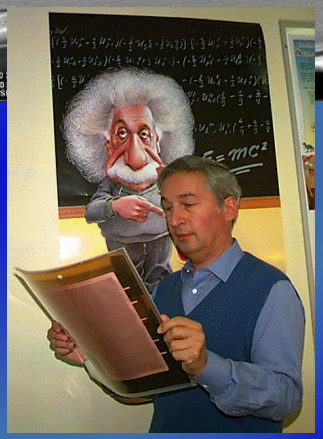

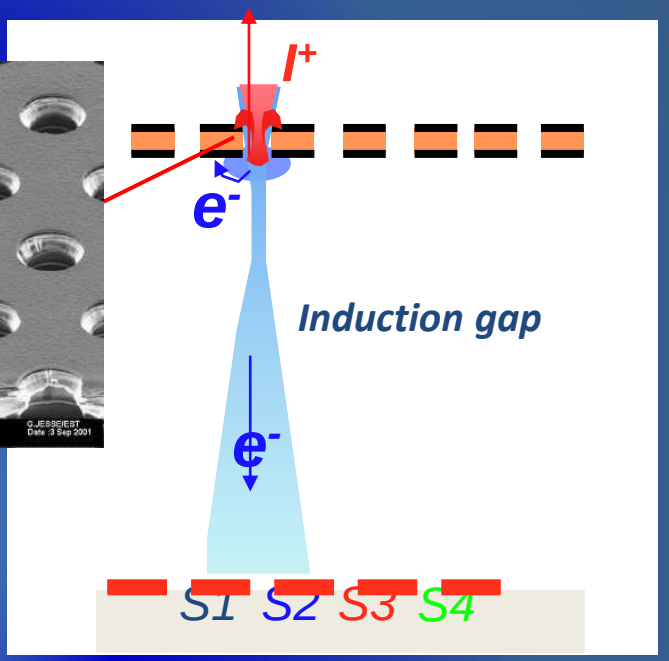

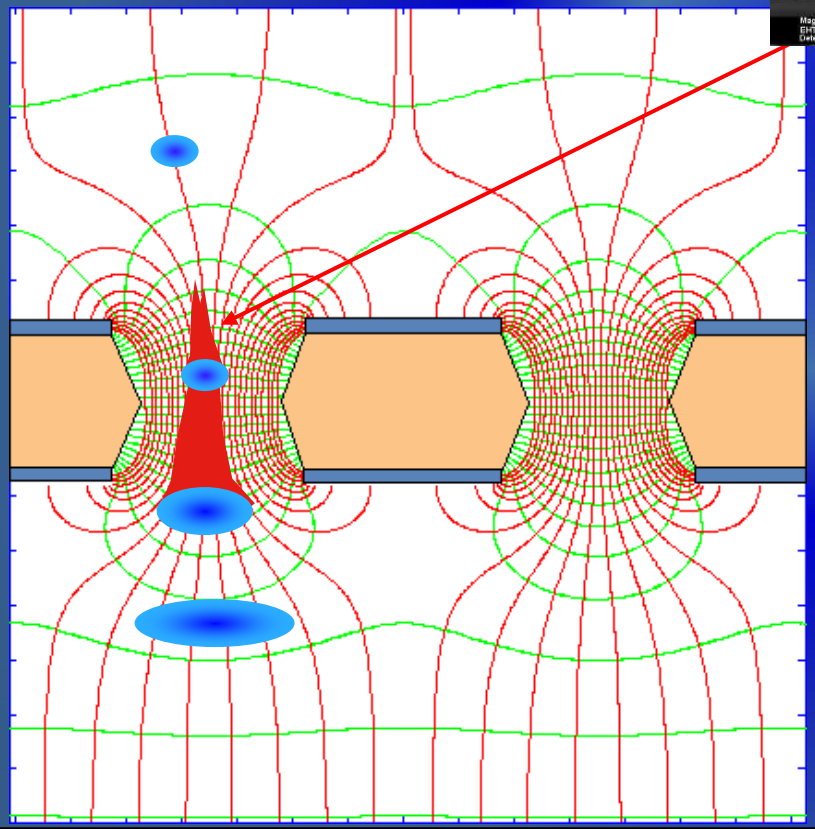

F. Sauli, NIMA386 (1997) 531

- ✓ Electrons are collected on patterned readout board.
- ✓ A fast signal can be detected on the lower GEM electrode for triggering or energy discrimination.
- ✓ All readout electrodes are at ground potential.
- ✓ Positive ions partially collected on GEM electrodes

Avalanche Simulation in GEM & Triple-GEM Structures

Animation of the avalanche process (Garfield++): ***monitor in ns-time electron/ ion drifting and multiplication in GEM***

http://cern.ch/garfieldpp/examples/gemgain

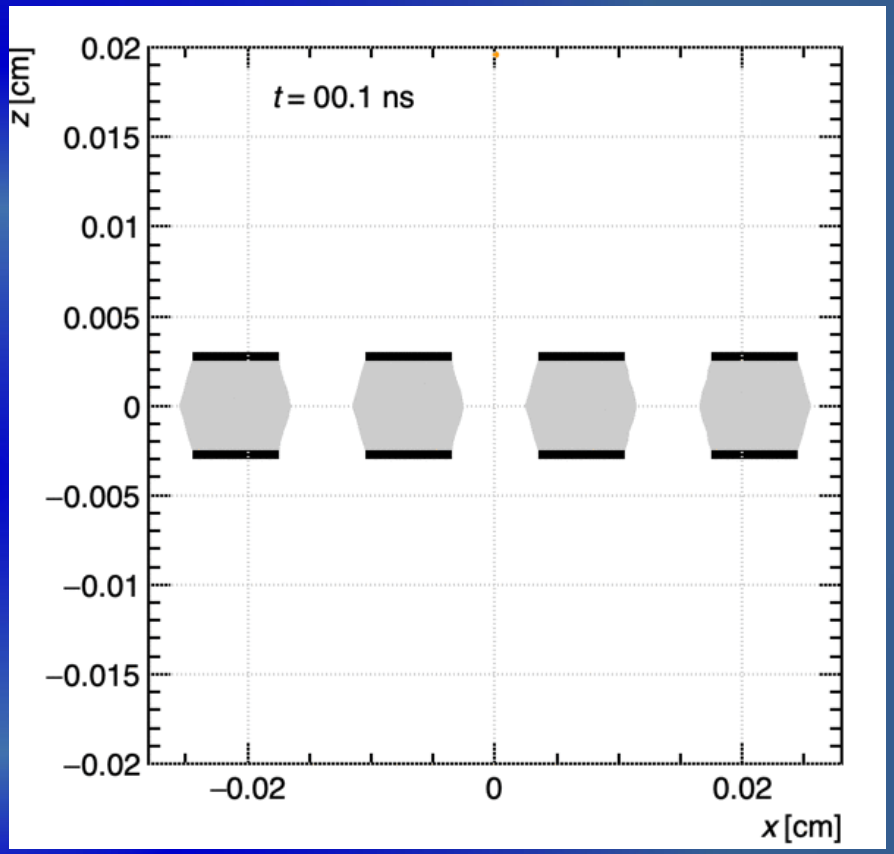

Full decoupling of amplification stage (GEM) and readout stage (PCB, anode)

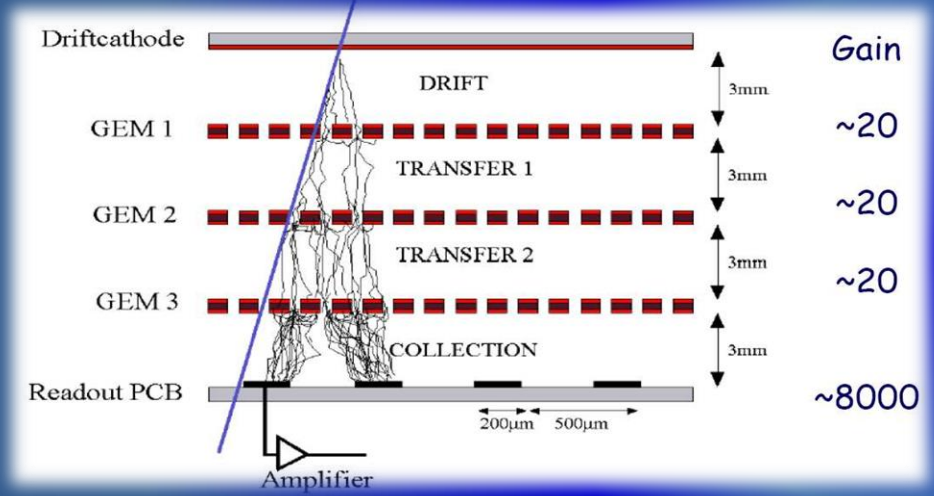

Amplification and readout structures can be optimized independently !

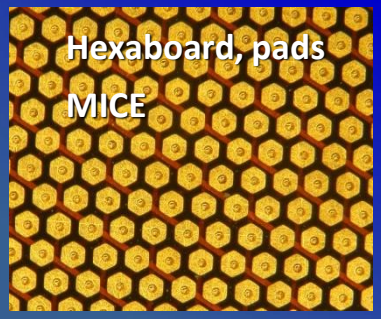

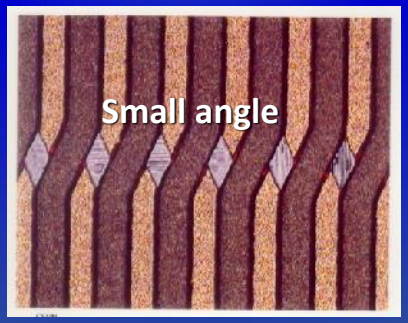

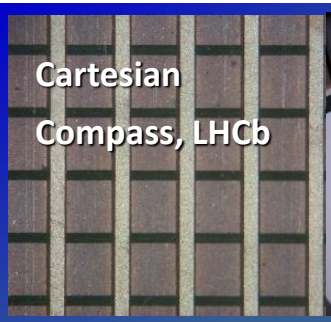

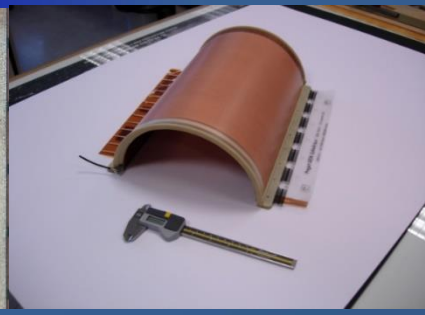

Micro Mesh Gaseous Structure (MICROMEGAS)

Micromesh Gaseous Chamber:
micromesh supported
by 50-100 mm insulating pillars

Small gap: fast collection of ions

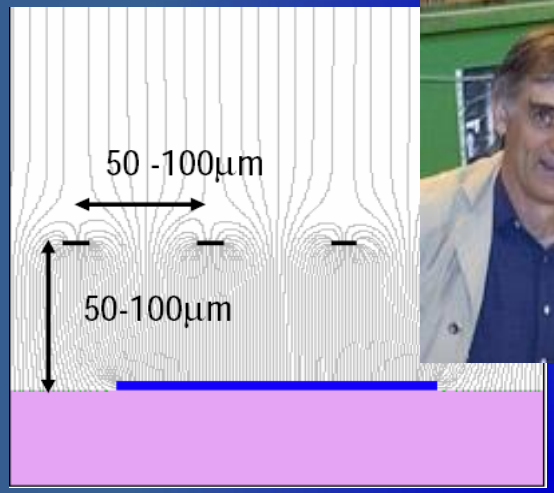

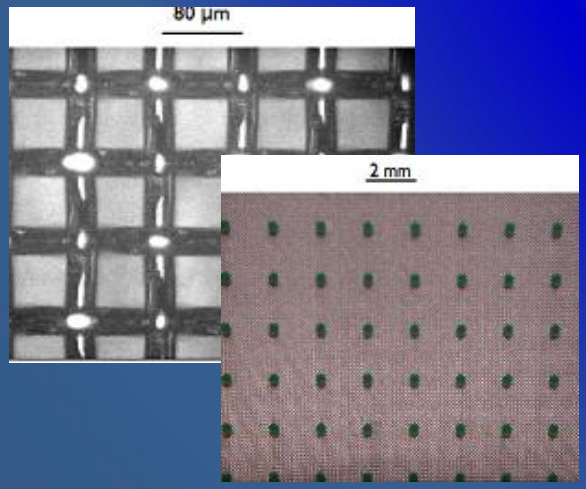

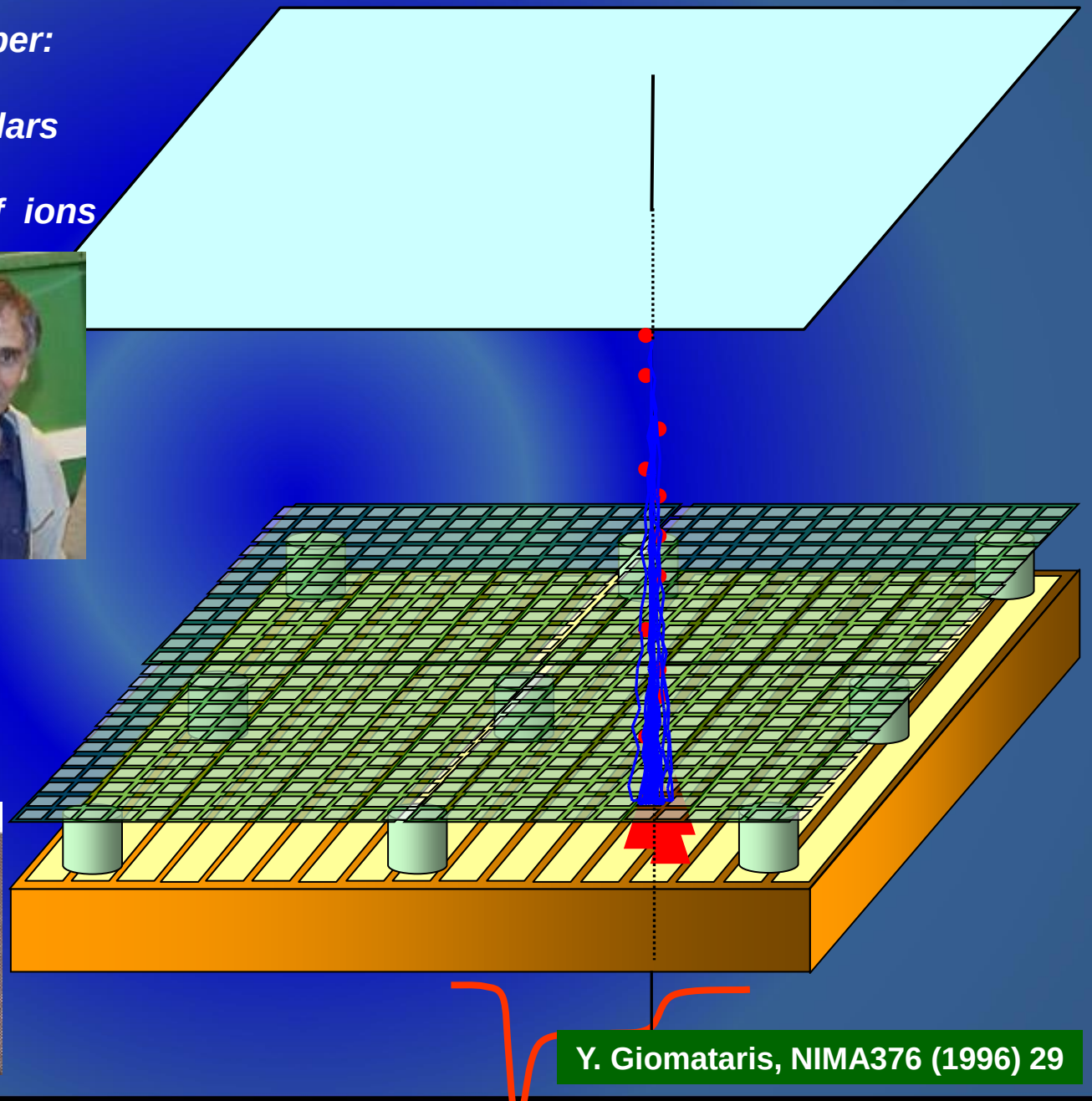

Y. Giomataris, NIMA376 (1996) 29

Other MPGDs Concepts: THGEM, µRWELL, RPWELL

THGEM Manufactured by standard PCB techniques of precise drilling in G-10 (and other materials) and Cu etching

STANDARD GEM

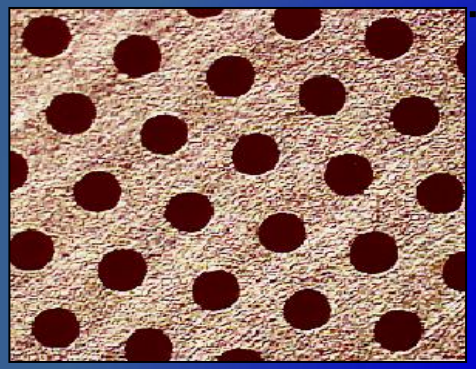

1 mm

THGEM

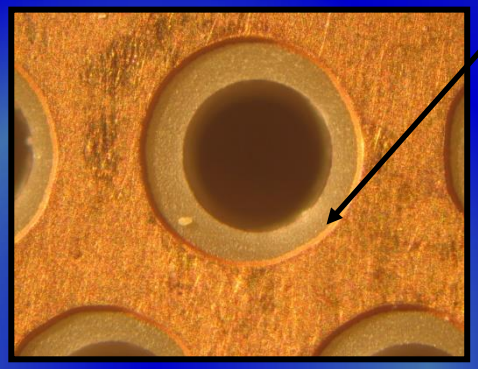

0.1 mm rim to prevent discharges

L. Periale, NIMA478 (2002) 377
LEM!: P. Jeanneret, PhD thesis, 2001

µRWELL and RPWELL

High-rate µRWELL prototypes made by new techniques

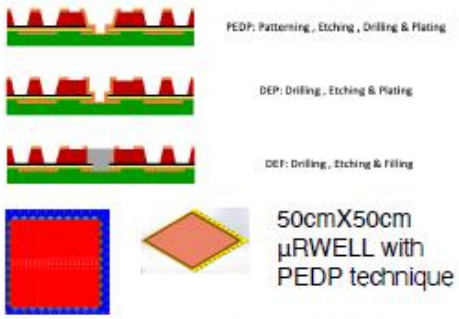

50cmX50cm µRWELL with PEDP technique

https://indico.cern.ch/event/889369/contributions/4020068/attachments/2115302/3560690/RD51_collabration_meeting_You..v.pptx

µRWELL with 2D-Strip Readout — For RD51 Tracker

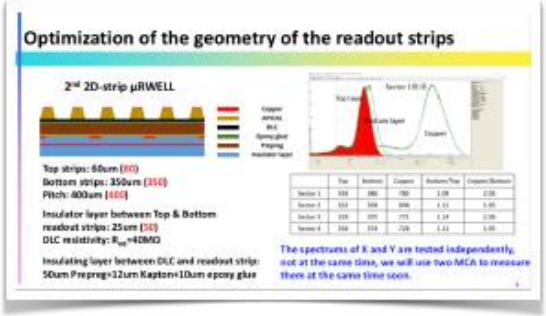

https://indico.cern.ch/event/1040996/contributions/4404219/attachments/2266859/3849374/2021-06-18_RD51-Collaboration%20Meeting-ZhouYi-Final.pdf

Development of RWELL detectors for large area & high rate applications

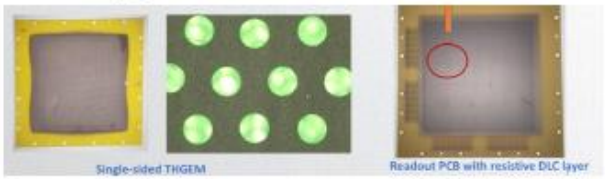

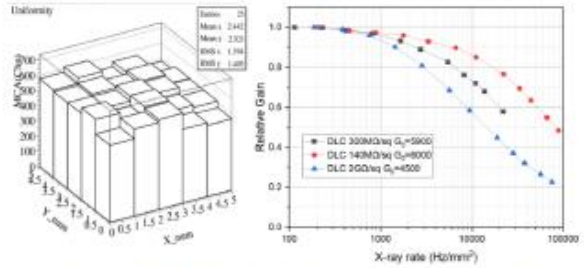

https://indico.cern.ch/event/889369/contributions/4020068/attachments/2115585/3559626/RD51CollaborationMeeting-sgf.pdf

COMPASS RICH Upgrade: Hybrid THGEM + MM with CsI PC

***COMPASS RICH I:* 8 MWPC with CsI since 2000**

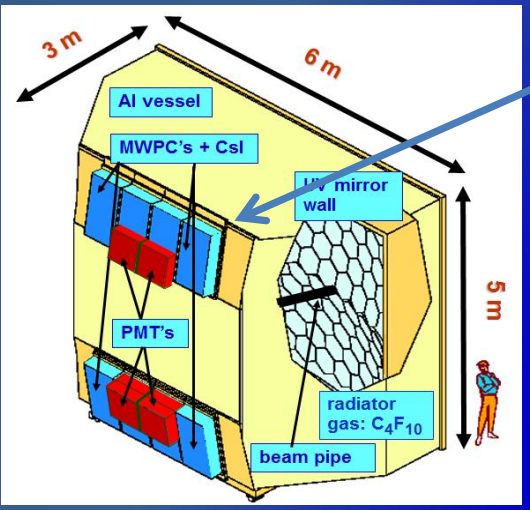

MWPC's + CsI

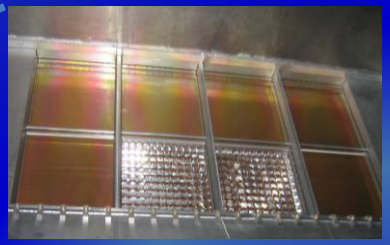

***MWPC+CSI:* successful but with performance limitations for central chambers**

8 Years of Dedicated R&D: THGEM+ CsI

New Hybrid THGEM + MM PDs:

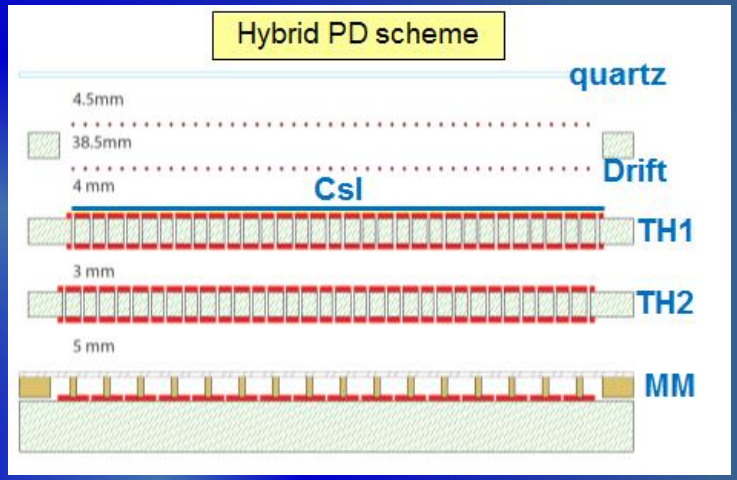

Production THGEM @ ELTOS Company:

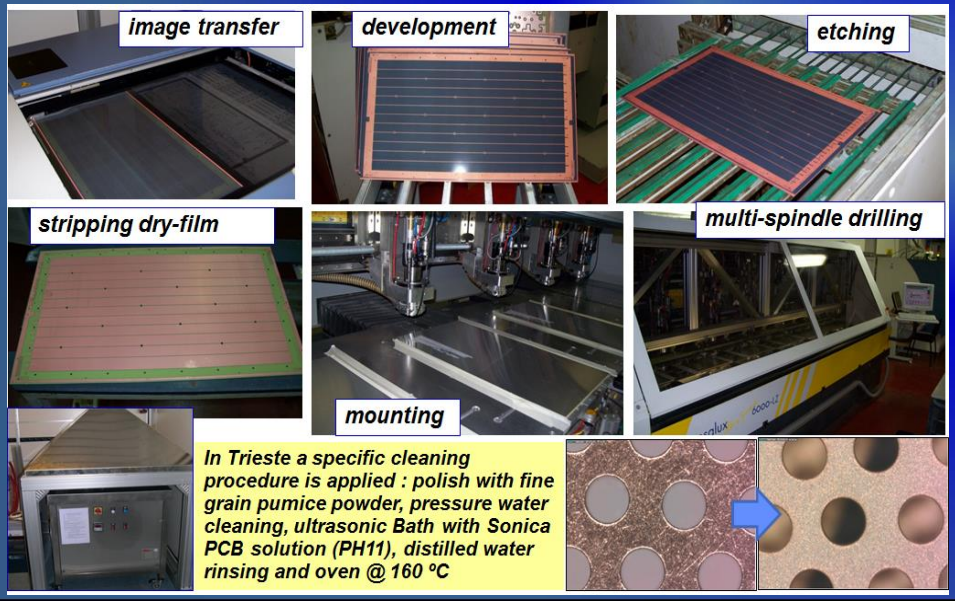

Assembly of Hybrid THGEM +MM:

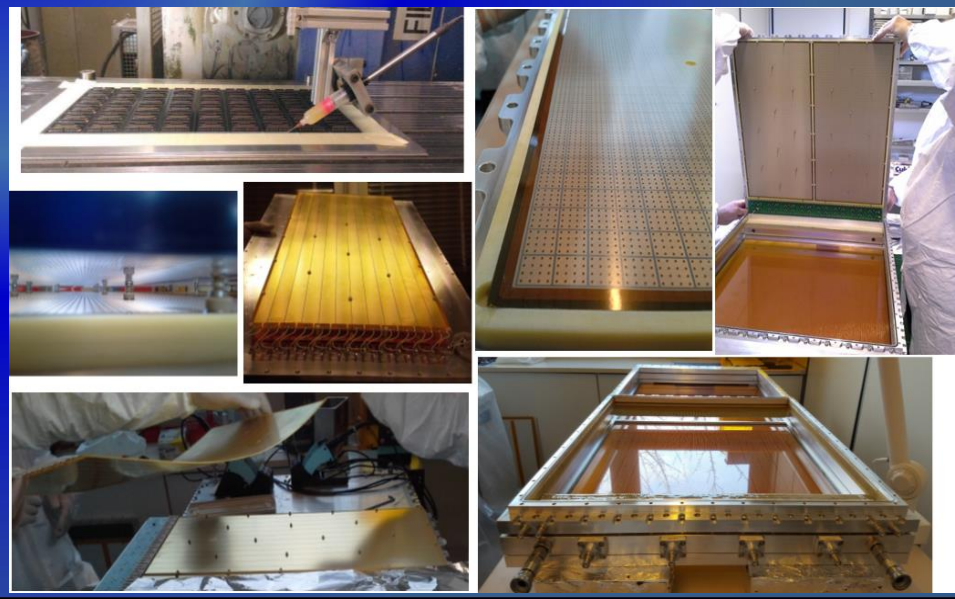

Simulation Tools and Modelling of MPGDs

MPGDs and the mean free path

- Recall:
  - Mean free path of electrons in Ar: 2.5 μm,
- Compare with:
  - Micromegas mesh pitch: 63.5 μm
  - GEM polyimide thickness: 50 μm
  - Micromegas wire thickness: 18 μm
  - GEM conductor thickness: 5 μm
- Hence:
  - mean free path approaches small structural elements;
  - such devices should be treated at a molecular level.
- In addition, MPGDs usually have structures for which no nearly-exact (e.g. 3d structures) fields are known.

Modelling and simulation are crucial for detailed understanding of detector physics and for developing and exploiting novel MPGD technologies

- **Resistive detectors:** modelling of signal induction, understand protection schemes and rate capabilities
- **Ion physics:** minimise ion backflow, understand ion-induced damages and feedback processes, ion species/clustering and mobility
- **Modelling of scintillation** processes for optical readout: light production, quenching, timing of light production processes

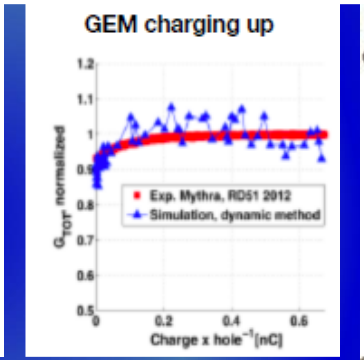

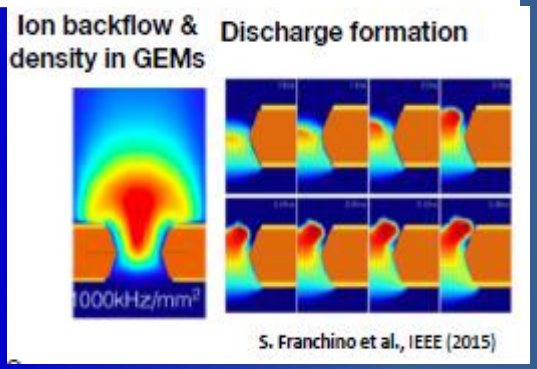

Gas mixture studies

Gain simulations in MPGDs including space charge effect using Elmer

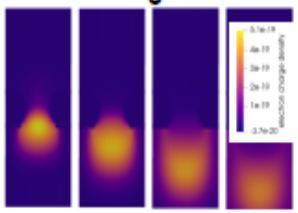

https://indico.cern.ch/event/889369/contributions/4039491/attachments/2115151/3558785/APellecchia_Elmer_RD51_Oct2020.pdf

F impurities with CF4-based gas mixtures

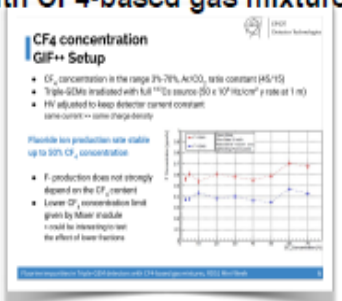

https://indico.cern.ch/event/989298/contributions/4230658/attachments/2191378/3703794/mcorbetta_RD51Feb2021.pdf

ATLAS NSW Micromegas mesh transparency

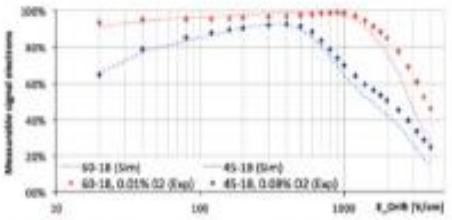

F. Kuger et al., https://doi.org/10.1016/j.nima.2015.11.011

A fast simulation method for THGEM charging-up study

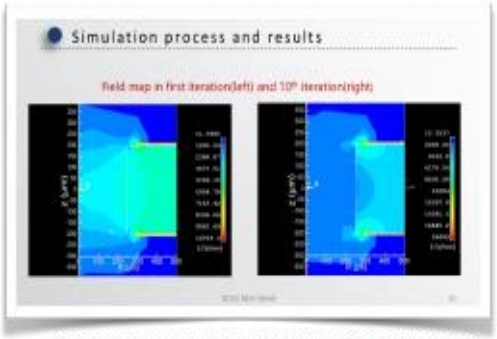

https://indico.cern.ch/event/989298/contributions/4225007/attachments/2192182/3705373/Guofeng-202102-RD51.pdf

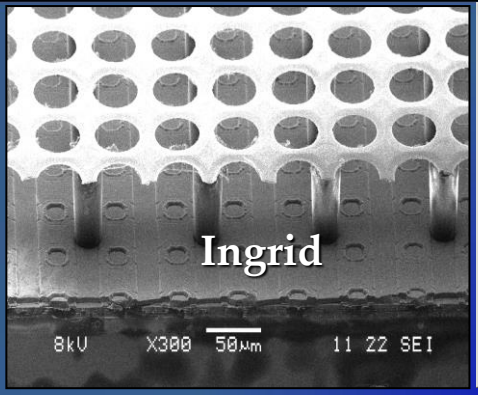

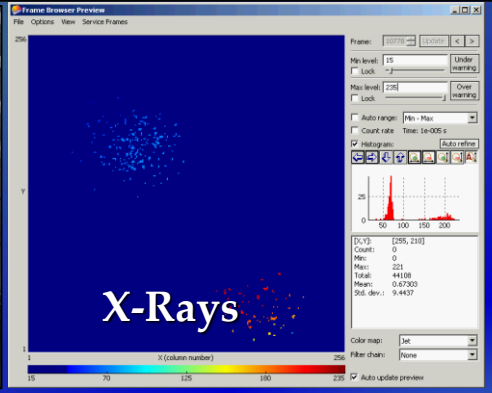

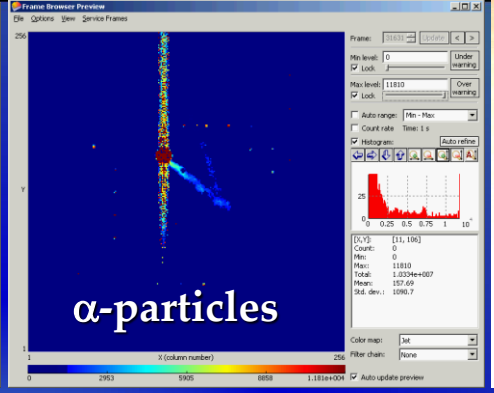

"Octopuce" (8 Timepix ASICs):

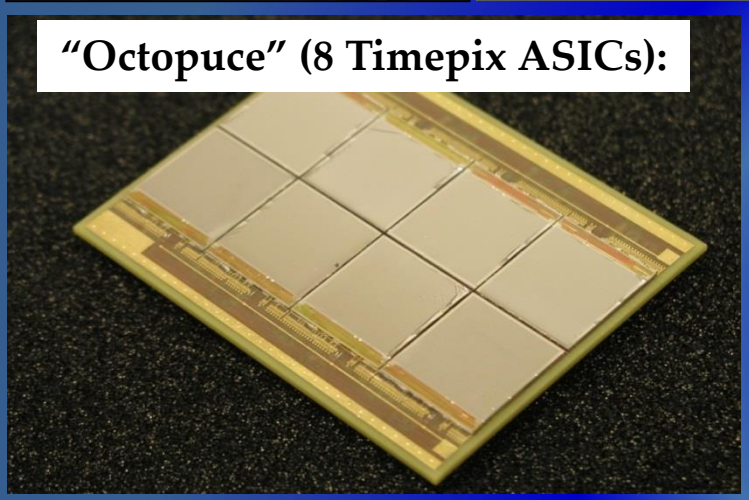

ULTIMATE INTEGRATION OF GASEOUS and SIICON DETECTORS –

PIXEL READOUT of MICRO-PATTERN GASEOUS DETECTORS

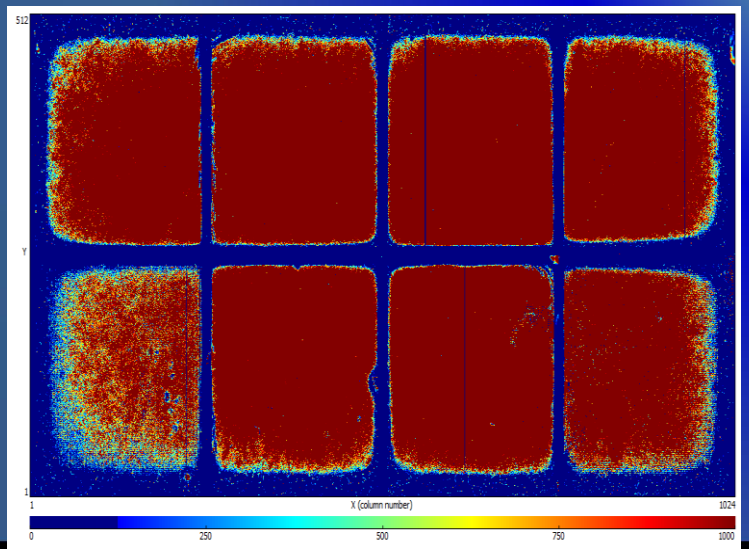

Triple GEM stack + Timepix ASIC (5 GeV e-):

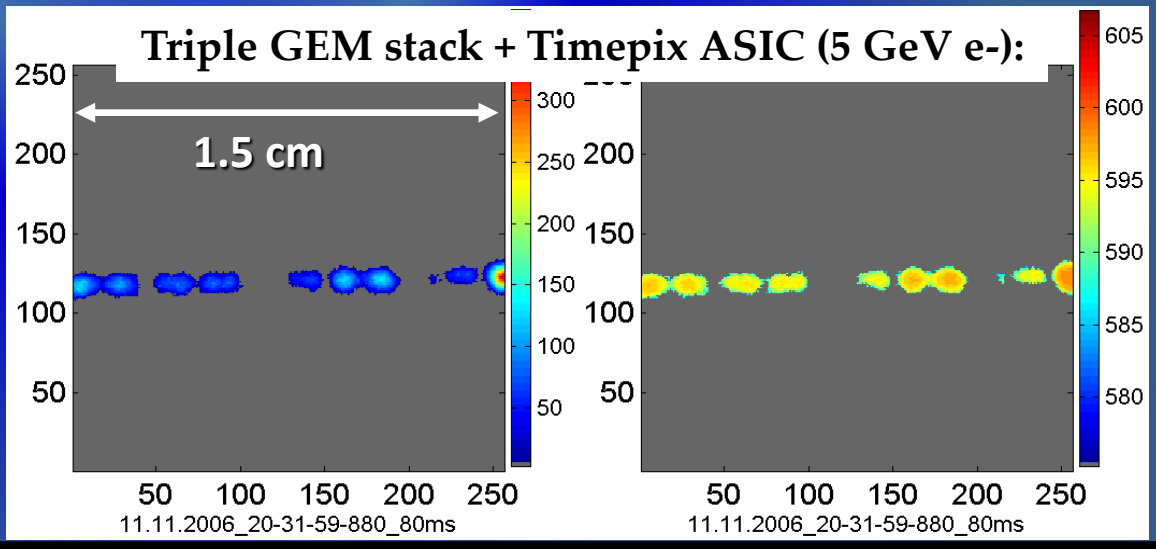

Pixel Readout of MPGDs: "GridPix" Concept

"InGrid" Concept: By means of advanced wafer processing-technology INTEGRATE MICROMEGAS amplification grid directly on top of CMOS ("Timepix") ASIC

3D Gaseous Pixel Detector → 2D (pixel dimensions) x 1D (drift time)

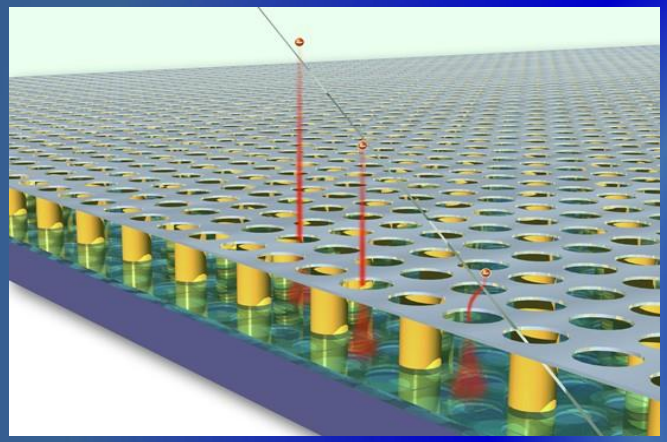

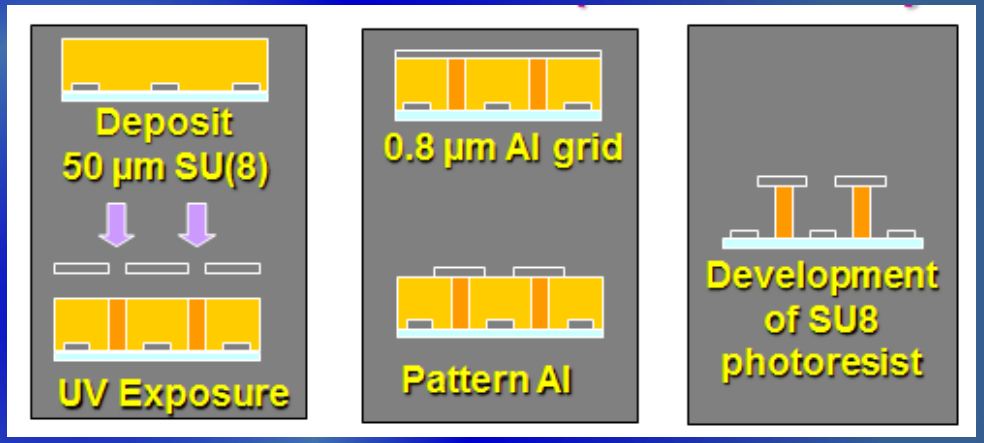

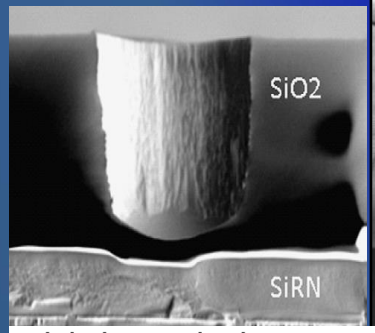

high resistive material
15 µm aSi:H (~10^{11} Ω·cm)
8 µm Si_XN_Y (~10^{14} Ω·cm)

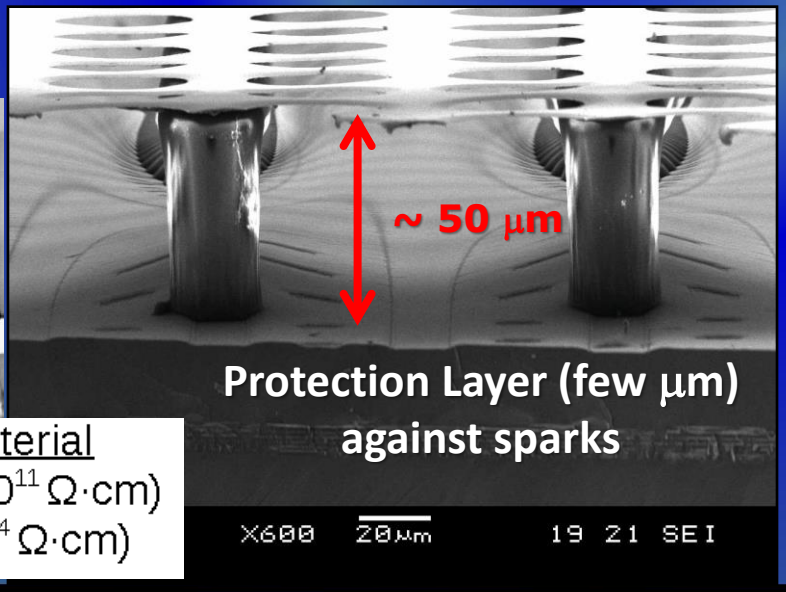

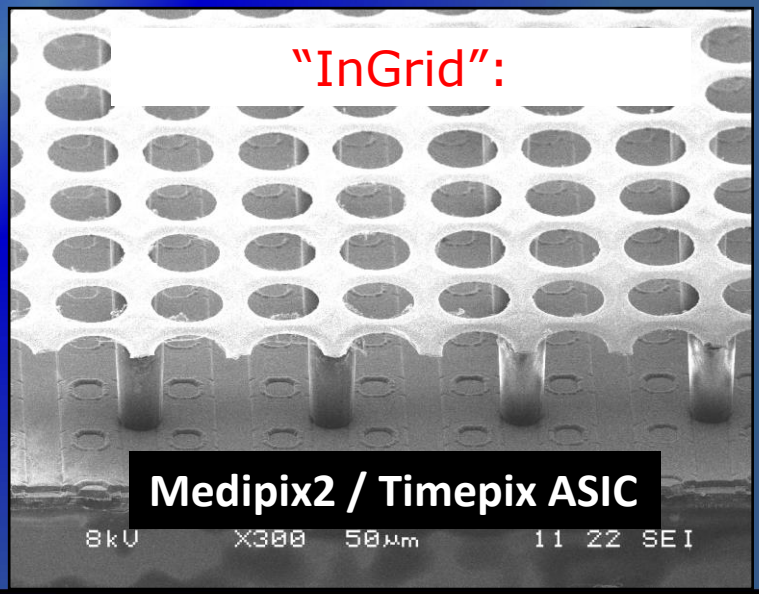

MPGD-Based Gaseous Photomultipliers

GEM or THGEM Gaseous Photomultipliers (CsI -PC) to detect single photoelectrons

Multi-GEM (THGEM) Gaseous Photomultipliers:

- ✓ *Largely reduced photon feedback (can operate in pure noble gas & CF_4)*
- ✓ *Fast signals [ns] → good timing*
- ✓ *Excellent localization response*
- ✓ *Able to operate at cryogenic T*

Semitransparent Photocathode (PC)

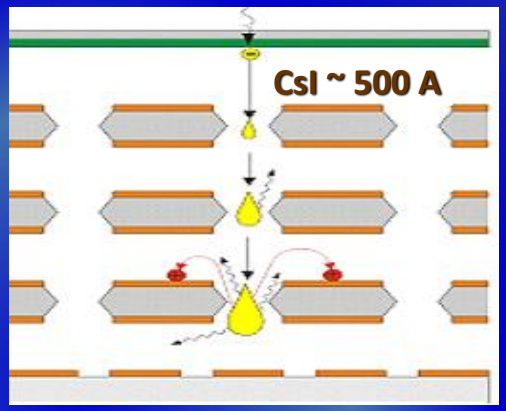

Reflective Photocathode (PC)

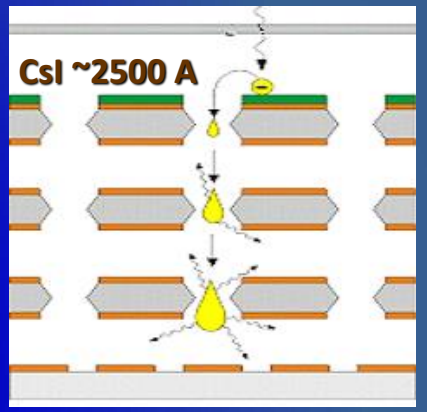

Single Photon Time Resolution:

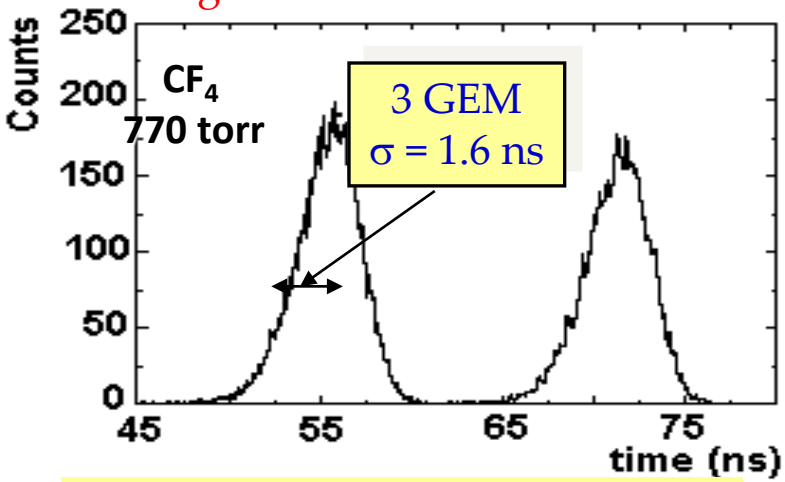

Micromegas: σ ~ 0.7 ns with MIPs

Single Photon Position Accuracy:

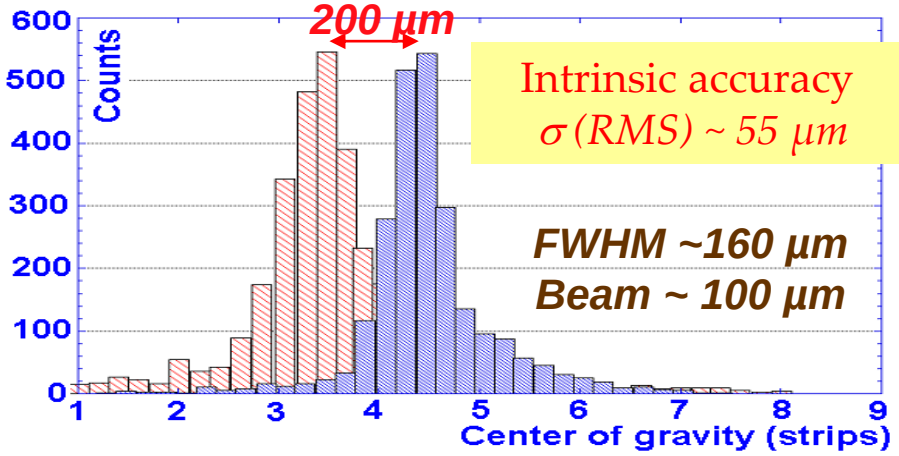

E.Nappi, NIMA471 (2001) 18; T. Meinschad et al, NIM A535 (2004) 324; D.Mormann et al., NIMA504 (2003) 93

Summary & conclusion

Christian Lippmann, 2nd ECFA High Luminosity LHC Experiments Workshop, Aix-les-bains, France, October 21-23 (2014)

Geiger- Müller (1908), 1928
Drift Tube (1968)

1)

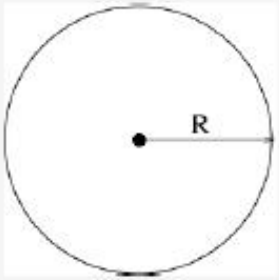

G. Charpak, 1968
Multi Wire Proportional Chamber

2)

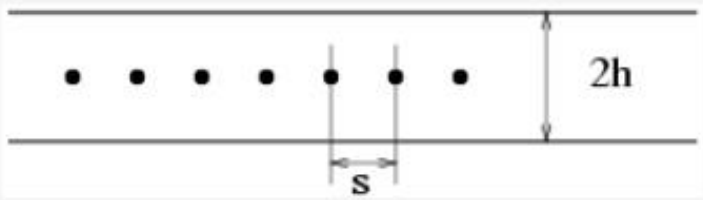

R. Santonico, 1980
Resistive Plate Chamber

3)

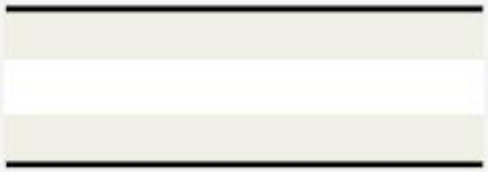

… will at HL-LHC be joined by:

F. Sauli (1997)
Gas Electron Multiplier

4)

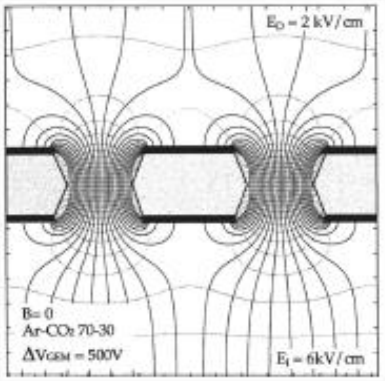

I. Giomataris et al. (1996)
Micro-mesh gaseous chamber (Micromegas)

5)

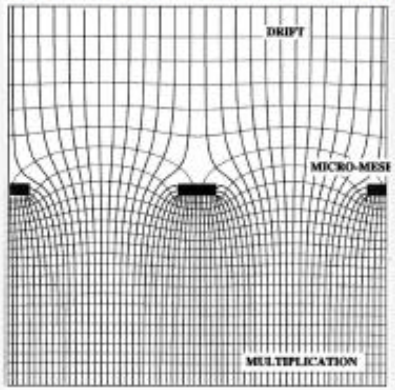

MPGD Technologies @ CERN Experiments

- The integration of MPGDs in large experiments was not rapid, despite of the first large-scale application in COMPASS at SPS in the 2000's

- Scaling up MPGD detectors, while preserving the typical properties of small prototypes, allowed their use in the LHC upgrades
  → Many emerged from the R&D studies within the CERN-RD51 Collaboration

Experiment / Timescale	Application Domain	MPGD Technology	Total detector size / Single module size	Operation Characteristics / Performance	Special Requirements / Remarks
COMPASS TRACKING > 2002	Fixed Target Experiment (Tracking)	3-GEM Micromegas w/ GEM preampl.	Total area: 2.6 m² Single unit detect: 0.31x0.31 m² Total area: ~ 2 m² Single unit detect: 0.4x0.4 m²	**Max.rate**: ~100kHz/mm² **Spatial res.**: ~70-100μm (strip), ~120μm (pixel) **Time res.**: ~ 8 ns **Rad. Hard.**: 2500 mC/cm²	Required beam tracking (pixelized central / beam area)
TOTEM TRACKING: > 2009	Hadron Collider / Forward Physics (5.3≤|η| ≤ 6.5)	3-GEM (semicircular shape)	Total area: ~ 4 m² Single unit detect: up to 0.03m²	**Max.rate**:20 kHz/cm² **Spatial res.**: ~120μm **Time res.**: ~ 12 ns **Rad. Hard.**: ~ mC/cm²	Operation in pp, pA and AA collisions.
LHCb MUON DETECTOR > 2010	Hadron Collider / B-physics (triggering)	3-GEM	Total area: ~ 0.6 m² Single unit detect: 20-24 cm²	**Max.rate**:500 kHz/cm² **Spatial res.**: ~ cm **Time res.**: ~ 3 ns **Rad. Hard.**: ~ C/cm²	Redundant triggering
COMPASS RICH UPGRADE > 2016	Fixed Target Experiment (RICH - detection of single VUV photons)	Hybrid (THGEM + CsI and MM)	Total area: ~ 1.4 m² Single unit detect: ~ 0.6 x 0.6 m²	**Max.rate**:100 Hz/cm² **Spatial res.**: <~ 2.5 mm **Time res.**: ~ 10 ns	Production of large area THGEM of sufficient quality
ATLAS MUON UPGRADE CERN LS2	Hadron Collider (Tracking/Triggering)	Resistive Micromegas	Total area: 1200 m² Single unit detect: (2.2x1.4m²) ~ 2-3 m²	**Max. rate**:15 kHz/cm² **Spatial res.**: <100μm **Time res.**: ~ 10 ns **Rad. Hard.**: ~ 0.5C/cm²	Redundant tracking and triggering; Challenging constr. in mechanical precision
CMS MUON UPGRADE CERN LS2	Hadron Collider (Tracking/Triggering)	3-GEM	Total area: ~ 143 m² Single unit detect: 0.3-0.4m²	**Max. rate**:10 kHz/cm² **Spatial res.**: ~100μm **Time res.**: ~ 5-7 ns **Rad. Hard.**: ~ 0.5 C/cm²	Redundant tracking and triggering
ALICE TPC UPGRADE CERN LS2	Heavy-Ion Physics (Tracking + dE/dx)	4-GEM / TPC	Total area: ~ 32 m² Single unit detect: up to 0.3m²	**Max.rate**:100 kHz/cm² **Spatial res.**: ~300μm **Time res.**: ~ 100 ns **dE/dx**: 11 % **Rad. Hard.**: 50 mC/cm²	- 50 kHz Pb-Pb rate; - Continues TPC readout - Low IBF and good energy resolution

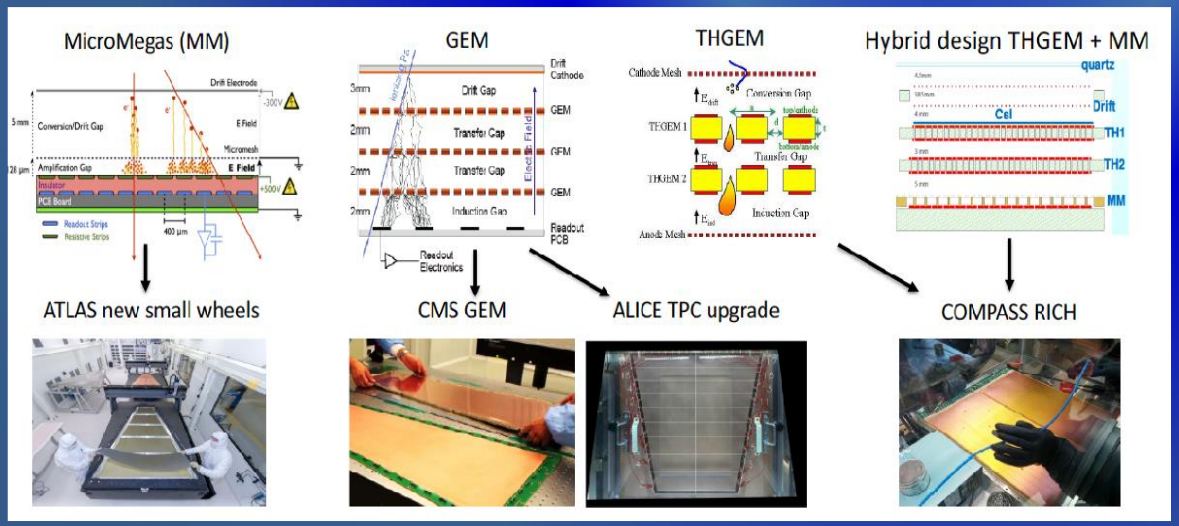

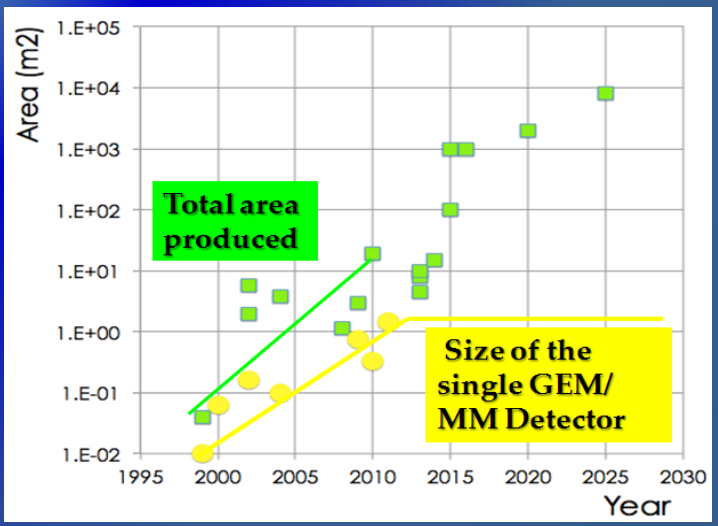

CERN Detector Seminars in 2022: LS2 Upgrades

Major MPGDs developments for ATLAS, CMS, ALICE upgrades, towards establishing technology goals and technical requirements, and addressing engineering and integration challenges … and first results from Run 3 !!!

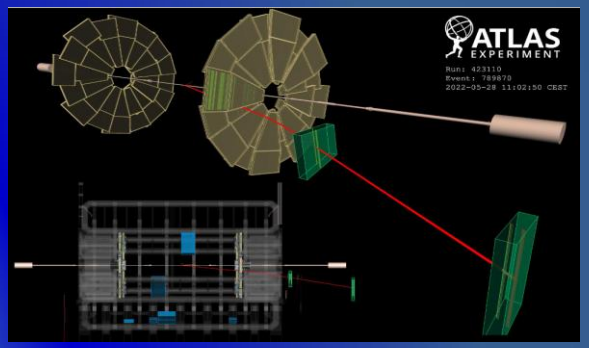

"The New Small Wheel project of ATLAS"
by Theodoros Vafeiadis (17 Jun 2022)
https://indico.cern.ch/event/1168778/

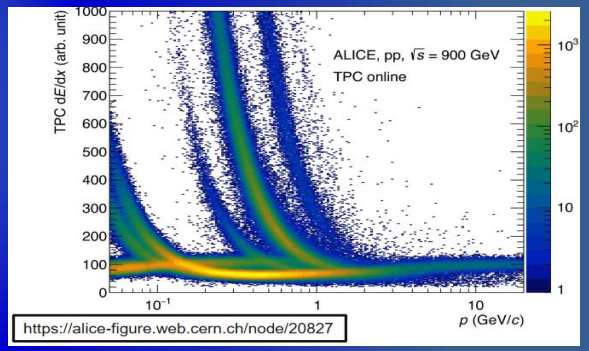

"Continuous data taking with the upgraded ALICE GEM-TPC"
by Robert Helmut Munzer (24 Jun 2022),
https://indico.cern.ch/event/1172978/

"The GEM detectors within the CMS Experiment"
Michele Bianco (08 Jul 2022)
https://indico.cern.ch/event/1175363/

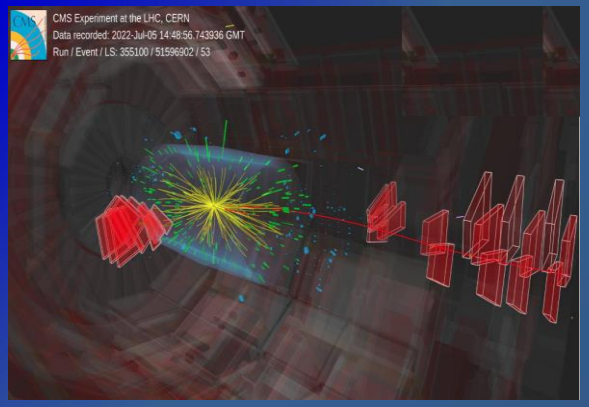

All three major LHC upgrades, incorporating MPGDs, started their R&D in close contact with RD51, using dedicated setups at GDD-RD51 Laboratory

Large-Area MM / GEM Detectors for ATLAS / CMS Upgrade

Resistive MM for ATLAS NSW Muon Upgrade:

Standard Bulk MM suffers from limited efficiency at high rates due to discharges induced dead time
Solution: Resistive Micromegas technology:

- Add a layer of resistive strips above the readout strips

- Spark neutralization/suppression (sparks still occur, but become inoffensive)

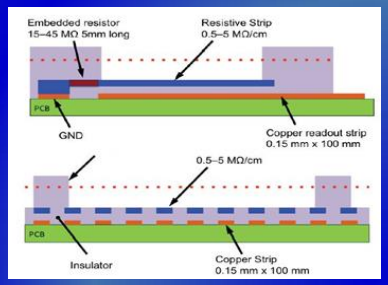

Still, main issue encountered: HV unstability
==> found to be correlated to low resistance of resistive strip anode
==> applied solutions + passivation in order to deactivate the region where R<0.8 MΩ

Production, sector integration (~1200m^2 resistive MM):

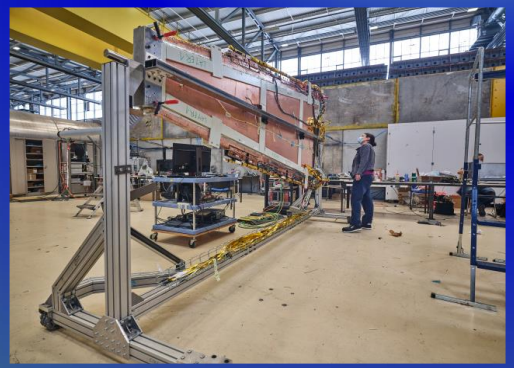

GEMs for CMS Muon System Upgrade:

- Single-mask GEM technology (instead of double-mask)
  → Reduces cost /allows production of large-area GEM

- Assembly optimization: self-stretching technique:
  → assembly time reduction to 1 day

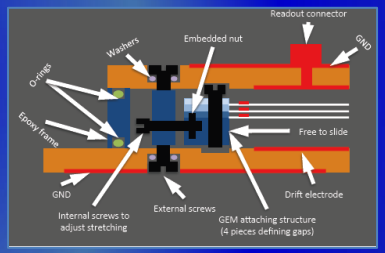

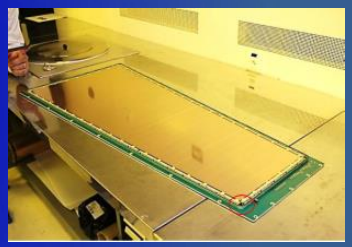

September 2020: 144 GEM chambers installed

TPC with MPGD Readout for ALICE Upgrade and ILC

ALICE TPC → replace MWPC with 4-GEM staggered holes (to limit space-charge effects)

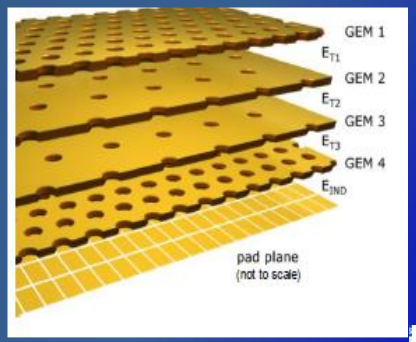

- Upgrade for continuous TPC readout @ 50 kHz Pb-Pb collisions

- Phys. requirements:
  IBF < 1%,
  Energy res. σ(E)E < 12%

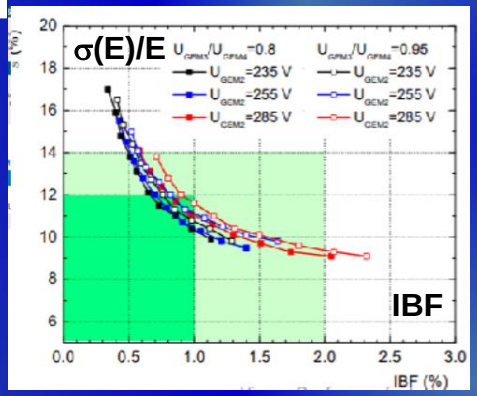

TPC reinstallation in the ALICE cavern (August 2020)

ILC –TPC with MPGD-based Readout

Target requirement of a spatial resolution of 100 um in transverse plane and dE/dx resolution < 5% have been reached with all technologies (GEM, MM and GridPix)

If dE/dx combined with ToF using SiECAL,
P < 10GeV region for pion-K separation covered

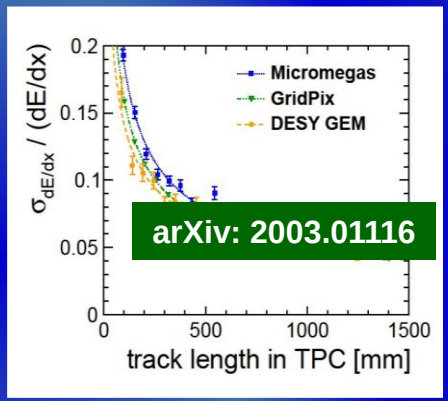

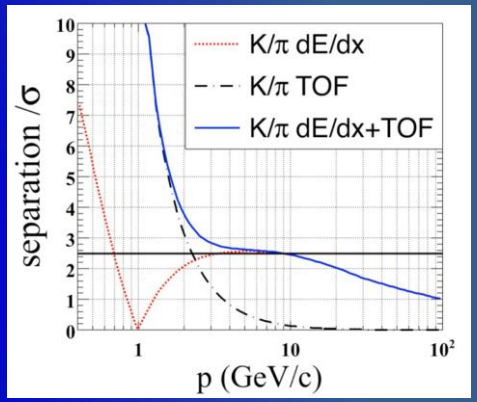

ILC: gating scheme, based on large-aperture GEM

→ Machine-induced background and ions from gas amplific.
→ Exploit ILC bunch structure (gate opens 50 us before the first bunch and closes 50 us after the last bunch)

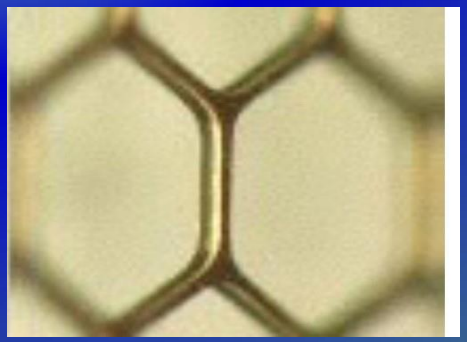

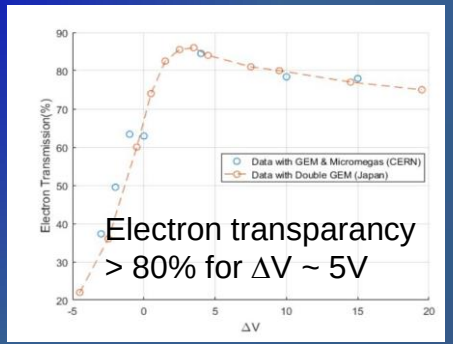

Towards Large-Scale Pixel "GridPix" TPC

Testbeams with GridPixes:
160 GridPixes (Timepix) & 32 GridPixes (Timepix3)

A PIXEL TPC IS REALISTIC!

NIM A956 (2020) 163331

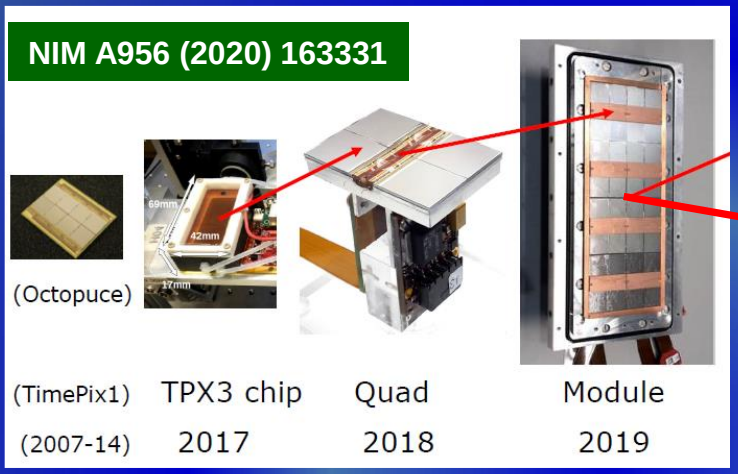

Physics properties of pixel TPC:

- Improved dE/dx by cluster counting
- Improved meas.of low angle tracks
- Excellent double track seperation
- Lower occupancy @ high rates
- Fully digital read out (TOT)

Quad board (Timepix3) as a building block
→ 8-quad detector (32 GridpPixs) with a field cage at test-beam @DESY in June 2021:

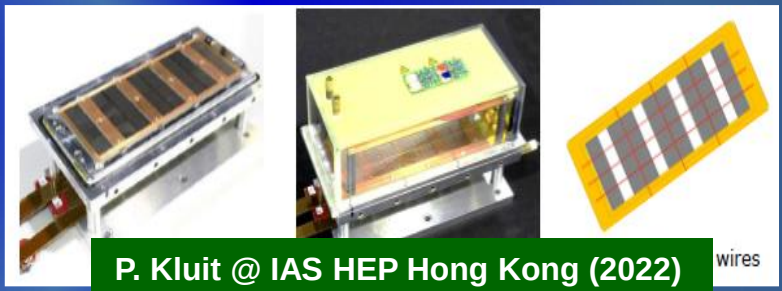

P. Kluit @ IAS HEP Hong Kong (2022)

3 modules for LP TPC @ DESY: 160 (1 x 96 & 2 x 32) GridPixs
320 cm² active area, 10,5 M. channels, new SRS Readout system

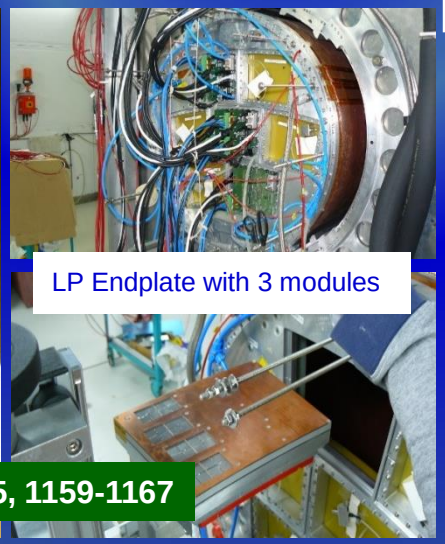

IEEE TNS 64 (2017)5, 1159-1167

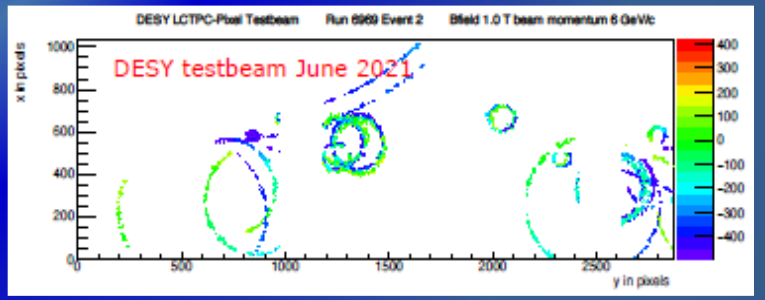

- ✓ ion back flow can be further reduced by applying a double grid.
- ✓ Protection layer resistivity to be reduced
- ✓ New Timepix4 developments

Dissemination of MPGD Applications in HEP & Other Fields

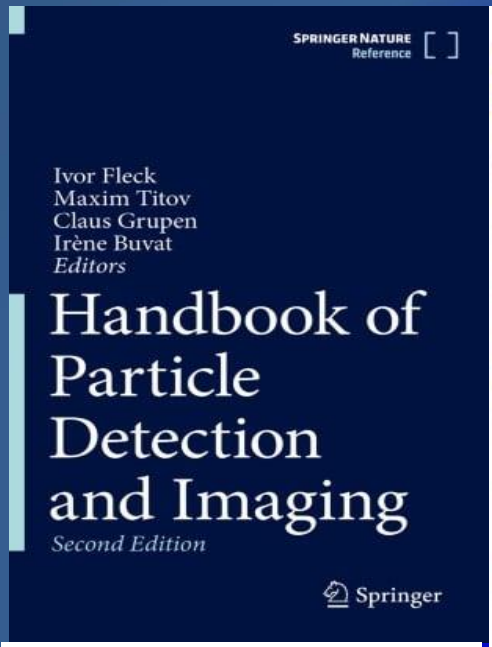

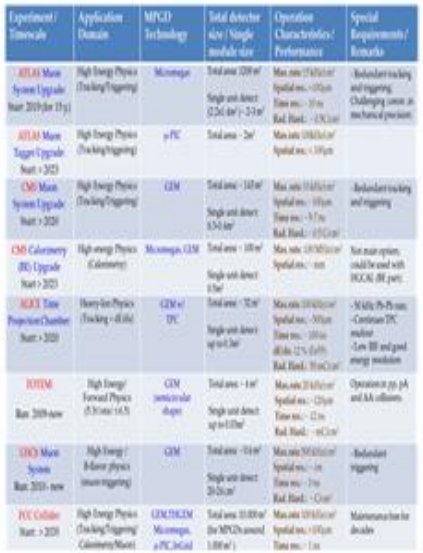

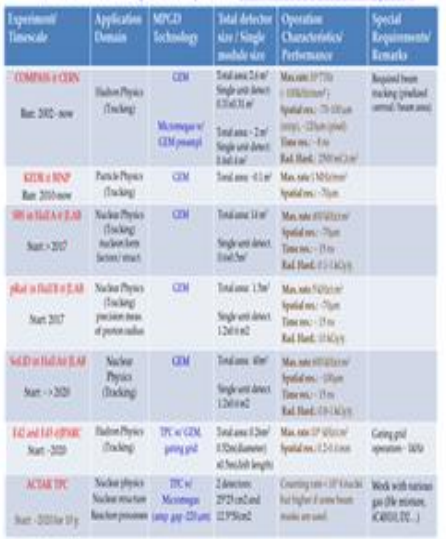

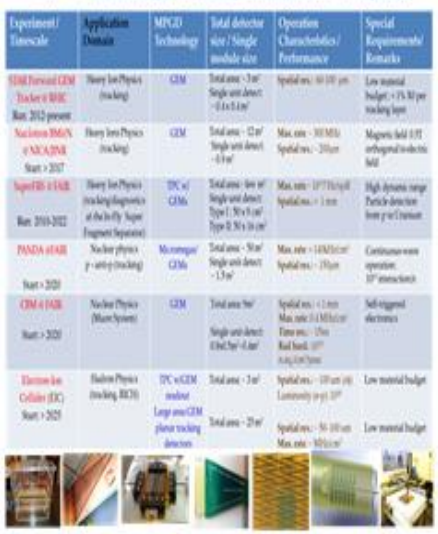

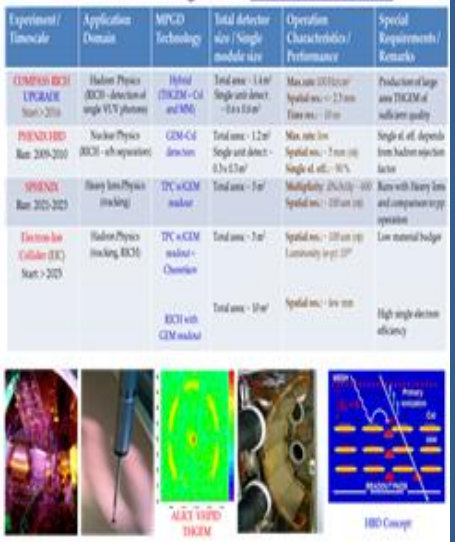

https://indico.cern.ch/event/581417/contributions/2558346/attachments/1465881/2266161/2017_05_Philadelphia_MPGD2017-ConferenceSummary_25052017_MS.pdf

MPGD Technologies @ Future R&D Trends

✓ ***RESISTIVE MATERIALS*** **and related detector architectures for single-stage designs (μPIC, μ-RWELL, RPWELL, resistive MM)**
→ improves detector stability; single-stage is advantage for assembly, mass production & cost.

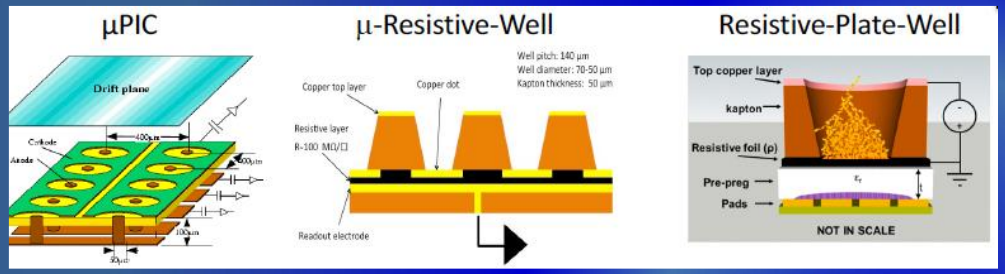

➢ ***Diamond-like carbon (DLC) resistive layers***
→ Solutions to improve high-rate capability (≥ MHz)

Resistive DLC Collaboration

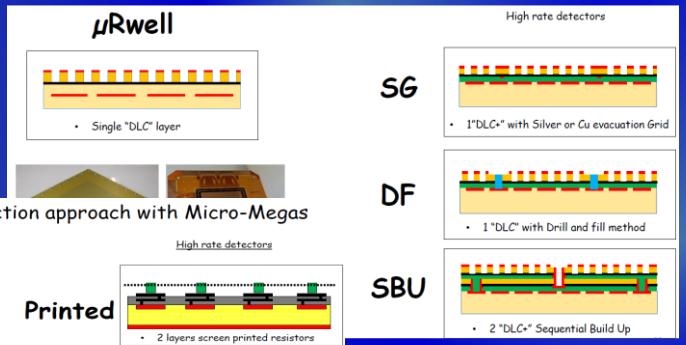

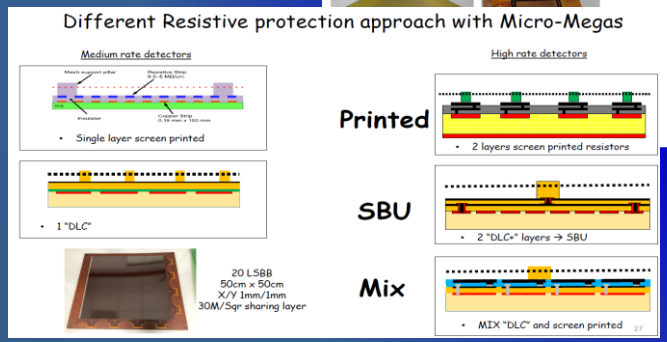

✓ ***Picosecond Timing Detector (RD51 PICOSEC Collaboration) – MM device*** with radiator and radiation-hard PC

➢ ***OPTICAL READOUT:*** hybrid approaches combining gaseous with non-gaseous in a single device (e.g. CYGNUS- TPC project):

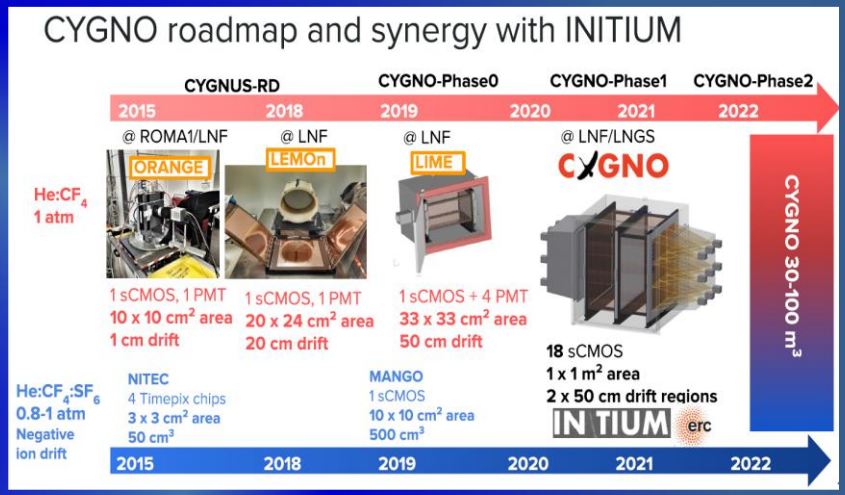

➢ **New manufacturing techniques & structures:**

- Solid-state photon and neutron converters, ***INNOVATIVE NANOTECHNOLOGY COMPONENTS (graphene layers);***

- Material studies (low out-gassing, radiation hardness, radio-purity, converter robustness and eco-friendly gases.

- Emerging technologies related to novel PCs, MicroElectroMechanical Systems (MEMS), sputtering, 3-D printing of amplifying structures and cooling circuits

Advanced Concepts Picosecond (a few 10's) Timing Detectors

Several types of technologies are considered for "Picosecond-Timing Frontier":

- Ionization detectors (silicon detectors or gas-based devices)
- Light-based devices (scintillating crystals coupled to SiPMs, Cherenkov absorbers coupled to photodetectors with amplification, or vacuum devices)

CONVENTIONAL MCP – PMT APPLICATIONS:

BELLE II TOP:

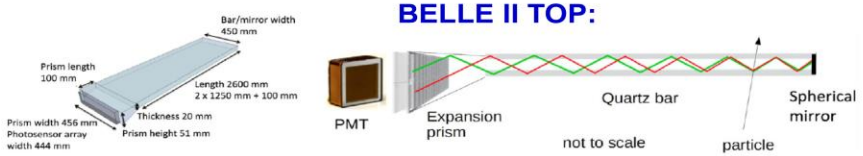

ATLAS HGTD (CMS ETL) TIMING WITH LGAD:

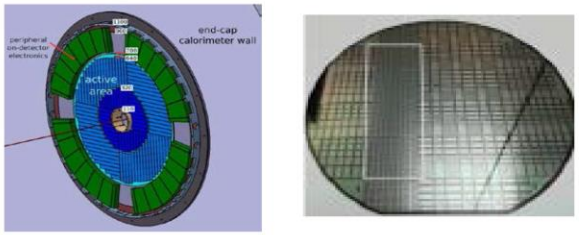

LHCb TORCH DIRC:

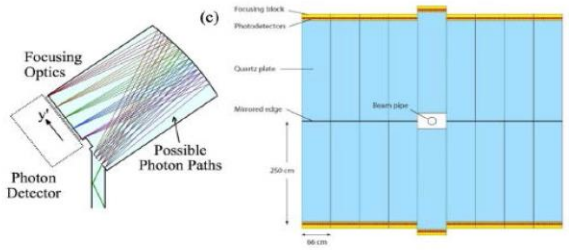

PANDA ENDCAP

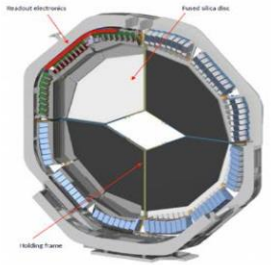

CMS BTL TIMING WITH LYSO:Ce / SiPMs

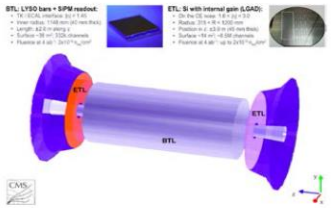

LAPPD TIMING PROJECT:

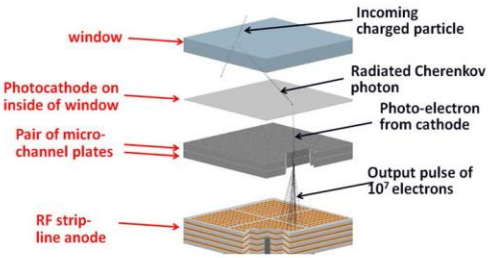

GASEOUS DETECTORS APPLICATIONS:

ALICE MPRC TOF:

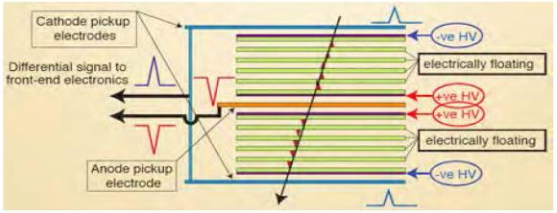

PICOSEC - MICROMEGAS:

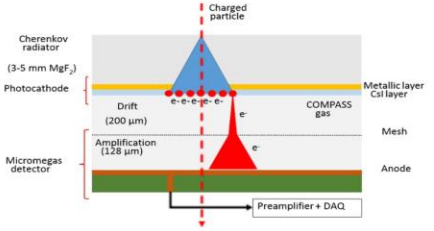

Examples of timing detectors at a level of~ 30 ps for MIPs and ~ 100 ps for single photons

Towards Large Area in Fast Timing GASEOUS DETECTORS

Multi-Gap Resistive Plate Chambers (MRPC):

- ✓ ALICE TOF detector (160m^2) achieved time res. ~ 60 ps
- ✓ New studies with MRPC with 20 gas gaps using a low-resistivity 400 μm-thick glass → down to 20 ps time resolution

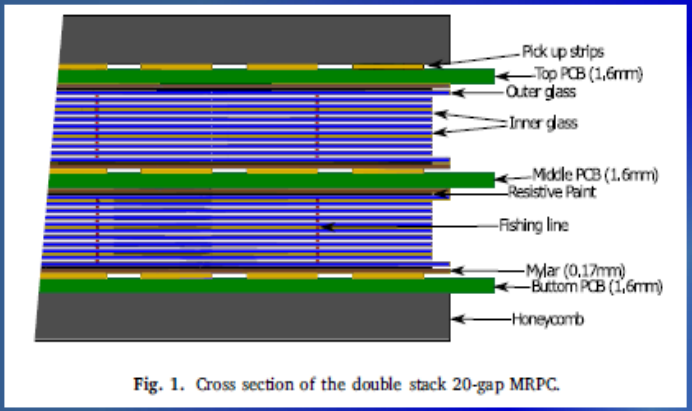

Fig. 1. Cross section of the double stack 20-gap MRPC.

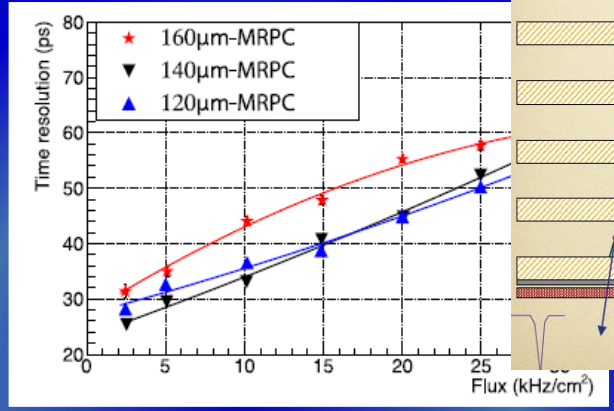

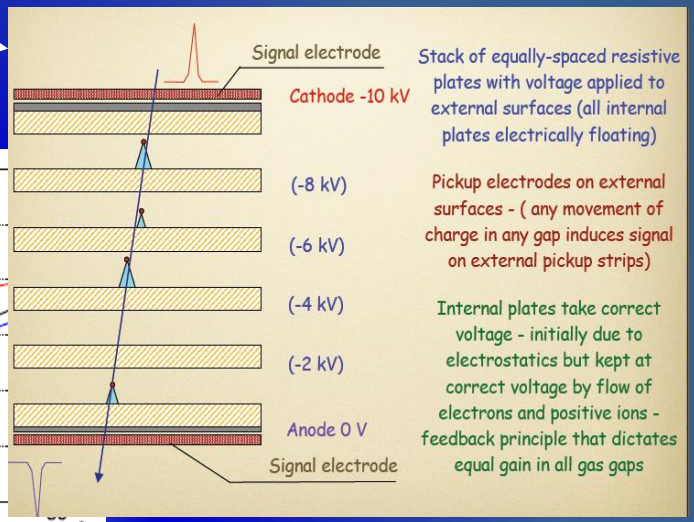

Gaseous Detectors: Micromegas with Timing (RD51 Picosec Collaboration)

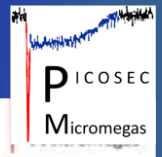

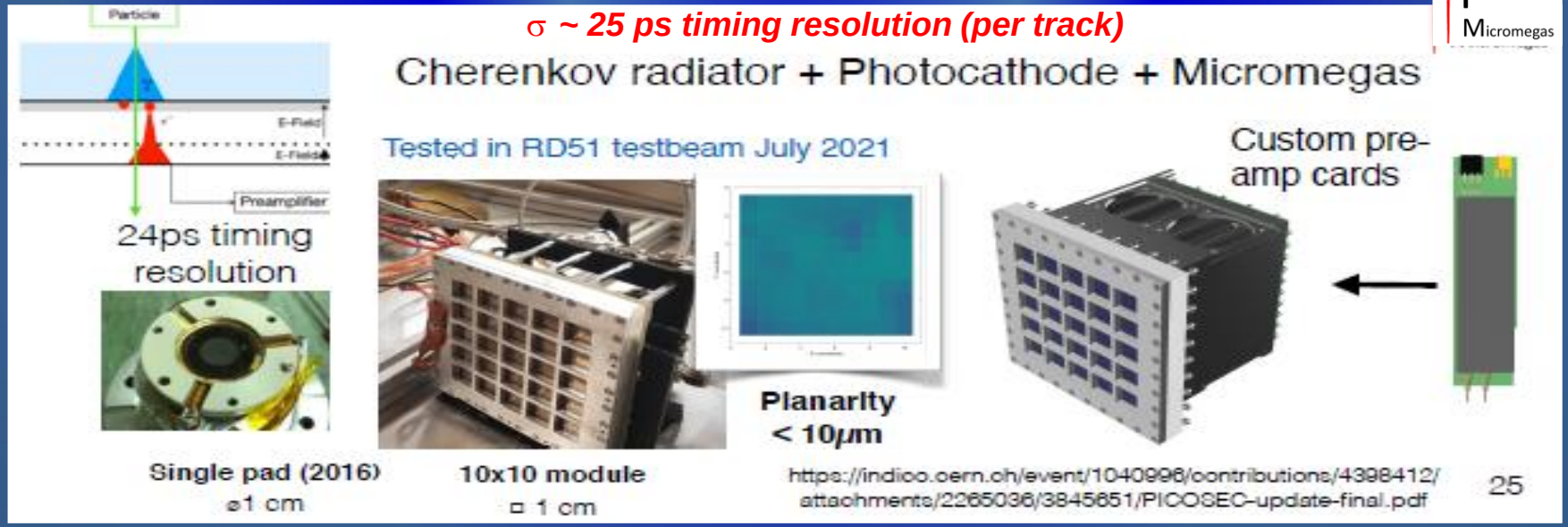

Optical Readout for Micro-Pattern Gaseous Detectors

Courtesy CERN GDD group

Concept

Scintillation light emitted during amplification processes in MPGDs can be read out with CCD or CMOS cameras.

GEM readout

Glass Micromegas readout

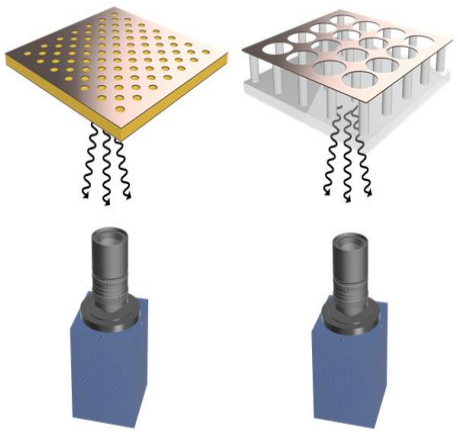

Emission spectrum of Ar / CF4 gas mixture with UV and visible scintillation

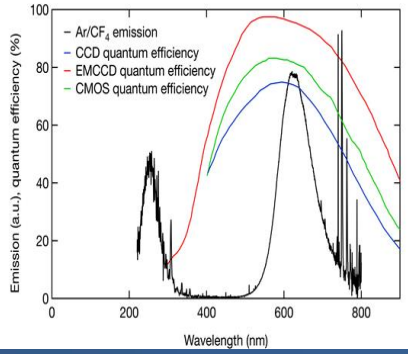

Examples and applications

X-ray radiography

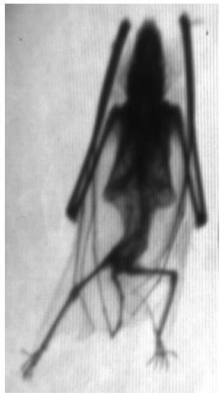

Energy-resolved imaging

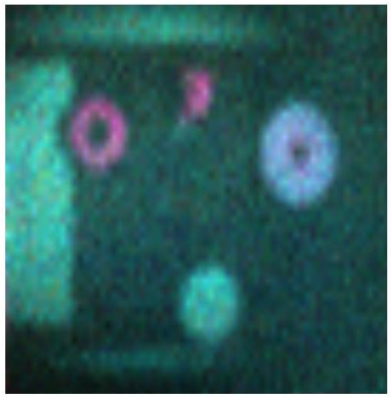

Track reconstruction

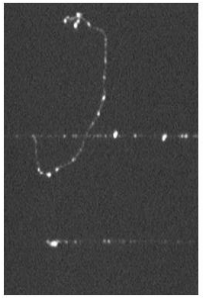

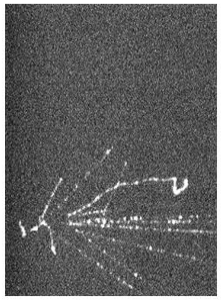

Beam monitoring

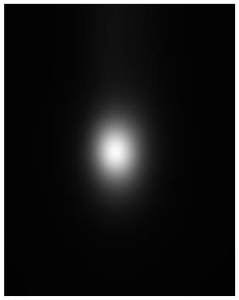

Rapid X-ray imaging (fluoroscopy) with sub-ms exposure per frame

R&D and current projects

Low-pressure optical TPC to resolve events with wide dynamic range (low energy X-rays in presence of alpha particle or nuclear recoils)

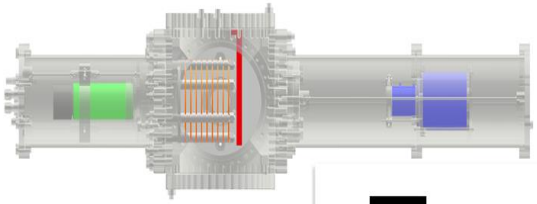

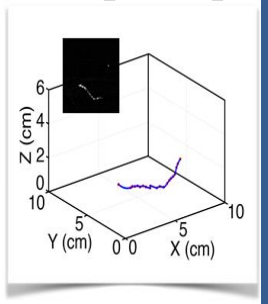

Use of high-speed cameras for 3D track reconstruction resolving drift time differences

The CYGNO TPC: Optical Readout for Directional Study of Rare Events

CYGNO is working in the framework of CYGNUS: international Collaboration for realization of Multi-side Recoil Directional Observatory for WIMPs & ν's

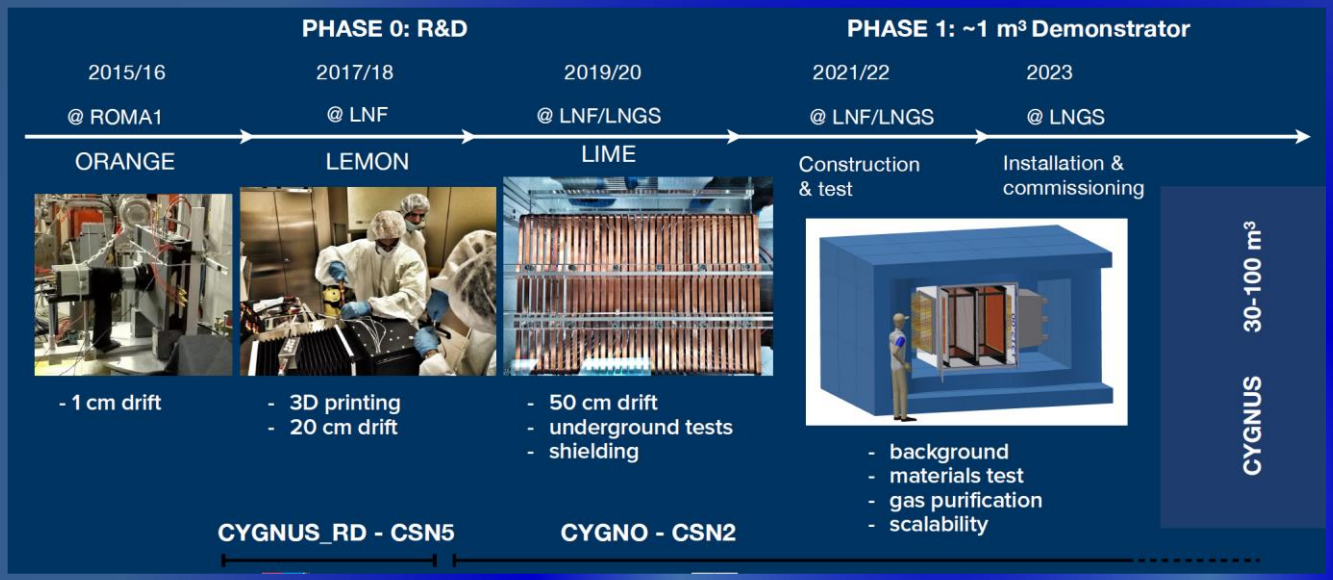

GEM Optical readout: Promising performance in a few keV region

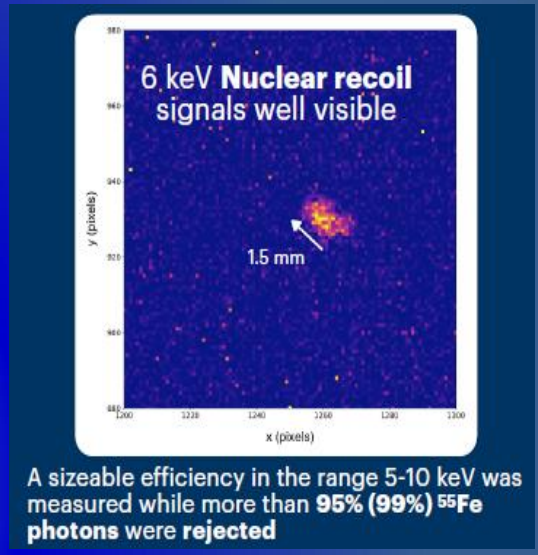

A sizeable efficiency in the range 5-10 keV was measured while more than **95% (99%)** ^{55}Fe **photons** were **rejected**

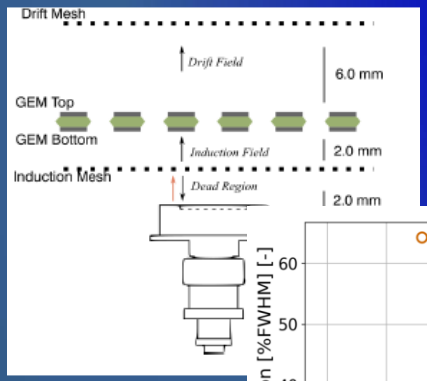

Electroluminiscence studies: readout light produced during multiplication process in GEMs

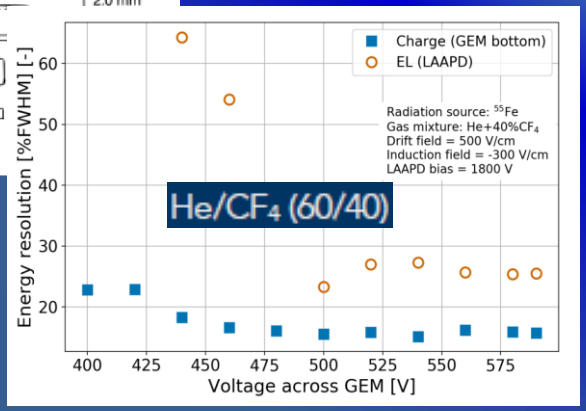

Optically readout TPC: 3D tracking (position and direction); total released energy measurement and dE/dx profile;

1M³ DEMONSTRATOR: BASELINE LAYOUT

1 m³ of **He/CF₄ 60/40** (1.6 kg) at **atmospheric pressure** with a composed by two 50 cm long TPC with a central cathode and a drift field of about 1 kV/cm;

Acrylic vessel ensuring gas tightness and high voltage insulation;

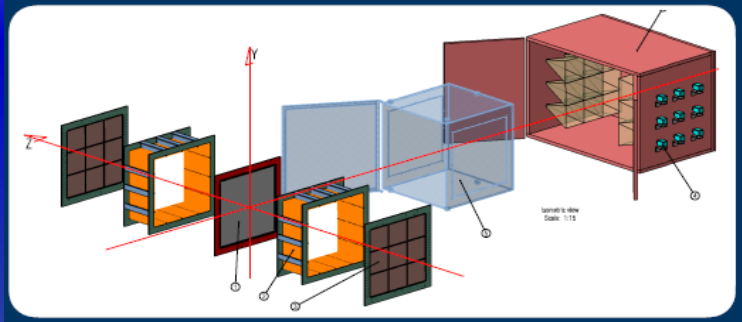

Each side equipped by a 3x3 matrix of LIME-like:

- sCMOS sensor 65 cm away;
- Almost 10^8 readout pixels 165 x 165 μm^2
- Fast light detector (PMT or SiPM).

Radioactivity shielding:

- **5 cm** thick **copper** box (Faraday cage too);
- **200 cm** of water.

Graphene-based Functional Structures and Nanostructures for novel MPGD Concepts

Graphene layers for: *ion-backflow suppression, protection of photocathodes, solid conversion layers*

PhD project of Giorgio Orlandini (FAU Erlangen-Nürnberg) in EP-DT-DD Gaseous Detector Development lab

The unique properties of two-dimensional materials such as graphene as well as carbon-based nanostructures offer new perspectives for novel gaseous radiation detectors. This may include performance improvements for detectors for HEP experiments as well as new application fields combining wideband sensitivity of advanced materials with high gain factors and granularity offered by Micro Pattern Gaseous Detectors.

Application 1:
Suspended graphene for ion back-flow suppression and gas separation

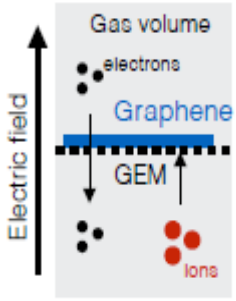

Previous work

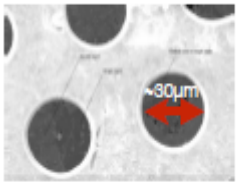

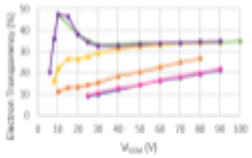

https://doi.org/10.1016/j.nima.2015.11.077

Suppressing ion back flow can significantly **improve high-rate capabilities** and **reduced electric field distortions** in Time Projection Chambers.

Application 2:
Protection of photocathodes with graphene layers

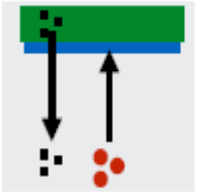

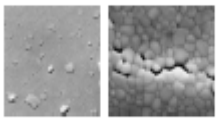

Damage of CsI

https://doi.org/10.1016/j.nima.2009.05.179

Protection and decrease of work function by coating layer

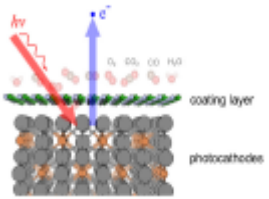

https://www.nature.com/articles/s41699-018-0062-6

Atomically thin coating layers could **protect sensitive photocathodes** such as CsI against environmental factors and ion bombardment, which is important for preserving specifications of precise timing detector in harsh ion-back flow conditions. Additionally, **modifications of the work functions**of converter layers can be used to increase QE.

Application 3:
Graphene and nanostructures for photoconversion and as solid converters

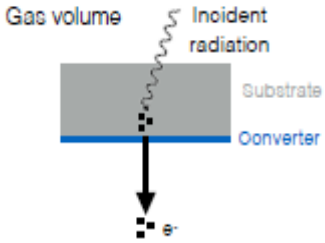

Possible system with UV-to-NIR response

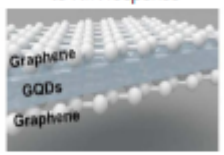

https://www.nature.com/articles/srep06603.pdf

Graphene quantum dots (GQD), carbon nanotubes and graphene have been shown to exhibit **broadband sensitivity** and could be used as versatile **conversion layers**. Utilising solid conversion layers enables high **detection efficiencies** and can be used for **precise timing** with gaseous radiation detectors.

First work on GEM & graphene layers: NIMA824 (2016) 571

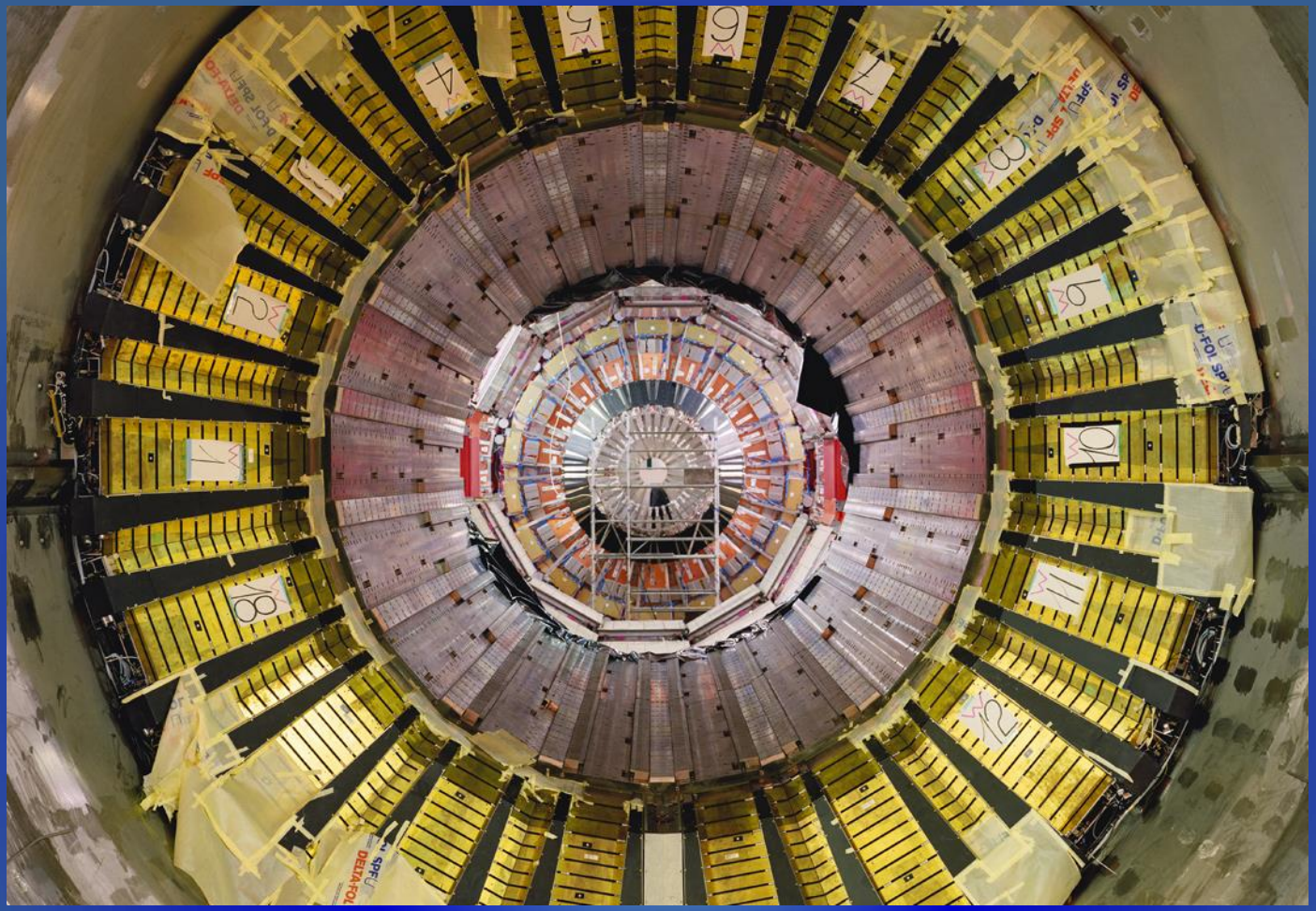

Knowledge is limited. Whereas the Imagination embraces the entire world… Albert Einstein

Bridge the gap between science and society …

The Role of Big High Energy Physics Laboratories: – innovate, discover, publish, share

… and bring the world closer together


BACK-UP SLIDES

Scintillating GEM for Dose Imaging in Radiotherapy

Scintillation Light (Optical) & Charge Readout:

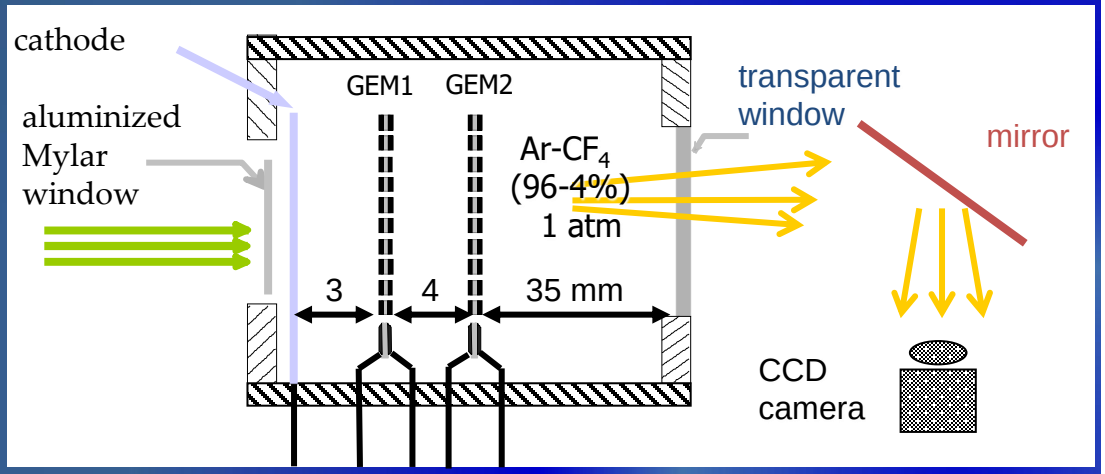

Light output for 138 MeV protons:

Scintillation type	Gas gain	Light signal (CCD) at 1Gy proton dose (ADU)
Screen (Gd_2O_2S:Tb)		2670
Ar/CO_2 (90:10)	3000	270
Ar/CF_4 (90:10)	1400	2350
Ar/CF_4 (95:5)	1300	4000
Ar/CF_4 (97,5:2,5)	770	2000

Bragg curve with 360 MeV a-beam

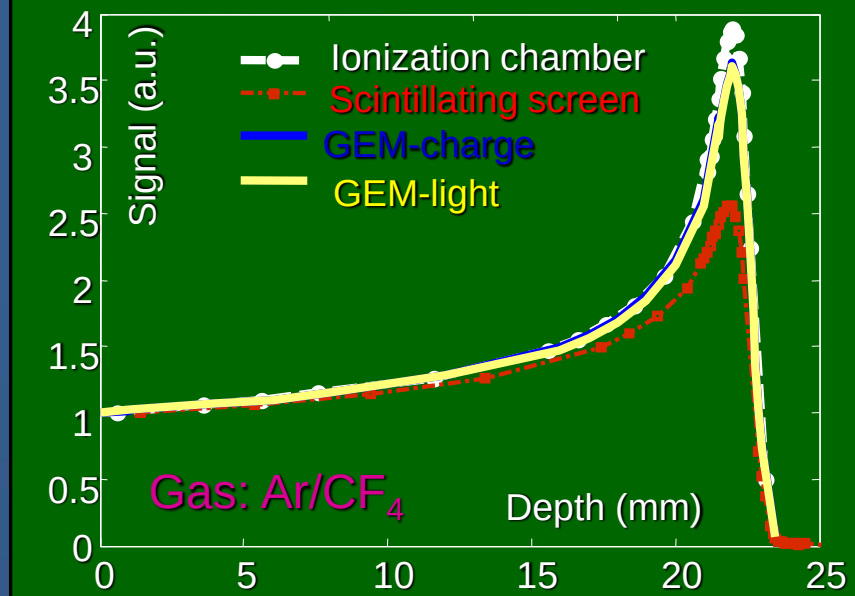

LIGHT SIGNAL FROM GEM:

(only 4% smaller than ionization chamber signal)

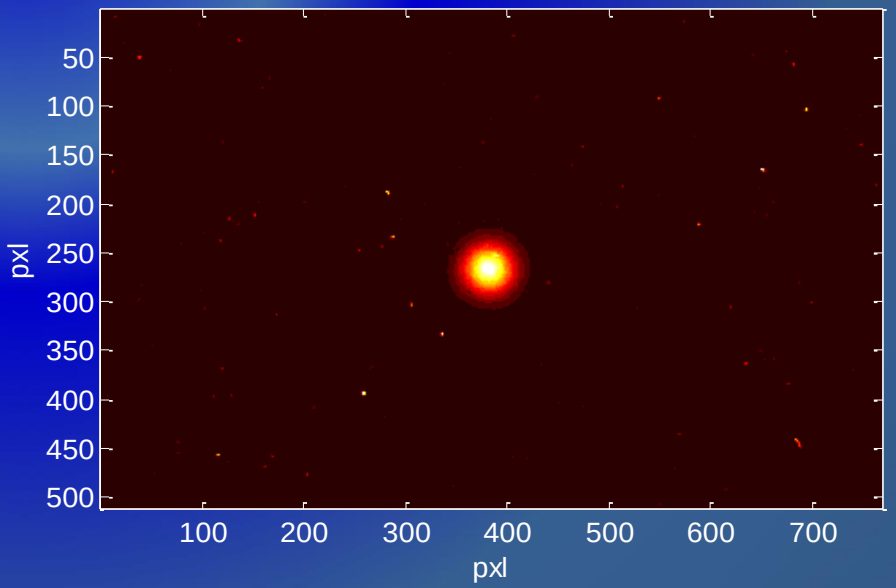

NEWS-G: Search for Dark Matter with Spherical Proportional Counters

NEWS-G Collaboration: 5 countries, 10 institutes, ~40 collaborators

Three underground laboratories:

- ✓ SNOLAB
- ✓ Laboratoire Souterrain de Modane
- ✓ Boulby Underground Laboratory

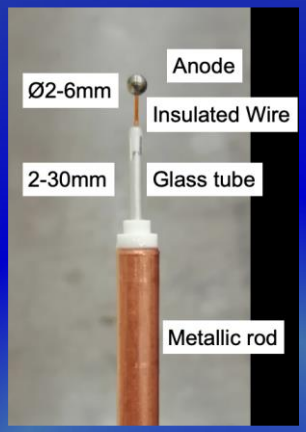

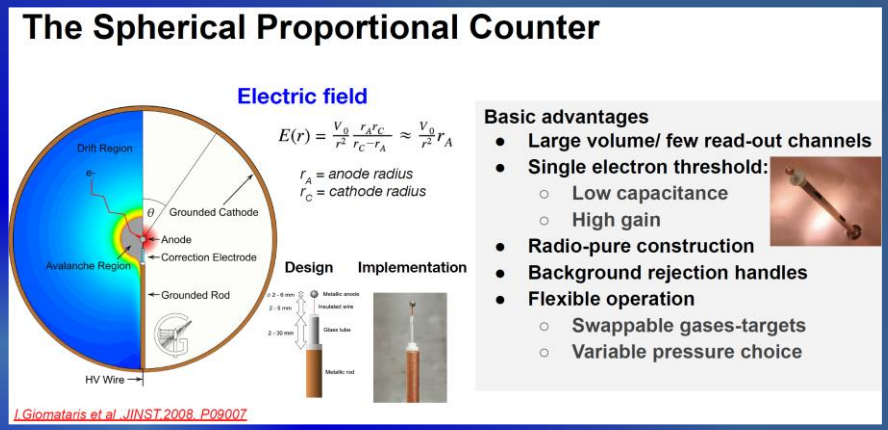

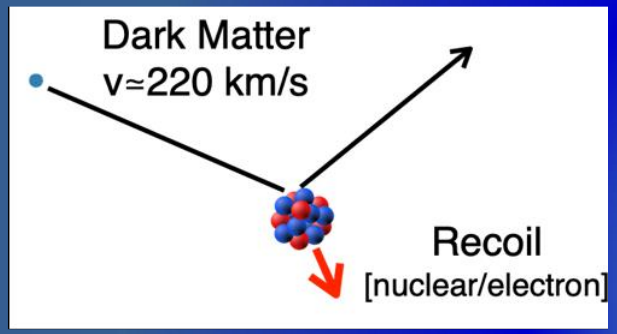

Nuclear Quenching Factor measurements:

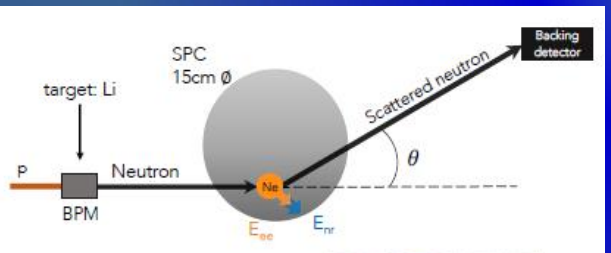

Run	E_{nr} [keV$_{nr}$]	θ [°]
8	6.8	29.02
7	2.93	18.84
14	2.02	15.63
9	1.7	14.33
10	1.3	12.48
14	1.03	11.13
11	0.74	9.4
14	0.34	6.33

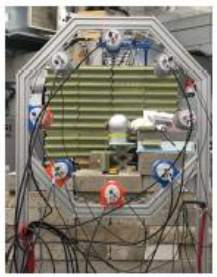

Increasing Target Mass and Reducing Background:

- ✓ **ACHINOS, electroformation, …**
- ✓ **Several detectors scheduled for the coming years**
- ✓ **Eventually sensitivity could reach neutrino floor**

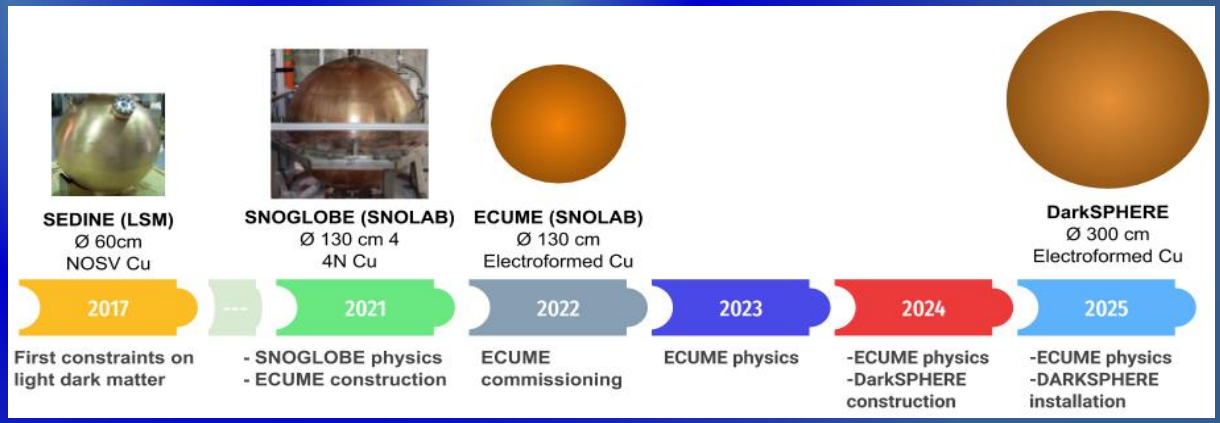

CEvNS & NEWS-G

- CEvNS opens a window to investigation non-standard neutrino interactions
  - First observations by COHERENT in NaI (2017) and Ar (2020)
  - Unique complementarity with DM searches as sensitivity reaches the neutrino floor
- NEWS-G3: A low-threshold low-background sea-level facility
  - Environmental and cosmogenic background studies towards reactor CEvNS studies
  - Shielding: Layers of pure copper, polyethylene, and lead, with active muon veto
  - Commissioning in 2021